Field-Flow Fractionation Techniques for Polymer and Colloid Analysis

Helmut Cölfen, Markus Antonietti

Max Planck Institute of Colloids and Interfaces, Colloid Chemistry Department, Am Mühlenberg 2, D-14476 Golm, Germany
E-mail: helmut.coelfen@mpikg-golm.mpg.de

Field-flow fractionation (FFF) is a family of flexible analytical fractionating techniques which have the great advantage that separation is achieved solely through the interaction of the sample with an external physical field and without a stationary phase. This has the advantage of avoiding the large variety of problems due to non-specific sample interactions with column materials associated with other chromatographic techniques. Furthermore, the range of information accessible is very broad and often complimentary when various FFF techniques are applied, so that even very complex systems with broad size distribution, heterogeneous mixtures or strongly interacting systems can be characterized. The range of particle sizes or hydrodynamic radii which can be separated is very broad ranging from 1 nm to 100 μm, covering the entire colloidal, polymeric and even most of the microparticle domain. No other fractionating technique can cover about 5 orders of magnitude of the particle size, even with complex distributions.
This review will introduce the basic principles, theory, and experimental arrangements of the various FFF techniques focusing on the most relevant for praxis: Sedimentation-FFF (S-FFF), Thermal-FFF (Th-FFF) and Flow-FFF (Fl-FFF). In a second part, selected applications of these techniques both to synthetic and biological samples will illustrate applications under a variety of conditions, where problems and potential pitfalls as well as recent developments are also considered.
Due to the wide spread of available information, an organized guide to the primary literature is given which contains the results from about 70% of the total literature published on FFF in listed journals so far.

Keywords: Field-flow fractionation, Chromatography, Separation, Polymers, Colloids

Advances in Polymer Science, Vol.150

List of Abbreviations

a_i	activity of component i in a solution
A_{Tot}	area of the accumulation wall
b	FFF channel breadth
b_0	channel width at the inlet
b_L	channel width at the outlet L
c	concentration
c^*	coil overlap concentration
c_0	concentration at the accumulation wall
d_H	hydrodynamic diameter
D	diffusion coefficient
D_T	thermal diffusion coefficient
E	electrical field strength
f	frictional coefficient
F	force
F_L	hydrodynamic lift force
F_{L_w}	hydrodynamic lift force by a near wall effect

F_{L_i}	inertial contribution to hydrodynamic lift force
$g(\dot{Y})$	zone spreading contribution to the FFF fractogram
G	gravitational/centrifugal acceleration
h(V)	experimental FFF fractogram
H_m	intensity of magnetic field
$\overline{H}$	theoretical plate height
J	flux density
k	Boltzmann's constant
l	average distance of the solute cloud from the accumulation wall
L	channel length
m	mass
m'	buoyant mass
M	molecular mass
n_c	peak capacity
N	plate number
N_A	Avogadro number
P	pressure
r	radius
r_c	radius from the center of rotation in S-FFF
$<r_G>$	radius of gyration
r_H	hydrodynamic radius
R	universal gas constant; also applied for the retention ratio
R_S	resolution between two separated components
s_0	fluid shear rate
S_m	mass based selectivity
S_D	diameter based selectivity
t	time
t_0	retention time of an unretained solute; void time
t_r	retention time
T	thermodynamic temperature
T_c	cold wall temperature in Th-FFF
$\lvert u_0 \rvert$	cross-flow velocity at the accumulation wall in A-Fl-FFF
U	solute drift velocity caused by the external field
v	flow velocity
$<v_s>$	mean velocity of the retained solute
<v>	mean velocity of the carrier fluid
$\overline{v}$	partial specific volume of the solute
$\overline{v}_i$	partial specific volume of component i in a multicomponent system
V	volume
V_0	volume of the separation channel
V_r	retention volume
$\dot{V}_c$	cross-flow rate for Fl-FFF
w	channel width

x	distance from the accumulation wall
y	distance perpendicular to the field axis and the carrier fluid flow
z	direction of the carrier fluid flow
z'	distance from the inlet to the focusing point for A-Fl-FFF
α	thermal diffusion factor=(D_T/D) T
χ_M	molar magnetic susceptibility
δ	distance of the particle bottom from the accumulation wall in hyperlayer FFF
ε_0	electrical permittivity of the free space
ε_m	relative electrical permittivity of the carrier medium
γ	thermal expansion coefficient
γ_s	steric correction factor
η	solvent viscosity
κ	thermal conductivity
κ_D	inverse of Debye length
κ_c	thermal conductivity at T_c
λ	retention parameter
μ_c^*	chemical potential
μ_e	electrophoretic mobility
ρ	solvent density
ρ_S	solute/particle density
σ	Gaussian half peak widths (time units) of eluting peaks
σ^*	complex conductivity
ω	angular velocity
ζ	ζ-potential
AC	adhesion chromatography
A-Fl-FFF	asymmetrical flow-field-flow fractionation
AUC	analytical ultracentrifugation
BSA	bovine serum albumin
CHDF	capillary hydrodynamic fractionation
DADMAC	diallyldimethylammonium chloride
DEP	dielectrophoresis
DEP-FFF	dielectrophoresis field-flow fractionation
DNA	desoxyribonucleic acid
DMSO	dimethyl sulfoxide
EAAS	electrothermal atomic adsorption spectroscopy
El-FFF	electrical field-flow fractionation
EM	electron microscopy
FFF	field-flow fractionation
Fl-FFF	flow-field-flow fractionation
GC-MS	gas chromatography coupled with mass spectrometry
Gr-FFF	gravitational field-flow fractionation
Gr-SPLITT-FFF	gravitational SPLITT-field-flow fractionation
HC	hydrodynamic chromatography

Helical Fl-FFF	three-dimensional flow-field-flow fractionation
HPLC	high performance liquid chromatography
ICP-MS	inductively coupled plasma mass spectrometry
IR	infrared
MALLS	multiangle laser light scattering
MS	mass spectrometry
MWCO	molar weight cut off
OFSC	opposed flow sample concentration
PCS	photon correlation spectroscopy
PEO	poly(ethylene oxide)
PET	poly(ethylene terephthalate)
PMMA	poly(methyl methacrylate)
PPO	poly(propylene oxide)
PS	polystyrene
PTFE	poly(tetrafluoroethylene)
P4VP	poly(4-vinylpyridine)
QELS	quasi-elastic light scattering
RI	refractive index
RNA	ribonucleic acid
RPM	revolutions per minute
SEC	size exclusion chromatography
S-FFF	sedimentation field-flow fractionation
S-Fl-FFF	symmetrical flow-field-flow fractionation
THF	tetrahydrofuran
Th-FFF	thermal field-flow fractionation

1 Introduction and Basic Principles

1.1 History/The Family of Field-Flow-Fractionation (FFF) Techniques

FFF techniques were pioneered by Giddings in 1966 [1]. Starting from this point, a remarkable development has taken place resulting in a diversity of different FFF methods. Figure 1 gives an overview of the different techniques with their time of invention. The number of different methods is directly related to the variety of force fields which can be applied for the separation of the samples. Practically, only three of those FFF methods are commonly used and commercially available at the present time; namely sedimentation-FFF (S-FFF), flow-FFF (Fl-FFF) and thermal-FFF (Th-FFF). The range of possible techniques was established in the early years whereas the main development of the last years is seen in a continuous optimization of the methodology and the instrumentation. This becomes most evident for the case of flow-FFF, where an asymmetrical channel with better separation characteristics has been developed.

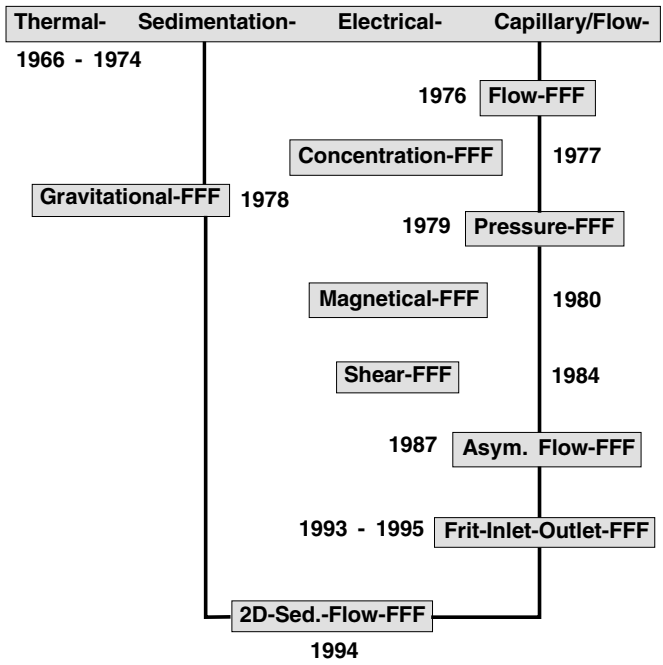

Fig. 1. A "family tree" of FFF methods with their date of birth

FFF techniques have also gained a broader and broader application, as reflected in the number of papers on the technique. This is shown in Fig. 2 in a plot of available papers versus time. Up to 1980, only few papers were published whereas there is a close to exponential increase afterwards. The FFF family has already been reviewed many times, covering both theoretical and practical aspects [2–26], and two books dedicated to FFF are available [27,28], the latter more generally treating separation techniques.

The first two experimental studies using FFF techniques were the fractionation of polystyrenes by Th-FFF [29] and the fractionation of *E. coli* bacteriophages and particles by sedimentation/gravitational-FFF [30–32]. Simultaneously, a theory of FFF was developed [33,34]. In 1972, electrical-FFF (El-FFF) was introduced as a technique for the separation of proteins [35,36]. The first flow-FFF setup was reported in 1974 applying circular tubes [37]. The experimental methodology and resolution of FFF were further improved by means of field programming which allowed the establishment of profiles of the applied physical field and thus an extension of the width of the separation range (see, e.g. [38–40]). Flow-FFF was introduced in 1976 in the principle setup which is still used today [41]. A year later the concepts for concentration FFF were published [42]. Other FFF methods, such as thermogravitational-FFF [43], pressure-FFF [44], magnetic-FFF [45] and shear-FFF [46], were developed but are rarely used

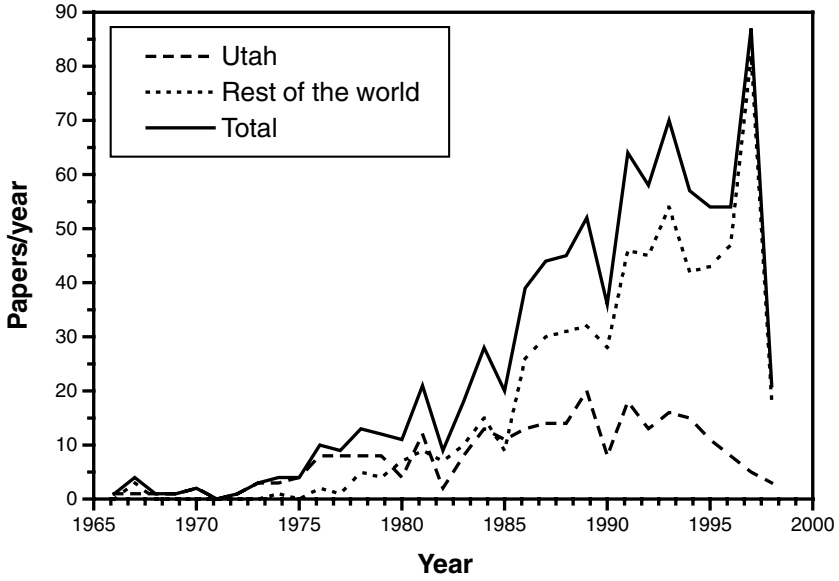

Fig. 2. Number of papers published on FFF. Source: Field-flow fractionation references web site update 14.10.1998 (see Sect. 6)

and are of minor importance. After 1984, principally flow-FFF was improved because it is the most simple and universally applicable FFF method for the whole range of systems. Asymmetrical flow-FFF was introduced in 1987 [47]. This technique has a better resolution than the so-far applied symmetrical flow-FFF due to the possibility of focusing the sample into a narrow band, whereas symmetrical flow-FFF could be improved by the introduction of frits for the sample injection [48–52]. Further improvement in the amount of accessible information of all FFF techniques was achieved by the modular combination of the fractionating FFF channel with an absolute molar mass measurement (multiangle laser light scattering; MALLS) at the beginning of the 1990s [53], a technique which can yield absolute molar mass distributions within a few minutes.

1.2 General Principles

The fundamental principle of FFF is illustrated in Fig. 3. The separation of the sample takes place inside a narrow ribbon-like channel. This channel is composed of a thin piece of sheet material (usually 70–300 μm thick Mylar or polyimide) in which a channel is cut and which is usually clamped between two walls of highly-polished plane parallel surfaces through which a force can be applied

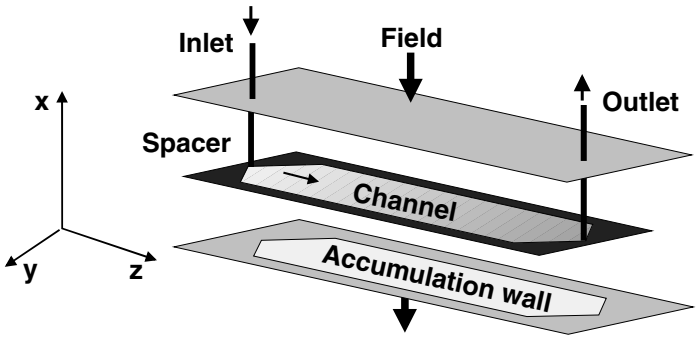

Fig. 3. Schematic representation of an FFF channel

(exceptions: flow- and electrical-FFF). The actual configuration varies with the type of field being utilized.

A carrier liquid is pumped through this channel from the inlet, where the sample is injected, to the outlet, to which a detector is connected. Inside the channel, a parabolic flow profile (laminar Newtonian flow) is established as in a capillary tube. Thus, flow velocities vary from zero at the walls to a maximum in the center of the channel. While the carrier liquid with the sample is flowing through the channel, an effective physical or chemical field is applied across the channel perpendicular to the flow direction of the carrier liquid. Interaction with the field concentrates the solute at one of the channel walls, called the accumulation wall. The center of gravity of the solute zones lies very near to the wall, usually extending only a few micrometers. Due to the established concentration gradient, a diffusion flux in the reverse direction is induced according to Fick's law. After a short time a steady state is reached, and the exponential distribution of the solute cloud across the channel can be described by a mean layer thickness (l). Due to the parabolic flow velocity profile, the solutes are transported in the direction of the longitudinal channel axis at varying velocities, depending on their distance from the channel walls. The nearer the solute is located to the accumulation wall, the later it will elute. Since smaller molecules (X) diffuse faster than larger ones (Y) and so establish a higher layer thickness l, the elution sequence proceeds from the smaller solutes to the largest ones. (See Fig. 4). Hence, the flow velocity profile of the carrier liquid amplifies very little distance differences between the solute clouds in the x-direction, leading to the separation. This FFF mode, when the intensity of driving forces induced by the applied outer field is homogeneous within the entire channel, is called classical or normal mode operation.

The intensity of the driving force can be varied in the course of the elution. This is called field intensity programming and permits analysis of very broadly distributed solutes (10^3–10^7 g/mol) [54] in one experiment over reasonable times with good resolution. The channel flow may also be programmed for shorter analysis times but with a cost to resolution.

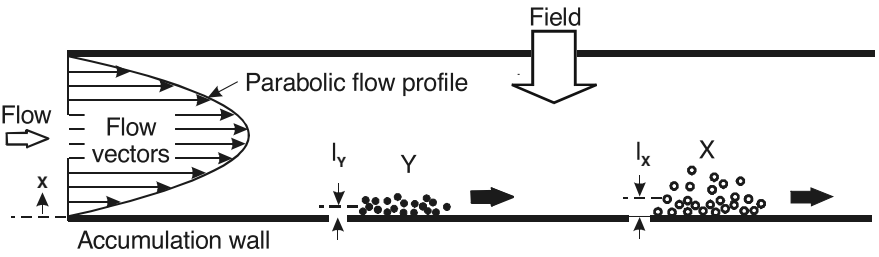

Fig. 4. Mechanism of an FFF separation of two components X and Y across the parabolic flow profile resulting in different flow velocities of X and Y. Reproduced from [14] with kind permission of the American Association for the Advancement of Science

The simple configuration with the defined channel geometry allows precise calculation of the flow hydrodynamics, unlike packed columns where flow patterns are very complex. In contrast to chromatography, the separation features of FFF techniques were conceived and developed from the beginning on theoretical grounds. Well-designed flow profiles were generated and different force fields were exploited to interact with a given specific particle property. Because of the theoretical basis of the resulting separation process, FFF is in principle also suited to determine absolute physicochemical properties of the sample components, such as the diffusion or thermodiffusion coefficient.

Compared to a packed high performance liquid chromatography (HPLC) column, the open channel also minimizes the shear effects exerted onto large molecules (as illustrated by the required pressure differences), and complex molecules and aggregates will remain intact. In addition, adsorption is kept to a minimum because of the greatly reduced surface area in an FFF channel. The carrier composition can affect the retention characteristics of polymers and particles in some cases. Factors including viscosity, ionic strength, type of detergent, and chemical composition have been discussed in the literature [55–62].

There are some special cases in FFF related to the two extreme limits of the cross-field driving forces. In the first case, the cross-field force is zero, and no transverse solute migration is caused by outer fields. However, because of the shear forces, transverse movements may occur even under conditions of laminar flow. This phenomenon is called the "tubular pinch effect". In this case, these shear forces lead to axial separation of various solutes. Small [63] made use of this phenomenon and named it "hydrodynamic chromatography" (HC). If thin capillaries are used for flow transport, this technique is also called capillary hydrodynamic fractionation (CHDF). A simple interpretation of the ability to separate is that the centers of the solute particles cannot approach the channel walls closer than their lateral dimensions. This means that just by their size larger particles are located in streamlines of higher flow velocities than smaller ones and are eluted first (opposite to the solution sequence in the classical FFF mode). For details on hydrodynamic chromatography, see [64–66].

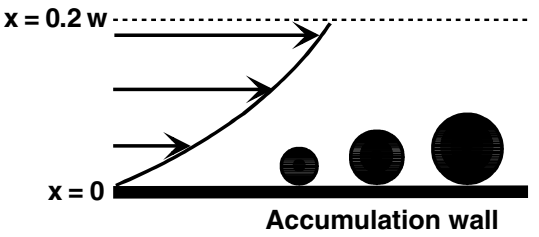

Fig. 5. Schematic representation of the steric-FFF mode

In the other limiting case of FFF, the intensity of the driving force is high enough to press all the solutes as close as possible to the accumulation wall of the channel, which is the basis of an independent FFF mode called steric field-flow fractionation [67]. This upper limit mode becomes operative when the mean diffusive layer thickness l is of approximately the particle size. As in hydrodynamic chromatography, the solute layer thickness is mainly controlled by steric exclusion of the particles from the accumulation wall. Again, larger particles are kept in streamlines of higher velocities than are smaller particles and are eluted more rapidly (see Fig. 5). In principle, any FFF technique can be operated in the steric-FFF mode by increasing the cross-field.

The transition between normal and steric-FFF mode depends on the particle size and lies for standard separation parameters at around 1 μm diameter (see Fig. 6). In this range, the elution behavior reverses, and the retention time is not any longer unique to a particle size. Consequently, the particle size determination of the size range can be erroneous, which can be a significant problem with polydisperse samples. However, most samples have sizes where the operation of one of the modes can be clearly assigned (see Fig. 6). The transition range between normal and steric-FFF mode has been considered in detail by Myers and Giddings [68].

For samples with a broad size distribution in the micron range, it is important to avoid the transition region between the normal and the steric mode during the measurement. This can be achieved by proper adjustment of the channel thickness, channel flow and the strength of the applied field [69]. The transition region in Fig. 6 can be experimentally determined by plotting the retention ratio vs. the particle size, as illustrated in Fig. 7 for the example of flow-FFF.

As the average velocity of the carrier in the channel increases, particles that are in close contact with the accumulation wall experience hydrodynamic lift forces which move them into a confined region from the wall that is thin relative to their size, or "focused," as shown in Fig. 8. This is the basis of another FFF operation mode called "hyperlayer mode" [71] which is characterized by an extremely high resolution in very short analysis times. However, the nature of the hydrodynamic lift forces is still only poorly understood.

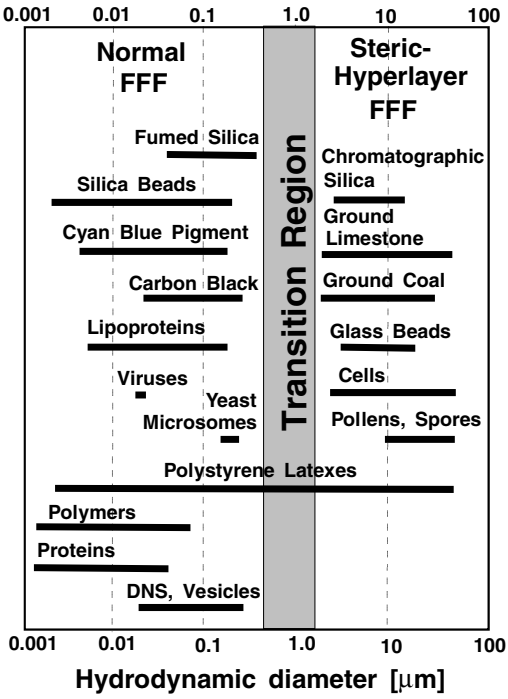

Fig. 6. Application of FFF to various materials spanning the whole range of applicability

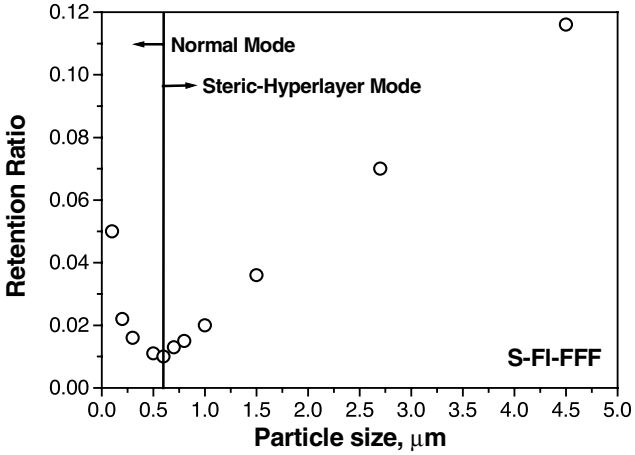

Fig. 7. Determination of the transition point between the normal and the steric mode for the example of S-Fl-FFF. Reproduced from [70] with kind permission of VCH Verlagsgesellschaft Weinheim

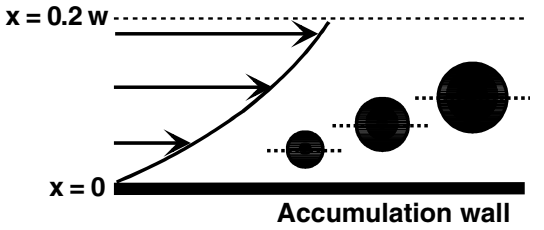

Fig. 8. Steric-hyperlayer mode

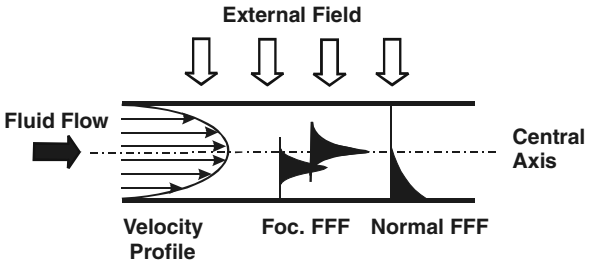

Fig. 9. Principle of focusing-FFF. Reproduced from [74] with kind permission of the American Chemical Society

Another FFF mode, focusing-FFF [71–74], exploits a counterbalance of the forces exerted on the solute via an external field gradient by dispersive diffusion processes. In contrast to classical FFF techniques, where the field strength is constant, the solute is focused to a position inside the channel where due to a balance of the driving force to the accumulation wall and the back diffusion the intensity of the driving force is zero. Thus a focused, Gaussian-shaped concentration distribution for each species is formed inside the channel, which migrate along the channel at different velocities and are longitudinally separated. Such a situation is shown schematically in Fig. 9. To illustrate the basic difference between the classical and all focusing-FFF methods, the exponential shape of the concentration profile of the solute in the case of classical FFF is also shown in Fig. 9.

1.3 Accessible Quantities

Depending on the separation mode, knowledge about the sample, and the FFF setup, four categories of operating an FFF experiment are identified:

1. Information about sample composition, homogeneity and purity from qualitative evaluation of the fractogram;

2. Application of the FFF channel as a separation column and determination of physicochemical quantities by following characterization (either on or off line);
3. Measurement of forces acting in the FFF channel;
4. Determination of absolute physicochemical quantities of the sample via the retention times in the FFF channel.

1. The simplest analytical information that can be obtained with the aid of FFF is the homogeneity of the sample or evidence for the presence of a compound of interest in the fractionated sample by the appearance of a peak in the expected interval of retention volume. In some cases, comparison of the retention volume and the peak shape of the investigated component with the peak shape of a reference sample can provide sufficient qualitative analytical information on sample purity and homogeneity. The peak areas in the fractogram can be used to evaluate quantitatively concentrations of the detected components provided that the relationship between detector response and concentration or quantity of the detected component is known. This relationship is usually determined by a calibration procedure. However some sample is lost in the void peak so that it is not possible to relate the detected concentration to that of the original sample; consequently, concentration determinations can more advantageously serve to compare the relative concentrations of the fractionated components.

2. Coupling FFF with other techniques can enhance measurement capabilities. Here, the possibility of taking fractions after the FFF separation is of great advantage. The use of photon correlation spectroscopy, for example, to determine the size of spheres eluted from sedimentation FFF yields both size and density [75]. Further comparison can be achieved with electron microscopy. In principle, every analytical technique (spectroscopy, microscopy, chemical analysis, etc.) can be performed off-line on fractions from FFF.

It is, however, more convenient to couple absolute flow-through detectors online with an FFF channel. For example, coupling multiangle laser light scattering (MALLS) with FFF has become highly popular among FFF researchers in recent years and is treated in detail in Sect. 4.3.2. Here, the molar mass distribution as well as the radii of gyration for each species are obtained on an absolute basis.

If a continuous viscosity detector is coupled to an FFF channel, viscosity distributions and intrinsic viscosities can be measured without calibrating the channel [76]. The coupling of one FFF instrument to another opens the possibility of obtaining two-dimensional property distributions of complex materials: the combination of sedimentation- and flow-FFF provides the size-density distribution of complex colloids, whereas a combination of thermal- and flow-FFF yields the composition-molecular weight distribution of copolymers.

3. FFF in an absolute configuration can be used to determine the often very weak cross-forces by the retention times which helps to understand the funda-

mental physicochemical phenomena which are reflected in these forces. For example, for poorly understood forces (e.g. hydrodynamic lift forces) or coupled transport phenomena (thermal diffusion), the measurement of forces exerted on model particles can help to explore and understand the principles. An FFF separation is sensitive to these very weak forces, and retention of colloids and macromolecules is induced by forces as little as 10^{-16} to 10^{-14} N per particle [77]. Thus forces as small as 10^{-16} N can be determined by measuring t_r. Force increments as low as 10^{-17} N can be detected as measurable shifts in t_r of 0.1 to 1 min (from $(\Delta t_r/t_0)=w\Delta F/6kT$; a change ΔF in F of 10^{-17} N at T=300 K with w=250 μm thus shifts the retention time by $\Delta t_r=0.106\ t_0$. Typically, the void time t_0 is 1 to 10 min, giving $\Delta t_r \approx 0.1$ to1 min) [14]. These forces are eight to nine orders of magnitude less than the force required to rupture one C–C bond (ca. 0.8×10^{-8} N [78]). The very high resolution of observable net forces is a result of the fact that they are balanced or "weighted" by similarly small entropic forces such as back diffusion due to the concentration gradient and so forth.

For micrometer-sized particles subject to steric- or lift-hyperlayer-FFF, the driving forces are higher (10^{-14} to 10^{-8} N per particle) but are not balanced by back diffusion as in the normal FFF mode. Steric- and lift-hyperlayer-FFF provide powerful means for the investigation of hydrodynamic lift forces [79]. Here, retention times have been measured for well-characterized particles such as latex spheres under widely varying conditions, and the hydrodynamic lift force F_L has been determined.

4. The dimensionless retention parameter λ of all FFF techniques, if operated on an absolute basis, is a function of the molecular characteristics of the compounds separated. These include the size of macromolecules and particles, molar mass, diffusion coefficient, thermal diffusion coefficient, electrophoretic mobility, electrical charge, and density (see Table 1, Sect. 1.4.1.) reflecting the wide variablity of the applicable forces [77]. For detailed theoretical descriptions see Sects. 1.4.1. and 2. For the majority of operation modes, λ is influenced by the size of the retained macromolecules or particles, and FFF can be used to determine absolute particle sizes and their distributions. For an overview, the accessible quantities for the three main FFF techniques are given (for the analytical expressions see Table 1, Sect. 1.4.1):

Sedimentation-FFF. Retention measurements give the effective particle mass m' (buoyant mass). If the particle density is known, the particle mass m, particle volume V_p, and hydrodynamic diameter d_H can be calculated [80,81]. Apart from the particle dimensions, the density can be determined as well [82] as the difference in the densities of the solute and the solvent, $\Delta\rho$, is linearly correlated to λ. Fractionation can be used in regions where the solvent density is lower than the solute density ($\rho<\rho_s$) as well as where $\rho>\rho_s$. The determination of particle density in a single experiment is possible by sedimentation-flotation focusing-FFF [72,73,83] analogous to density gradient ultracentrifugation.

Flow-FFF. The measurement of retention in flow-FFF directly yields the diffusion coefficient D and the related hydrodynamic diameter d_H which is related to D by the Stokes–Einstein equation $D = \frac{kT}{3\pi\eta d_H}$. As the solute density does not influence retention, information from flow-FFF can be advantageously combined with that of sedimentation-FFF yielding particle size and density distributions.

Thermal-FFF. The retention rate directly yields the Soret coefficient D_T/D. If D is known (for example from flow-FFF), the thermal diffusion coefficient D_T can be obtained which can give information about the chemical sample composition. Unfortunately, no context is known which analytically relates D_T with the sample composition [84]. On the other hand, for known D_T values (material constant), the diffusion coefficient distribution is directly obtained.

1.4 General Theoretical Considerations

If the geometry of an FFF channel is known exactly and a parabolic flow profile in the channel can be assumed (see Sect. 1.2), it is possible to make exact predictions about the separation of the sample as well as the separation efficiency. In this section, only the general theoretical expressions universally applicable to all FFF techniques operating in the normal mode are provided. Specialities of the different FFF methods are given during their detailed discussion in Sect. 2.

1.4.1 *Elution in an FFF Channel*

The theory of FFF has undergone significant developments since the general introduction of the "non-equilibrium theory of FFF" by Giddings in 1968 [33] especially motivated by the various FFF techniques. Examples that include general discussions for FFF are [5,25,30,85–102], Th-FFF [34,103], magnetic-FFF [45] dielectrical-FFF [104], S-FFF [105,106], hyperlayer-S-FFF [83,107], focusing-FFF [108], Fl-FFF [41] and shear-FFF [46].

For the concentration profile of a sample which has been driven towards the accumulation wall by the physical field, the general transport theory yields for the flux density J_x of the solute:

$$J_x = \underbrace{Uc(x)}_{\substack{\text{External}\\ \text{field}}} - \underbrace{D\frac{dc(x)}{dx}}_{\text{Diffusion}} \qquad (1)$$

where D is the translational diffusion coefficient, x is the distance from the accumulation wall, c(x) is the concentration gradient and U is the drift velocity of

the solute caused by the external field. As indicated in Eq. (1), there are two contributions to the flux density of the solute: (a) the flux caused by the solute drift due to the external field and (b) the back diffusion away from the accumulation wall according to Fick's law due to the established solute concentration gradient. After a short time, a steady state is established. Due to the transport character of the solute distribution, this is not an equilibrium state as erroneously stated in many literature references but in fact a stationary non-equilibrium state. In the steady state, the resulting flux vanishes and by integration of Eq. (1) the following relationship is obtained:

$$c(x) = c_0 \exp\left(-\frac{x|U|}{D}\right) \tag{2}$$

where c_0 is the concentration at the accumulation wall. The diffusion coefficient can be related to the frictional coefficient f by the Stokes–Einstein relation:

$$D = \frac{kT}{f} \tag{3}$$

where k is the Boltzmann constant and T is the temperature. The frictional coefficient furthermore relates the drift velocity U to the force F which acts on the solute by:

$$U = \frac{F}{f} \tag{4}$$

A parameter $l=D/|U|$ can now be introduced which is a measure of the average distance of the solute from the wall. From Eqs. (3) and (4) the following relationship for l is obtained:

$$l = \frac{kT}{F} \tag{5}$$

or in the form of the dimensionless retention parameter λ

$$\lambda = \frac{l}{w} = \frac{kT}{Fw} \tag{6}$$

where w is the channel thickness. The parameter λ is not directly experimentally accessible, but can be related to experimental quantities. This can be done by using the retention ratio R. R is defined as the ratio of the retention time of an unretained solute t_0 to the retention time of the retained solute t_r or equivalently in terms of retention volumes $R=V_0/V_r$ of the two species. V_0 is the volume of the separation channel which in the ideal case can be calculated from its geometry, but is experimentally obtained from the position of a low molecular weight sol-

ute. R can also be defined as the ratio of the mean velocity of the retained solute $<v_s>$ to the mean velocity of the carrier fluid $<v(x)>$.

$$R = \frac{t_0}{t_r} = \frac{V_0}{V_r} = \frac{< v_s >}{< v(x) >} = \frac{< c(x)v(x) >}{< c(x) >< v(x) >} \tag{7}$$

or as the integral form:

$$R = \frac{\int_0^w c(x)v(x)dx}{\int_0^w c(x)dx \int_0^w v(x)dx} \tag{8}$$

For the isothermal, isoviscous flow profile v(x) of a Newtonian liquid between two parallel infinite plates, one obtains:

$$v(x) = \frac{\Delta P}{2\eta L} x(w - x) \tag{9}$$

where ΔP is the pressure drop along the channel with length L and η is the viscosity of the solvent. For a parabola-shaped flow profile, the mean velocity $<v(x)>$ is 2/3 of the maximum velocity in the center of the channel at x=w/2. Thus, $<v(x)>$ can be written:

$$< v(x) >= \frac{\Delta P w^2}{12\eta L} \tag{10}$$

Using Eqs. (9) and (10), the integrals in Eq. (8) can be solved and a relationship between λ and the experimentally accessible R obtained [34]:

$$R = 6\lambda \left[\coth\left(\frac{1}{2\lambda} \right) - 2\lambda \right] \tag{11}$$

For small values of λ, one can approximate $\coth(2\lambda)^{-1}=1$ and thus Eq. (11) is simplified:

$$R = 6\left(\lambda - 2\lambda^2 \right) \tag{12}$$

or if λ approaches 0 by:

$$\underbrace{\lim}_{\lambda \to 0} R = 6\lambda \tag{13}$$

For $\lambda<0.3$, deviations from the exact Eq. (11) are negligible [85]. Once λ is known, it can be related to physicochemical quantities of the solute depending

Table 1. Relationship between λ and the physical solute properties using different FFF techniques [27,109] with R=gas constant, ρ=solvent density, ρ_s=solute density, $\omega^2 r$=centrifugal acceleration, V_0=volume of the fractionation channel, $\dot{V}_c$=cross-flow rate, E=electrical field strength, dT/dx=temperature gradient, M=molecular mass, d_H=hydrodynamic diameter, D_T=thermal diffusion coefficient, μ_e=electrophoretic mobility, χ_M=molar magnetic susceptibility, H_m=intensity of magnetic field, ΔH_m=gradient of the intensity of the magnetic field, $\Delta\mu^*_c$ = total increment of the chemical potential across the channel

FFF technique	Expression for λ	Physicochemical parameters
Sedimentation-FFF	$\lambda = \frac{RT}{\omega^2 r M\left(1-\frac{\rho}{\rho_s}\right)w}$	ρ_s, M
	$\lambda = \frac{6kT}{\pi d_H^3 \omega^2 rw\left(\rho_s-\rho\right)}$	d_H
Thermal-FFF	$\lambda = \frac{D}{D_T(dT/dx)w}$	D, D_T
Electrical-FFF	$\lambda = \frac{D}{\mu_e E w}$	D, μ_e
Flow-FFF	$\lambda = \frac{DV_0}{\dot{V}_c w^2}$	D, d_H
Steric-FFF	$\lambda = \frac{d_H}{2w}$	d_H
Magnetic-FFF	$\lambda = \frac{RT}{Mw\chi_m H_m \Delta H_m}$	M, χ_m
Concentration-FFF	$\lambda = \frac{RT}{\Delta\mu^*_c}$	$\Delta\mu^*_c$

on the nature of the applied physical field. For the various FFF techniques, these relationships can be found in Table 1.

The theoretical treatment above was based on the following assumptions: (a) The channel is placed between infinite parallel plates, (b) the flow profile is parabolic, (c) a steady state concentration profile of the sample is established after action of the physical field, (d) uniform force of the physical field in the channel, and (e) absence of extraneous non-uniform forces. These assumptions are usu-

ally fulfilled for the various FFF techniques, but significant errors and artifacts can be generated in the other cases (see also Sect. 4.2.1).

1.4.2
Resolution, Theoretical Plate Heights and Peak Capacity

Successful separation of two components requires that a difference Δt_r in retention time t_r is generated by sufficiently different molecular parameters of the components subjected to fractionation. However, separation also requires a consideration of peak broadening so that peaks with a finite Δt_r do not overlap. In FFF, theoretical guidelines can be developed to reach band broadening and resolution objectives through optimization of the flow rates V and $\dot{V}_c$.

As in chromatography and related techniques, the resolution R_s between two components can be defined by [28]:

$$R_s = \frac{t_{r2} - t_{r1}}{2\sigma_2 + 2\sigma_1} \cong \frac{\Delta t_r}{4\sigma} \tag{14}$$

where σ_1 and σ_2 are the Gaussian widths (in time units) of the two eluting peaks. For well-defined, neighboring components with similar properties one can assume that the σ values are similar [41], and a mean common σ is used which is the average of the σ_i. In elution methods such as FFF and chromatography, σ is – in analogy to fractionation systems – related to the height equivalent of a theoretical plate, $\overline{H}$, by [28]:

$$\overline{H} = \frac{L\sigma^2}{t_r^2} = \frac{\sum_i L_i \sum_i \sigma_i^2}{\left(\sum_i t_{r,i}\right)^2} \tag{15}$$

where L is the channel length. The plate number N can be calculated from $\overline{H}$ by $N = L/\overline{H}$. $\overline{H}$ is only an average value as several contributions to the average plate heights exist:

$$\overline{H} = \overline{H}_{neq} + \overline{H}_{long} + \overline{H}_{inj} + \sum \overline{H}_i \tag{16}$$

where the non-equilibrium term $\overline{H}_{neq}$ is due to the velocity profile, $\overline{H}_{long}$ due to longitudinal diffusion, $\overline{H}_{inj}$ is caused by the broadness of the sample zone when starting elution and $\sum \overline{H}_i$ is due to the sum of instrumental effects. The last three terms are for a modern instrument usually small and can be neglected as compared to the magnitude of the first one.

A combination of Eqs. (14) and (15) gives:

$$R_s = \frac{L^{1/2}}{4} \frac{\Delta t_r}{t_r \overline{H}^{1/2}} \tag{17}$$

which relates the resolution R_s to the plate height $\overline{H}$.

Furthermore, R_s is related to the peak capacity n_c which is the number of peaks that can be separated at a specified resolution R_s over the channel length L by [28]:

$$n_c = \frac{L}{4\sigma R_s} = \frac{(L\overline{H})^{1/2}}{\sigma t_r} \tag{18}$$

To make use of Eqs. (17) and (18), $\overline{H}$ needs to be related to the experimental parameter λ. Hence, an expression for the plate height must be sought which varies for each FFF technique. In general, $\overline{H}$ can be expressed as [28]:

$$\overline{H} = \chi \frac{w^2 \langle v \rangle}{D} \tag{19}$$

where <v> is the mean cross-sectional fluid velocity and χ a dimensionless parameter. χ equals 24 λ^3 for small λ and l [85].

For example, in the case of Fl-FFF, the non-equilibrium contribution to the plate height, which is the minimum value of $\overline{H}$, is closely approximated by [41]:

$$\overline{H} = \frac{2}{3} R^2 (1 - R) \frac{V}{\dot{V}_c} L \cong \frac{2}{3} R^2 \frac{V}{\dot{V}_c} L \tag{20}$$

where the final approximation is applicable for R (or λ) <<1. When this latter approximation is substituted into Eq. (17), we obtain:

$$R_s = \frac{1}{4} \left(\frac{3\dot{V}_c}{2V} \right)^{1/2} \frac{\Delta t_r}{t_r R} \tag{21}$$

1.5 Comparison of FFF with Other Analytical Techniques

1.5.1 *Comparison of FFF (Th-FFF and Fl-FFF) with SEC*

As FFF is similar to other chromatographic techniques it is interesting for the reader to compare their performance. The most extensive comparison is with size exclusion chromatography (SEC). The reason for this is that SEC and Th-FFF have similar application ranges, mainly synthetic polymers in organic solvents, and were developed at about the same time. Both FFF and SEC are used to obtain molecular weight information, but they use different fundamental mechanisms and therefore have different capabilities and limitations. For example, SEC can be advantageously applied to low molecular weight polymers while, for Th-FFF, very high temperature gradients are needed for the retention of these oligomers/polymers. On the other hand, Th-FFF is more

suited to ultrahigh molecular weight polymers susceptible to shear degradation in the packed SEC column. In this respect, SEC and Th-FFF are complimentary.

A significant difference can be found in the theoretical basis of the separation. The open Th-FFF channel allows retention to be precisely related to physicochemical parameters and experimental variables (even if the nature of thermal diffusion is not yet completely understood), whereas separation conditions in SEC channels lack the possibility of a rigid physicochemical basis. But although Th-FFF has a more rigorous theoretical background than SEC and a much wider application range with regard to separable molar masses, and although both techniques require almost the same supplemental equipment, it is astonishing to note that SEC has found widespread application and was the subject of intense research whereas Th-FFF was more or less a "Cinderella" in the analytical ballrooms. Both techniques were established in the 1960s but, even today, the application of FFF is in general by no means comparable with that of SEC. The following discussion compares SEC and FFF in detail, including calibration procedures, separation efficiencies and the general applicability of both techniques to polymer analysis.

Methodology and Universal Calibration. FFF calibration curves relating the retention of the solute to the molar mass can be expressed as:

$$\log V_r = a + S_m \log M \tag{22}$$

where a and S_m are constants; S_m is referred to as the mass based selectivity. Since the V_r of a component is related to its transport coefficients (D in Fl-FFF and D/D_T in Th-FFF), the calibration constants contain the inherent dependence of these transport coefficients on M; the appropriate algebraic scaling relations are well known in polymer and colloid physics:

$$D/D_T = \phi_0 M^{-n} \text{ for Th-FFF and} \tag{23}$$

$$D = AM^{-b} \text{ in case of FI-FFF} \tag{24}$$

The parameters ϕ_0, n, A and b are universal constants for a given polymer-solvent system. (Since D_T is independent of M and the degree of branching for a given polymer-solvent system [110,111], n≈b.) Differences between n and b arise primarily from the temperature dependence of the transport coefficients, which plays a role in Th-FFF and makes n slightly larger than b [112].

Combining Eq. (23) with the expression for $l = \frac{wD}{D_T \Delta T}$ for Th-FFF and, respectively, Eq. (24) with $l = \frac{w^2 D}{\dot{V}_c}$ for Fl-FFF yields the following universal calibration equations:

$$\lambda = \frac{\phi_0}{\Delta T} M^{-n} \tag{25}$$

for Th-FFF and

$$\lambda = \frac{wA}{\dot{V}_c} M^{-b} \tag{26}$$

for FI-FFF.

The parameter λ can be calculated from experimental values of V_r using Eq. (11), or M can be directly related to V_r by using the approximation $R \cong 6\lambda$ (accurate to within 2% when $R<0.06$):

$$V_r = \frac{V_0 \Delta T}{6\phi_0} M^n \text{ for Th} - \text{FFF and} \tag{27}$$

$$V_r = \frac{V_0 \dot{V}_c}{6Aw} M^b \text{ for FI} - \text{FFF} \tag{28}$$

A comparison of these separation equations with the universal calibration curve (Eq. 22) leads to the prefactors of Eq. (22):

$$a = \log \frac{V_0 \Delta T}{6\phi_0} \text{ and } S_m = n \text{ for Th} - \text{FFF} \tag{29}$$

$$a = \log \frac{V_0 \dot{V}_c}{6Aw} \text{ and } S_m = b \text{ for FI} - \text{FFF} \tag{30}$$

It is seen that for all FFF techniques the dependence of the retention volume on molecular weight is not linear. Practically, this restricts the accessible range of particle sizes in one single normal mode separation to about one order of magnitude. Broad molar mass distributions can be efficiently analyzed by FFF in a single run in the field programming mode. Theoretical guidelines and examples (including temperature programming) that can be found in the literature [15] show how experimental time and fractionating power in Th-FFF can be manipulated through changes in flow rate and ΔT. In contrast to FFF, the elution volume in SEC is proportional to the logarithm of hydrodynamic size or molecular weight of the sample, and molecular weight distributions can be as broad as five orders of magnitude in weight and are still accurately determined. Such molecular weight ranges, however, require connection of several columns in series, which significantly increases both run time and operating pressure.

FFF calibrations are universal in the sense that calibration constants apply to all other FFF setups under a wide range of experimental conditions [113] which are somewhat different from SEC as explained below. For characterizing molecular mass distributions with SEC, the calibration constants must be determined empirically for a whole set of standard samples. FFF channels are also calibrated empirically with standards for polymer-solvent systems where the Mark–Houwink coefficients for the dependence of the transport coefficients on M are un-

known. When this dependence is accessible, Fl-FFF does not require calibration, and since D_T is independent of M, universal calibration in Th-FFF can be performed with a single standard of known M to determine D_T. Once the calibration constants have been determined, no additional information is needed to characterize the molar mass distribution of a given polymer on every Th-FFF apparatus.

Both FFF and SEC require careful control of the temperature for universal calibration. For SEC and Fl-FFF, this means controlling the temperature of the room or of the channel/column. For Th-FFF, it is important to maintain the specified cold-wall temperature, T_c. Fortunately, the temperature at the center of gravity of a component is independent of the field strength in Th-FFF, so that universal calibration constants do not change when ΔT is tuned to optimize the analysis of a particular range in M, provided T_c is held constant.

The resolution of polymer components in FFF and SEC is governed by two factors: the change in retention with M and the plate height $\overline{H}$. The former is defined by the selectivity S_m and governed by transport coefficients and the separation mechanism; the latter is used to define the extent of remixing of separated zones [114]. If the remixing occurs more slowly than the retention, a net gain in the separation of different components is obtained. Plate height varies with experimental conditions, with lower $\overline{H}$ corresponding to more efficient separations. Selectivity in FFF depends on the polymer-solvent system but is as high as 0.5–0.65; this compares favorably with SEC where S_m is 0.1–0.2.

The higher selectivity of FFF results in more precise values of M compared with SEC [115]. However, SEC has a lower plate height, so the question of which technique is superior cannot be answered definitely. Several workers have compared Th-FFF with SEC in a systematic fashion. Early studies [115] focused on the mass-based fractionating power F_m, defined as the smallest relative molecular weight increment ($\Delta M/M$) that can be separated with unit resolution. For low molecular weight polymers, the greater efficiency of SEC leads to a superior fractionating power. In addition, Th-FFF is not applicable below 10^4 g/mol because the ratio of the transport coefficients (D/D_T) becomes too unfavorable for significant retention to occur. However, SEC efficiency deteriorates with M so that, around 10^5 g/mol, the higher selectivity of Th-FFF more than compensates for its lower efficiency. The advantages of Th-FFF over SEC continue to increase with increasing M.

Time requirements have been the subject of more recent comparisons between Th-FFF and SEC [116,117]. The time required to separate two components that differ in molecular mass by ΔM can be expressed as [118]:

$$t_r = \left(\frac{4R_S}{b} \frac{M}{\Delta M} \right)^2 \frac{\overline{H} V_r}{V_0 \langle v \rangle} \tag{31}$$

Here, R_s is the resolution defined in Eq. (17). When the resolution between two components is unity, the components are almost completely resolved. In

FFF, $\overline{H}$ can be precisely related to experimental parameters, allowing a closed form for t_r to be obtained:

$$t_r = \frac{1}{D}\left(\frac{4V_0 w}{3bV_r}\frac{M}{\Delta M}R_S\right)^2 \tag{32}$$

This equation indicates that faster separations are achieved with thinner channels and higher levels of retention. However, V_r is generally limited to under 20–50 times the channel volume in order to avoid undesirable interactions with the accumulation wall. For polymers in the size range of 10^6 g/mol, a 20% difference in molecular mass can be separated with unit resolution in about 6 min, while smaller differences and larger molecular weights require more time. Although channels as thin as 51 μm have been used to increase efficiency, as t_r is proportional to w^2, problems with sample overloading increase [119–121], particularly for polymers with $M>10^6$ g/mol. As more sensitive detectors become available, smaller sample loads become possible and, thereby, overloading problems diminish so that thinner channels may be used with increasing separation efficiency.

An analysis of separation time in SEC on an exact basis is not possible because column efficiency cannot be theoretically derived. Stegemann et al. [116] used empirical efficiency models to compare the time requirements of Th-FFF, SEC and hydrodynamic chromatography, and a critical M value of 10^5 g/mol was obtained above which Th-FFF is superior to SEC.

For Th-FFF, column dispersion is well defined and can therefore be accounted for and removed from the elution profile [122,123]. In removing the effects of column dispersion, the smaller fractionating power of Th-FFF for $M<10^5$ g/mol can be partially compensated. Similar findings were also published by Gunderson and Giddings [115] who found that, after dispersion corrections, Th-FFF shows a better resolution than SEC with the exception of low molar mass samples.

For laboratories that analyze a broad range of polymers on a routine basis, it is important to have a technique that can be tuned to maximize the efficiency of each particular analysis. In FFF the field strength is variable, while in SEC the column must be changed. Although several SEC columns can be purchased for the price of a single FFF channel, the SEC columns must be replaced periodically as a result of degradation of the packing material. Other advantages also make Th-FFF more attractive than SEC for a universally broad application: First, since the FFF channel is open, it has little tendency to clog, even in the presence of particles (including gels) up to 75 or 100 μm diameter, which is the typical range for the channel thickness. Secondly, the absence of a separation gel which can degrade also allows harsh chromatographic conditions. In this respect Th-FFF is particularly promising for high temperature polyolefin analysis. Another important aspect of the comparison is shear sensitivity. For random coil polymers with $M>10^6$ g/mol, SEC starts to become unreliable because shear forces in the packed column can degrade single polymer strands, whereas the FFF flow pattern subject shear-sensitive molecules to less disruptive conditions [124,125].

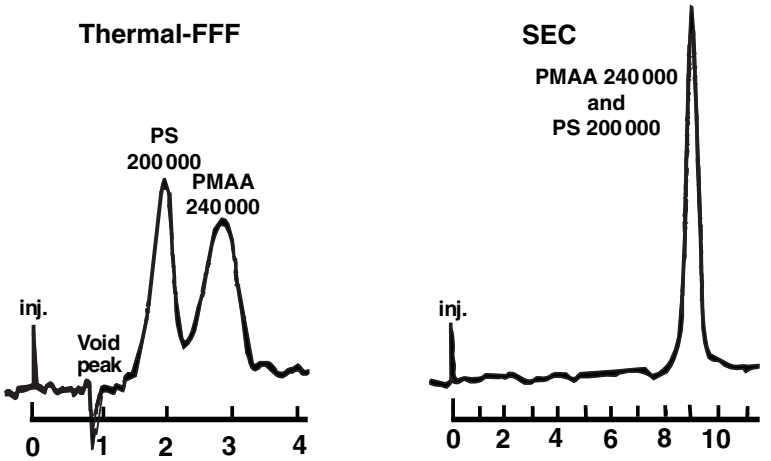

Fig. 10. Elution profiles of similarly sized polystyrene and poly(methyl methacrylate) polymers by Th-FFF and SEC illustrating the chemical selectivity of Th-FFF. Reproduced from [2] with kind permission of Pergamon Press

Th-FFF has been used successfully on many occasions to fractionate polymers with $M>10^6$ g/mol and in one case for $M>10^7$ g/mol [126].

One of the unique characteristics of Th-FFF is that retention depends not only on the molar mass but also on the chemical composition of the polymer. This "chemical" differentiation is due to the dependence of the underlining thermal diffusion process on polymer (and solvent) composition [84]. This effect can likely be used to determine compositional distributions in copolymers and blends [111]. Figure 10 compares the resolving power of Th-FFF and SEC on two polymers of similar molecular weight but varying chemical composition. The polymers coelute in SEC because their sizes are similar; whereas Th-FFF resolves the polymers because they differ in chemical composition.

1.5.2
Comparison of FFF (Th-FFF and Fl-FFF) with Other Analytical Techniques

The theoretical separation capabilities of Th-FFF have also been compared with those of capillary hydrodynamic fractionation (CHDF) [116]. Th-FFF was found theoretically to have the highest separation potential (also compared with SEC) and high selectivity which, however, is not fully accessible due to experimental restrictions. For CHDF, low selectivity but high efficiency as well as a very high analysis speed was predicted for samples with lower M but, experimentally, capillaries with very small tube diameters are not available in sufficient quality. In addition, such capillaries are very sensitive to clogging with minor amounts of impurities, e.g. dust. SEC was found to reach selectivities between Th-FFF and CHDF and had a high separation speed for lower molar masses $M<10^5$ g/mol.

S-FFF has been compared with analytical ultracentrifugation (AUC) with respect to the fractionation of a 10-component latex standard mixture with narrow particle size distribution, known diameters (67–1220 nm) and concentration [127]. With an analytical ultracentrifuge, the particle sizes as well as their quantities could be accurately determined in a single experiment whereas in S-FFF deviations from the ideal retention behavior were found for particles >500 nm resulting in smaller particle size determination in the normal as well as in the programmed operation. It was concluded that, without a modified retention equation which accounts for hydrodynamic lift forces and steric exclusion effects, S-FFF cannot successfully be used for the size characterization of samples in that size range.

Another comparison of AUC and FFF was reported for the Fl-FFF separation of native ferritin which exhibits a particle size distribution (monomer, dimer, trimer) as well as a density distribution due to non-uniform amounts of FeOOH in the core [128]. Such samples are notoriously difficult to characterize by sedimentation techniques like S-FFF and AUC because size and density distributions are superimposed whereas Fl-FFF was found to yield baseline resolved peaks for each of the oligomers due to the separation dependent only on diffusion coefficients.

Several authors [9,129–131] have to a certain extent compared S-FFF with hydrodynamic chromatography HC [129], disk centrifugation [9,129,130] and with some other non-separating methods such as transmission electron microscopy [9,130], light scattering [9], quasi-elastic light scattering [9,131], among others. Approximately 5–50 times higher resolution of S-FFF, in comparison with SEC or HC, was reported. In the majority of cases these authors concluded that the advantages of FFF were more important than the minor drawbacks.

1.6 Experimental Methodology

The setup of an FFF system and the experimental procedure are discussed in the following section.

1.6.1 *General Equipment for FFF*

The basic experimental equipment for FFF is, except for the channel and its support, in general identical to the equipment used for liquid chromatography. It is usually composed of a solvent reservoir, a pump, and an injection system; the chromatographic column is replaced by the FFF channel, followed by a detector. The FFF channel can require additional supporting devices, such as a centrifuge for sedimentation FFF or a power supply, and other electronic regulation devices for electrical FFF. If necessary, this basic equipment is complemented by a flow meter at the end of the separation system. For special semipreparative purposes, a fraction collector can be attached to the system.

In the following subsections, the different components of an FFF system apart from the FFF channel are given. A more detailed description is available elsewhere [27].

Solvent Reservoir. The requirements for the solvent reservoirs are similar to those in liquid chromatography. Regarding the applied solvent, the reservoirs must be manufactured of an inert material and must neither change the solvent properties nor react with the mixed solvent components. Filling and emptying the reservoir must be easy, as must be the solvent exchange and cleaning. It is necessary in some cases to keep the solvent under an inert gas to prevent dissolution of the air components in the solvent. Bubbling through with an inert gas, ultrasonic or vacuum treatment, or a combination of these methods can be used to degas the solvent as well as using a commercially available degasser.

Solvent Delivery System. Solvent delivery systems provide the flow rate of the carrier liquid through the whole separation system. Highly stable liquid flow rates free of pulsations, a broad range of adjustable flow rates, repeatability, and reproducibility of the adjusted flow rate are their most important parameters. A broad range of adjustable flow rates is important. The pumps must be corrosion resistant and inert to the solvents used. The channels for FFF have very low hydrodynamic resistance and, consequently, the solvent delivery systems should not rely on high pressure operation. Furthermore, it is very important that the flow rate is free of pulsation. The stability of the flow rate and, consequently, of the velocity profile inside the separation channel is the most important requirement for the validity of all the theoretical relationships for retention and dispersion and thus for the choice of the solvent delivery system.

Sample Injection. In principle, the samples can be injected in two ways: with a syringe through a septum, or through a multiport valve at the channel inlet. The septum material must be inert to the solvent, but usually cannot withstand more than 30 punctures before replacement is necessary. Furthermore, the septum variant of injection complicates the entire FFF operation and is rarely used anymore. Sample injection by multiport valves does not suffer from these complications.

Elution Volume Measurements. The majority of commercially available pumps provide a high constancy of flow rate and reproducibility of setting. In these cases, measurement of the retention times and knowledge of the flow rate in a given time interval make it possible to calculate the retention volumes and/or retention ratios directly from the retention times (see Eq. 7). Nevertheless, an independent flow rate or retention volume measurement at the end of the separation system is often useful. This applies especially for S-FFF, focusing S-FFF, and Fl-FFF. Small but fluctuating solvent leakage through the rotary passage sealing at the head of the separation system may occur in the first two cases, and the determination of the retention volume from the flow rate may cause serious errors.

Several commercially available devices can be employed at the outlet of the separation system. The use of an optical drop counter is advantageous if aqueous solvents are used as eluents. With respect to usually very low concentrations of separated substances in the eluate, the surface tension and the size of the droplets are usually not affected. A siphon equipped with a photo-optical sensor may also be used to measure the retention volume. If water is used as the eluent, there are problems with the drops adhering to the inner siphon surface.

Detectors. Most detectors for liquid chromatography can also be used in FFF systems. Refractive index detectors [132] are the most popular for soluble macromolecules. Designed as differential detectors, they measure differences in refractive indices of eluate relative to pure eluent, Δn_r. This difference is proportional to the solute concentration in the eluate through the refractive index increment dn_r/dc. The major problem associated with the use of a refractometer is the dependence of the refractive index on temperature and pressure, which can cause baseline drifts and fluctuations.

Photometric detectors focus on the interaction of light with the solute, e.g. absorption of light, fluorescence, optical rotation, or light scattering. A combination of these phenomena (e.g., both absorption and light scattering) may sometimes occur even for simple absorption optics. The notation "photometric detector" describes the fact that light intensity is always measured photometrically after passing through a measuring cell filled with the detected sample.

Absorption photometers operating in the ultraviolet (UV) or visible (VIS) range have gained the widest application. Detectors operating in the infrared (IR) range are also commercially available. The foregoing photometric detectors are designed to operate at one or more fixed wavelengths, or they may be equipped with a source of polychromatic light and a monochromator that makes it possible to vary the wavelength continuously.

Fluorescence detectors measure the intensity of the fluorescence of the eluate, stimulated either by monochromatic light or a laser. As most polymers and colloids do not exhibit fluorescence, applications of this detector have been very limited.

The final group of photometric detectors are instruments that measure the intensity of scattered light either from non-homogeneous dispersions (turbidimetric detectors, nephelometers) or from molecularly homogeneous systems (light scattering photometers). Depending on the ratio of the mean particle size to the wavelength of the scattered light, three basic regions of light scattering are distinguished: the region of Rayleigh scattering, where the particle diameter is substantially less than the wavelength of the applied light (approximately 20-fold); the region of Mie scattering, where the diameters of the scattering particles are roughly comparable with the wavelength of the light and; finally, the geometric region, where the particle diameter is significantly greater than the wavelength of the light. All these three regions of particle sizes are accessible by FFF so that a quantitative determination of a particle size distribution is very difficult at the limits of each domain. For the same reasons, the interpretation of the response of turbidimetric detectors is also not easy to evaluate.

A low-angle laser light scattering (LALLS) detector was developed for use in size exclusion chromatography [133] and has been used coupled with FFF [134]. The advantage of this detector is that it can, in combination with a concentration detector (refractometer, UV/VIS, or IR photometric detector), provide direct data on molar masses of the eluted sample.

In recent years, multiangle laser light scattering (MALLS) detectors have become highly popular in SEC and also in FFF (see, e.g. [135–140]), since they also determine molar masses and molecular dimensions on an absolute basis. Here, the scattered light is simultaneously detected at various angles so that an extrapolation to zero angle is possible. Such instruments are commercially available from several companies. As an important development, the FFF-MALLS combination is discussed in a separate chapter (see Sect. 4.1.2).

An interesting alternative to the use of the conventional laser-light-scattering detector are evaporative light scattering detectors [141], which are also commercially available. The eluent containing particles after FFF separation is sprayed, the solvent is vaporized, and the light scattering of the aerosol is measured.

A viscometric detector together with a concentration detector can provide information on molar masses of macromolecules emerging from the FFF system [76,134,142–144] using the Mark-Houwink-Kuhn-Sakurada coefficients. If these coefficients are not available, an intrinsic viscosity distribution can still be determined without calibration. Detailed features of this distribution are unique to a given polymer sample, and are not affected by changes in experimental conditions [145]. In fact, since the intrinsic viscosity distribution is more directly related to end-use properties, its measurement is preferred in certain applications.

Detectors capable of continuously measuring the density of the flowing liquid have been designed by Kratky et al. [146]. They are based on the measurement of frequency oscillations of a quartz tube through which the eluate flows. The oscillation frequency depends on the tube mass and, thus, for the given eluent, on the concentration and density of the solute. Their application to size exclusion chromatography has been described by Trathnigg and Jorde [147]. Kirkland applied such a detector for FFF [148].

Beckett described inductively coupled plasma mass spectrometry (ICP-MS) as an off-line detector for FFF which could be applied to collected fractions [149]. This detector is so sensitive that even trace elements can be detected making it very useful for the analysis of environmental samples where the particle size distribution can be determined together with the amount of different elements/pollutants, etc. in the various fractions. In case of copolymers, ICP-MS detection coupled to Th-FFF was suggested to yield the ratio of the different monomers as a function of the molar mass. In several works, the ICP-MS detector was coupled on-line to FFF [150,151]. This on-line coupling proved very useful for detecting changes in the chemical composition of mixtures, in the described case of the clay minerals kaolinite and illite as natural suspended colloidal matter.

In a recent paper, electrospray mass spectrometry was applied as a detection system for Fl-FFF [152]. This detector is especially useful for low molar mass

samples as the MALLS detector suffers from poor sensitivity at molar masses below 10^4 g/mol [153]. The method was tested with poly(styrene sulfonate) standards (M_w=1.4×10^3–4.6×10^4 g/mol) and poly(ethylene glycol) standards (M_w= 1.0×10^3–4.0×10^3 g/mol). For the polyelectrolyte samples, the high ionic strengths were a problem as matrix ion clusters and adducts formed a background in the mass spectra. However, this detector is complementary to the MALLS detector and also provides molar mass distributions on an absolute basis together with the diffusion coefficient distribution from the retention behavior. Another advantage is that in cases of mixtures of different polymers, the molecular weight distribution of each individual polymer can be obtained by their mass chromatograms.

Many other on-line detectors suitable for SEC columns as reviewed [154], including chemiluminescent nitrogen detection, dynamic surface tension detection, high frequency detection and Fourier transform infrared detection, can be applied to FFF; the latter being capable of delivering polymer compositions on-line.

There are also many possibilities for the off-line combination of FFF with various detectors, and virtually any analysis technique can be applied to the fractions as long as the sample quantity is sufficient. One useful combination is electron microscopy on fractions collected from an FFF channel [155]. Electrothermal atomic adsorption spectroscopy (EAAS) [156] has also been described.

1.6.2 *The FFF Experiment*

An FFF experiment involves several phases. In most FFF experiments, the carrier liquid flow is started and the cross-field is adjusted. The sample is then injected and a careful procedure of sample introduction and relaxation must be followed [28,97]. This procedure is illustrated in a schematical FFF fractogram (Fig. 11). One can see five basic phases of an FFF experiment. Special care must be taken to determine the time the sample spends in the tubing and connections outside the channel, t_{extra}, as this shifts the void peak as well as the sample peak towards longer retention times.

1.6.2.1 Relaxation

After the sample has entered the channel it relaxes into a steady-state concentration profile at the accumulation wall under the influence of the applied field (step 2 in Fig. 11). The carrier liquid flow is stopped just after the sample injection because otherwise it would experience the full range of flow velocities existing across the channel, in turn causing extensive band broadening. Although the flow can be stopped by simply turning off the pump, the pressure pulse associated with restarting the pump can result in severe baseline distortions. Therefore, it is better to interrupt the channel flow during sample relaxation, routing

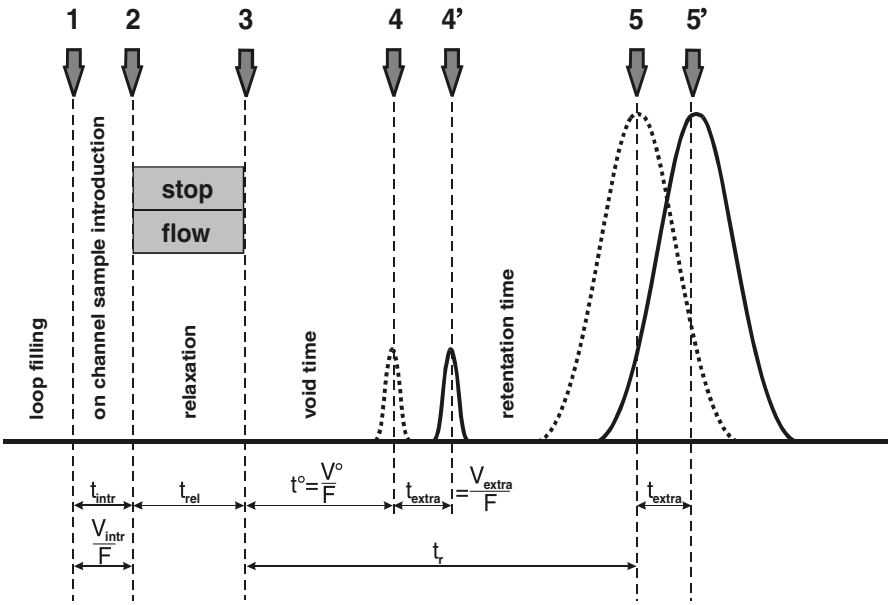

Fig. 11. Schematic FFF fractogram with the different phases of an FFF experiment. Reproduced from [157] with kind permission of Societá Chimica Italiana

flow around the channel with a pair of three-way valves and a pressure matching device.

As an alternative to stopping the flow, the sample can be rapidly compressed against the accumulation wall by flow rather than field-driven transport [48]. After compression, the sample zone quickly relaxes into its steady-state concentration profile without appreciable zone broadening. This method requires a special inlet configuration where either a splitter divides the channel thickness into two flow spaces near a pair of inlets located on opposite walls [158,159], or the carrier substream enters the channel through a frit imbedded in the wall opposite the accumulation wall [160]. The advantages and disadvantages of the two configurations for hydrodynamic relaxation have been summarized [160]. The most important advantage of the frit inlet is the gentle relaxation limiting sample adsorption on the membrane and decreased shear effects, but it requires careful sample introduction. While the flow splitter can be used in any FFF subtechnique, the frit inlet was designed for flow-FFF, where it is easily implemented into the existing design. Figure 12 shows the two methods for hydrodynamic relaxation.

1.6.2.2 Field Programming

If samples to be fractionated are very polydisperse, a high external field strength must be applied in order to separate the least retained macromolecules or par-

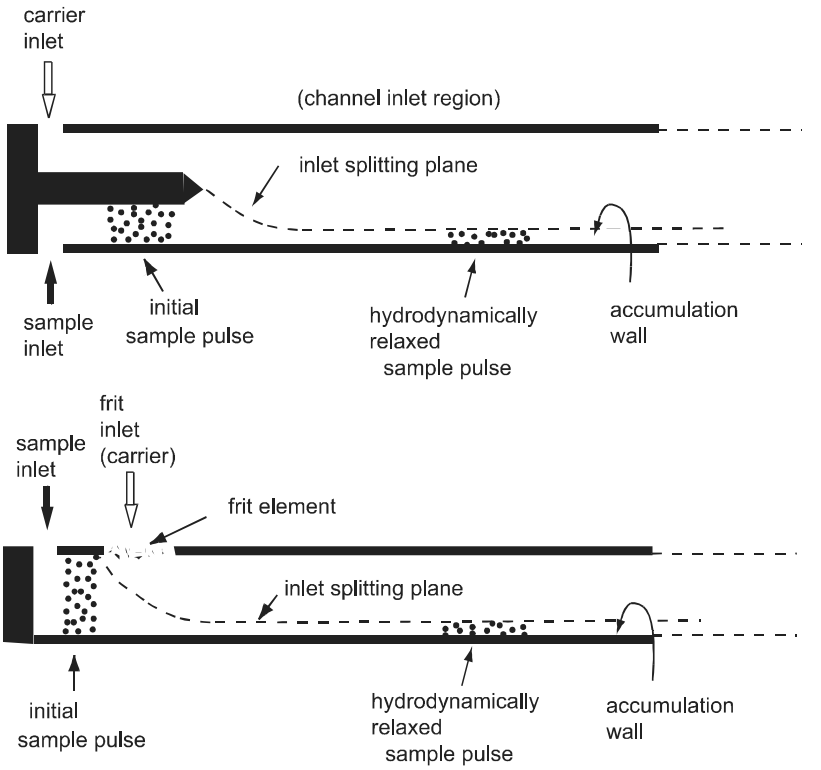

Fig. 12. Schematic illustration of hydrodynamic relaxation achieved in a split inlet system (*above*) and a frit inlet system (*below*). Reproduced from [160] with kind permission of the American Chemical Society

ticles [161]. As a result, well-retained species leave the fractionation channel after an excessively long period. This problem can be solved by gradually decreasing the intensity of the forces affecting the retained solute. In principle, there are two ways possible: decreasing the external field strength, or changing the solute property that is decisive for its retention [162]. For various FFF techniques the means for such variations can be deduced directly from equations for λ. However, other possibilities even exist which are not expressed explicitly by these equations but can be employed effectively.

Yang et al. [38] classify programming into two basic categories: uniform programming and solvent programming. Uniform programming means that some parameters (e.g. external field strength) are being changed equally and simultaneously throughout the channel. Changes in the physical field can be, for example, a change in the temperature gradient for Th-FFF, the speed of rotation or the density of the used carrier liquid for S-FFF, the electric field gradient for El-FFF, the ratio of longitudinal flow to cross-flow for Fl-FFF, the gradient of magnetic field strength for magnetic-FFF, and so on.

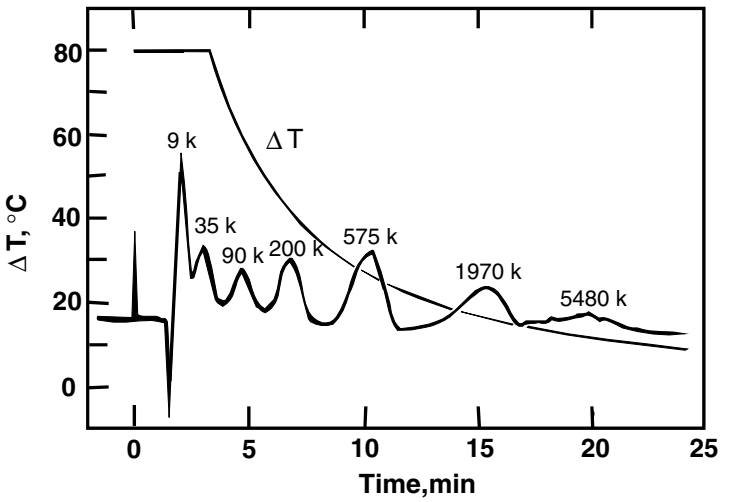

Fig. 13. Separation of seven polymers of indicated molar mass by power-programmed Th-FFF. Reproduced from [54] with kind permission of the American Chemical Society

In solvent programming the change is induced by the inflowing carrier liquid and continues gradually in time and distance from the beginning of the channel (e.g. the change in the carrier liquid density in sedimentation-FFF). The change in solute properties can be influenced by, for example, changing pH and thereby altering the diffusion coefficient and/or electrophoretic mobility in El-FFF.

Programming, however, not only complicates the evaluation of the experimental data [27,38,39] but, furthermore, secondary relaxation phenomena [91], solute-solute and solute-accumulation channel wall interactions occur at high field strength and, thus, high solute concentrations in the vicinity of the accumulation wall must also be considered. Thus whether to use programming or not is always a compromise between the speed versus precision of the measurement. Advantages and disadvantages of such programming procedures have been discussed by Giddings and Caldwell [163]. Experimental results [38,39,164–166] confirmed the utility of the programming in FFF, and good agreement of experimental retention with the theoretical values was found [89,167].

Several mathematical functions have been used for programming field decays in both thermal- [39,54,164,168] and flow-FFF [165]; these include linear [39,165], exponential [164,165,167,168], parabolic [39], and power [54,169] functions. The exponential decay function produces a linear calibration plot of log M versus retention time, that provides convenient and accurate calibrations over a wide molar mass range without the need for frequent recalibration [168]. The effects of operating parameters on the accuracy of the determined molar masses were investigated so that nomographs containing optimum operating conditions could be given on the basis of a preliminary separation [170]. The

power function can be used to maintain a fractionation power that is independent of molecular weight, which is desirable for the characterization of highly polydisperse samples. The power program developed by Williams [169] gives nearly constant fractionating power over the entire separation which is not provided by the other types of programs. Figure 13 illustrates the use of power programming to separate seven polymers ranging in molecular weight from 9.0×10^3 to 5.5×10^6 g/mol.

Kirkland et al. [6,167,171] dealt with the programming of S-FFF in an analysis of particle size distribution. They also used time-delayed exponential decay programming of the centrifugal force intensity, which allowed them to linearize the dependence of retention time to a logarithm of solute dimensions. Moreover, the total analysis time was shortened without sacrificing the resolution.

Flow-rate programming was elaborated theoretically and verified experimentally [40]. Slowing down the channel flow, field programming, and an increase in the field strength applied [172] have provided a higher resolution of particle separation by S-FFF within three orders of magnitude of masses in a single experiment.

1.6.2.3 Optimization of the FFF Experiment

Once an FFF measurement has been completed, it is useful to investigate the same sample under different experimental conditions (such as field strength, etc.). If the same distribution is obtained at markedly different retention times, one can exclude the presence of artifacts. Another approach is to compare the fractionation of a narrowly distributed sample with a sample whose size distribution is broader and that spans the entire size range of the narrower sample under identical fractionation conditions. This technique is described in the literature [173].

It has already been stated that a simple way to enhance the resolution of an FFF measurement is to reduce the channel thickness. This however can lead to other problems as the effects of surface irregularities are enhanced, due to the increase of the surface-to-volume ratio of the channel, and lead to increasing, unpredictable solute–wall interactions, etc. Furthermore, non-uniformities in the channel planarity will also be a problem with very small channel thicknesses, especially in Fl-FFF where the accumulation wall is a membrane. Another possibility for the reduction of $\overline{H}$ is to reduce the flow velocity of the carrier liquid <v> which, in turn, leads to longer retention times and slower separation. However, in Fl-FFF, one has the possibility to increase the flow rate with cost to resolution but simultaneously increase also the cross-flow rate. Nevertheless, this enhances sample absorption onto the membrane. The third possibility for the reduction of $\overline{H}$ is to increase the solute diffusion. This can be done by decreasing the solvent viscosity by increasing the temperature.

Another method for experiment optimization concerns the sample. Here, it is desirable to inject the sample with the lowest detectable concentration, as high

concentrations increase sample–sample interactions or overloading effects (see Sect. 4.2.1). Significant effort has been spent on concentrating the sample past FFF so that it is possible to operate at much lower sample concentrations (see, e.g. the frit outlet system, Sect. 4.3.3). It is also important to choose a suitable carrier liquid to prevent coagulation of particles or phase separation of polymers.

Thus the optimization of an FFF experiment depends greatly on the analytical demands. If a rapid separation is required, one would apply field programming with cost to resolution and precision of the measurement. For very precise measurements, on the other hand, one must consider long experimental times as well as repetitions of the experiment under partly significant differing conditions. Sometimes many problems have to be addressed before a suitable fractionation can be achieved. For a good description of such a method optimization process see [166].

2 FFF Techniques and Modes of Operation

The different FFF techniques all have their special applications and compliment each other in a favorable way. As well as discussing the various FFF methods, the typical application ranges of the most important FFF techniques are given in Table 2.

Table 2. Typical application ranges of various FFF techniques

FFF technique	Typical application range	Modes
S-FFF	Polymers $>10^6$ g/mol, and colloids or particles >30 nm, useful for particular matter and biological applications. Applicable to water and organic solvents. The only technique operating in all modes of FFF	Normal, steric, focusing, adhesion
Gr-FFF	Particles >1 μm. Applicable to water and organic solvents	Steric, adhesion
Th-FFF	Lipophilic synthetic polymers $>10^4$ g/mol. Very useful for large shear sensitive polymers or aggregates. Applicable to water and organic solvents	Normal, steric
Fl-FFF	Polymers, colloids and particles from 1000 g/mol or 1 nm to ≈50 μm. Most universal of all FFF techniques. Applicable to water and organic solvents	Normal, steric
El-FFF	Biopolymers and colloids from 40 nm to >1 μm. Applicable to water	Normal, steric

2.1 Sedimentation-FFF (S-FFF)

S-FFF is one of the oldest FFF techniques (see Fig. 1). It was designed in theory independently by both Giddings [1] and Berg et al. [30–32] and experimentally realized a few years later in the principal arrangement still used today [174]. Either gravitational or centrifugal forces act as the effective field.

The sedimentation force F acting on the solute particles or macromolecules is given by the relationship:

$$F = \frac{\pi d_H^3 G |\Delta\rho|}{6} \tag{33}$$

where G is the gravitational/centrifugal acceleration and $|\Delta\rho|$ the difference in the densities of the particles and the solvent used. Note that the sign of the density difference just determines the direction of movement in the field. A positive value means sedimentation whereas a negative value indicates flotation.

If Eq. (33) is combined with Eq. (6) a relationship is obtained for the retention parameter [174]:

$$\lambda = \frac{6kT}{\pi d_H^3 G w |\Delta\rho|} \tag{34}$$

Thus, colloidal particles can be separated (see Eqs. (33) and (34)) based on differences in m',d_H or $|\Delta\rho|$, with the separation adjustable by the spin rate of the rotor used to control $G=\omega^2 r$ where ω is the angular velocity and r is the distance from the axis of rotation.

Berg and Purcell [30] presented an elementary theoretical analysis of the fractionation of particles by using gravitational or centrifugal forces in the centrifuge. In their first experimental paper [32] they described the fractionation of polystyrene (PS) latex with particle sizes of 0.796 and 1.305 μm. Their experimental arrangement was quite simple, but the time of the analysis was very long (76 to 125 h). In a subsequent paper [31] the separation of R17 *E. coli* bacteriophage with a molar mass of 4×10^6 g/mol was described. The time of the analysis was substantially shorter in this case, approximately 4 to 12 h due to a higher centrifugal field.

Finally, Giddings et al. [174] described an S-FFF device in which the channel was coiled along the internal wall of the centrifuge basket (see Fig. 14A,B and also Fig. 15). The basic theoretical and experimental aspects of S-FFF were discussed and the fractionation of a series of monodisperse spherical polystyrene latexes was demonstrated [174]. The principle of a rotor for S-FFF capable of being applied at low centrifugal fields corresponding to speeds up to 6000 rpm is shown in Fig. 15 [175].

The channel itself, in which separation proceeds, is formed between two stainless steel polished strips that include a stainless steel spacer. The stainless

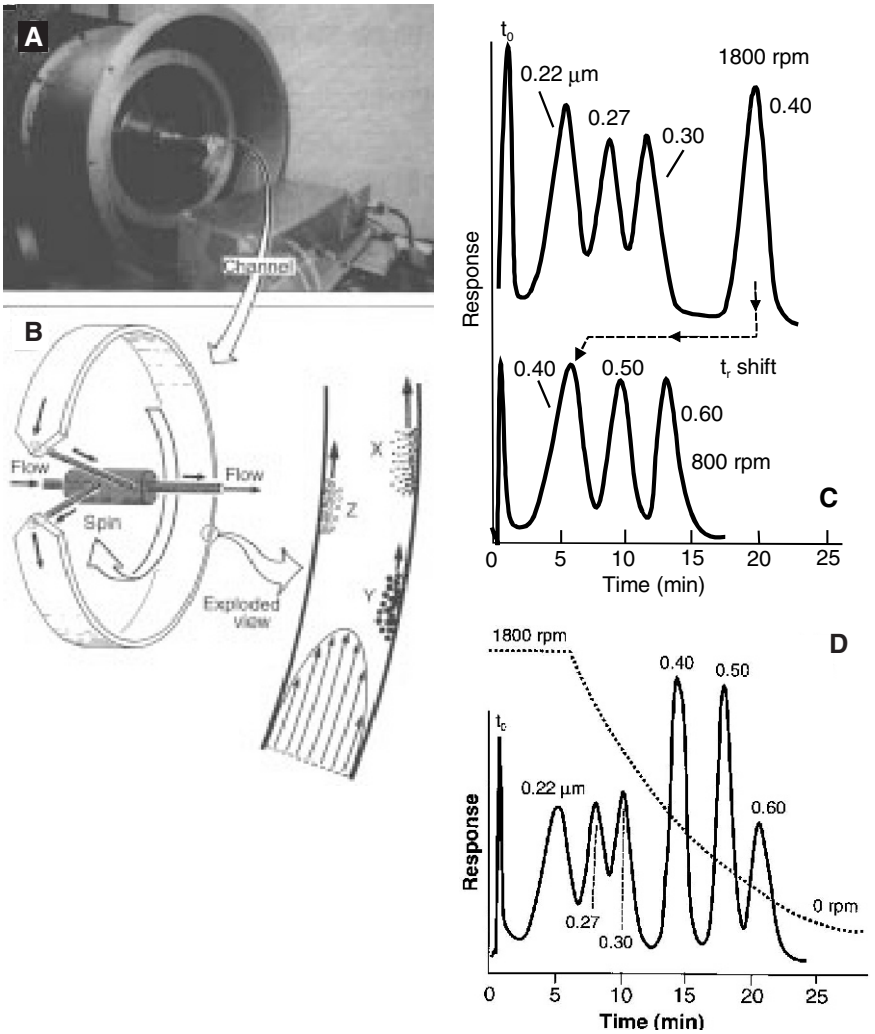

Fig. 14. S-FFF apparatus designed by Giddings' group (**A**) the separation principle with smaller particles (*X)*, bigger particles (*Y*) and floating particles (*Z*) with a density smaller than that of the solute [These particles are equally well separated as retention depends on $|\Delta\rho|$ (**B**)]. **C** Fractogram of a separation of polystyrene latexes of different sizes at two different rotational speeds. The ability to shift retention by changing the rotational speed is demonstrated. **D** The same mixture analyzed by a programmed field run demonstrating that a wider particle size range can be condensed into a reasonable elution span. Reproduced from [14] with kind permission of the American Association for the Advancement of Science

steel strips are coiled into a ring whose outer diameter adjoins closely the inner surface of the rotor basket. The strips are welded together, coiled into a ring and placed properly in the rotor basket. Inlet and outlet tubes are welded to the beginning and the end of this channel. An injection port with a septum is situated

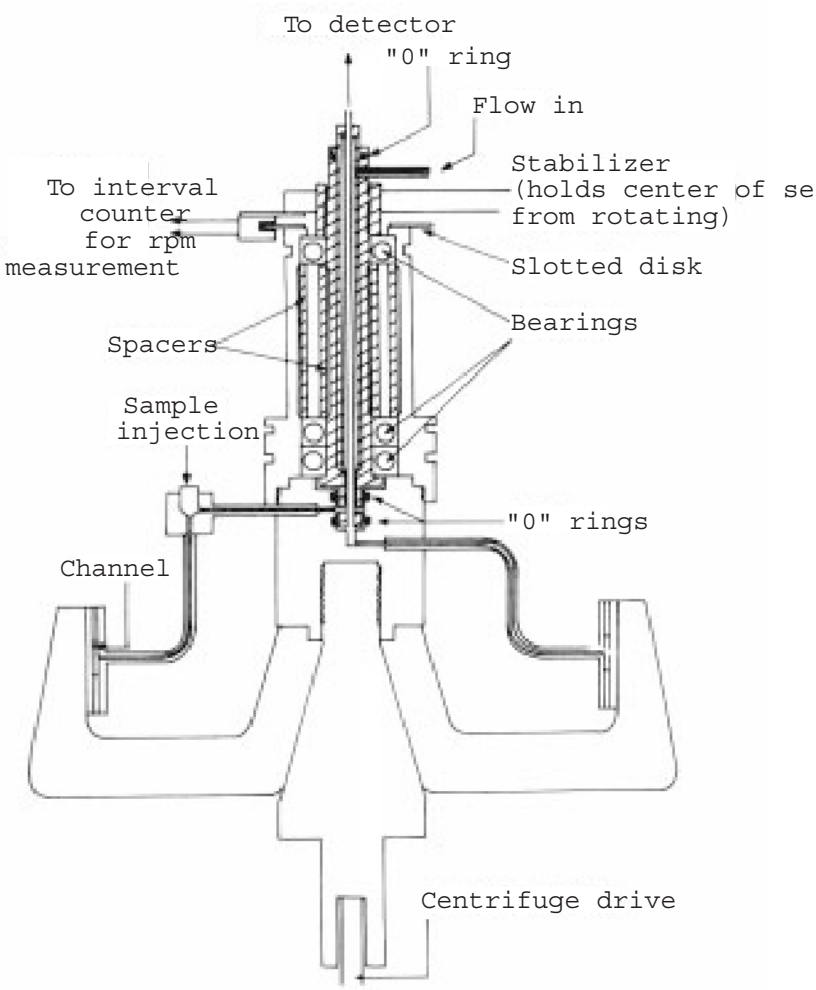

Fig. 15. Schematic representation of a rotor for S-FFF. Reproduced from [175] with permission of John Wiley and Sons

at the inlet tube. Both inlet and outlet tubes must be connected to a rotary passage. Solvent is introduced to the rotor and channeled into the detector by a system of two concentric tubes inside the rotary passage. The rotor is further equipped with an element permitting measurement of the rotation speed. The sealing rings and the whole rotary sealing unit, made of ethylene-propylene rubber, are a critical and troublesome part of the instrument. This rotor design allows injection of the sample only with the rotor at rest. The flow of liquid must then be stopped and the rotor set to the required rotation with the flow stopped

in the course of relaxation. Only then can the pump with an adjusted flow rate be put into operation and the separation performed. Prior to subsequent injection, the rotor must again be stopped. Common dimensions of the S-FFF channel are as follows: thickness, approximately 250 μm; width, about 20 mm; and length, approximately 500 mm. The radius of coiling is usually 80–100 mm.

Improvements in the rotor design by Kirkland et al. [6] using a split ring, which expands during rotation, thereby sealing the channel itself permitted an increase in centrifugal acceleration up to 20,000 rpm. Further improved channels for sedimentation-FFF made it possible to work up to 32,000 rpm which, at the given rotor dimensions, corresponded to an acceleration of about 100,000 gravitational units [176].

The separation of a mixture of different sized PS latex beads at two different spin rates is shown in Fig. 14C. As predicted (Eqs. 33 and 34), t_r increases with both d_H and G. The rough proportionality of t_r to the particle mass and thus to d^3_H explains why particles differing only slightly (down to 5 to 10%) in size can be well separated. In some respects, the size selectivity ($S_d \cong 3$) is too great. A fivefold size difference elutes over a t_r range of ~125-fold, making t_r excessively long for larger particle sizes. The long separation time is unacceptable. This problem can be circumvented by programming the decreasing field strength so that late-eluting particles hasten out of the channel [38] (Fig. 14D). The resolution is most uniform when G is reduced with time according to a special power program [169] but other types of field programming have also been successfully employed (see Sect. 1.6.2.2). When programming is used, Eqs. (11) and (34) are no longer valid as the retention behavior is complicated by the varying field. This is an important difference to analytical ultracentrifugation (AUC) which can also make use of field programming to fractionate particles in the size range of 30 nm to 10 μm in a single experiment (see, e.g. [177,178]). This ultracentrifuge technique is common laboratory practice today and the theory remains the same for the programmed field, in contrast to FFF, as the sedimentation coefficient is calculated on the basis of the run time integral $\int \omega^2 t$ which is continuously monitored by the ultracentrifuge.

Elution in S-FFF requires rotating seals which are troublesome at high spin rates and, therefore, S-FFF is difficult to apply to particles smaller than 10 to 30 nm in size (for usual density differences) and polymers $<10^6$ to 10^7 g/mol, i.e. for most linear polymers. Thus, S-FFF is more attractive for biological applications, large colloids and microparticles, and several applications have been described [179].

For new systems, the particle density ρ_s is often unknown. This uncertainty is resolved by measuring retention at two or more carrier liquid densities ρ [82] in analogy to corresponding procedures in AUC which yield particle size and density distributions [180,181]. Measurements made close to the point of neutral buoyancy yield ρ_s to four digits accuracy which is equivalent to the maximum accuracy of density gradient ultracentrifugation. Carrier densities far removed from neutral buoyancy provide ρ_s by extrapolation. This approach, used for viruses [182,183], can yield ρ_s without exposing fragile particles to highly modified dense media but at the cost of accuracy.

S-FFF can be advantageously used to characterize complex particulate objects. For example, for a superstructure the overall weight is $m'=\sum m'_I$, where m'_I is the effective mass of the component i. Examples for such composed systems include core-shell latexes and filled liposomes [184], where m'= m'(shell)+m'(core). If the carrier density is adjusted to make the core neutrally buoyant, m'(shell) and its distribution can be obtained from retention measurements. However, this is not a simple task, as physically attached solvent also contributes to the shell density. For liposomes, where the shell is a uniform phospholipid bilayer, m'(shell) gives a measure of the shell area A. On the other hand, if the shell is made neutrally buoyant, m'(core) can be measured. This can then be used to measure the loading of a substance like a drug in the liposome or to determine the core volume [184]. Such measurements are otherwise only possible with contrast variation scattering techniques such as neutron scattering using very expensive equipment. Nevertheless, care must be taken with any technique relying on variation of the solvent density as density variation of a solvent always requires the addition of either another solvent or a salt which in turn can lead to extensive conformation changes. The addition of the same solvent in the deuterated form, such as H_2O/D_2O, is feasible for such purposes.

If the change in m' is measured in two different solvents (see the note of caution above), the mass or thickness of adsorbed layers on particles can be determined [185,186]. Before adsorption, only the effective particle mass is determined. After adsorption, the measured gain $\Delta m'$ corresponds to the adsorbed layer. Eqs. (33) and (34) give for $\Delta m'$:

$$\Delta m' = \frac{6kT\Delta t_r}{Gwt_0} \tag{35}$$

The detectable amount of adsorbed species can be extremely low. A retention time shift of $\Delta t_r=0.3\ t_0$ at a modest G (10^3 g) with w=250 μm results in only ~10^{-17} g of adsorbed mass (density 1.4 g/cm^3). This mass corresponds to a very small layer, only ~0.6 Å thick on a 0.2 μm sphere [186]. The above approach has been used to measure protein adsorbed on latex surfaces [186–188], which is relevant to immunodiagnostic assays and biomedical implants. Complete adsorption isotherms can be measured [186] and antigen–antibody binding ratios determined [187].

When the diluted sample of solute is injected during rotation, it is concentrated at the beginning of the channel, due to the fact that the average volume flow rate of the retained solute is lower than the average flow rate of the injected solution. Hence diluted colloidal samples can be concentrated by sedimentation-FFF [189]. One can even operate such that the injection is run at a higher field force and, after the entire sample solution is injected, the field force is decreased to the required value.

The good agreement between theory and experiment in S-FFF was confirmed by experiments with standard samples [81]. Good agreement was also found for the determination of molar masses of different biopolymers [171] and sizes of

poly(vinyl chloride) latex fractions compared with those from electron microscopy [190]. The underlying theory of retention and dispersion in S-FFF was experimentally verified by measurements of polystyrene standard latexes in comparison with electron microscopy [191]. Differences in the sizes could be attributed to shrinkage of the latex in the electron beam of the microscope.

2.2 Gravitational-FFF (Gr-FFF)

Gr-FFF is based on the same principle as S-FFF. However, as the applied field is simply the Earth's gravitational field, it is clear the lower separable particle size is limited depending on the particle density. In fact, particles with sizes lower than 1 μm are usually not well retained so that, in Gr-FFF, particles usually elute only in the steric mode (see Fig. 6).

The channel for Gr-FFF has the simplest design of all FFF methods and is also the cheapest to make (material cost of ca. 20 US$). It can be formed by cutting the required shape of the channel into a cellulose acetate, Teflon or Mylar foil. The channel foil, equipped with inlet and outlet tubes, can be clamped between two plates of glass or Plexiglas with the aid of screws. Such a channel was described by Giddings et al. [175]. Dimensions should be chosen depending on the size of separated particles. The channel is usually 70–250 μm thick, 10–25 mm wide, and up to 2000 mm long. An example of the design of a channel of this type is shown in Fig. 16. The spacer is sandwiched between two mirror-finished

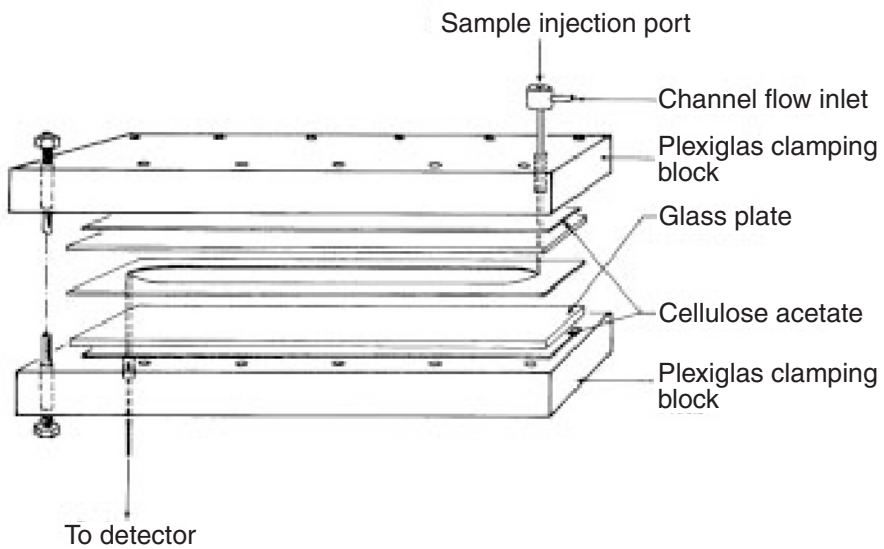

Fig. 16. Schematic representation of a channel for steric-FFF in the natural gravitational field. Reproduced from [175] with permission of John Wiley and Sons

plates made of either floating glass or polycarbonate. The foils between the glass or Plexiglas plates function as cushions that balance the pressure on the edges and in the center of the glass or Plexiglas plates. It is advisable to use rubber washers under the screws to distribute the local pressure and avoid cracking.

Giddings theoretically suggested a gravitational-FFF operating with a cyclical field by rotating the channel frequently 180° around its long axis [192]. This method however never gained importance.

2.3 Thermal-FFF (Th-FFF)

Like S-FFF, Th-FFF is one of the oldest FFF techniques [29,193]. Thompson described a basic experimental arrangement and a successful fractionation of polystyrene (PS) standards with narrow distribution of molar masses [29,193] followed by studies on some fundamental theoretical and experimental aspects of Th-FFF [34,194]. The theory of the retention of macromolecules in Th-FFF was advanced later [195]. The dependence of retention on the molar mass of polystyrene samples was proven experimentally [109,194], since D is a linear function of M of the form $D=A\times M^{-b}$. It was possible to find a linear dependence of λ values on $M^{-0.5}$ [194]. Analogous experimental results, confirming theoretical relationships for retention in Th-FFF, were also reported for other polymers [196,197]. In a critical review of polymer analysis by Th-FFF, Martin and Reynaud [197] specified the requirements for successful separation.

A channel for Th-FFF is relatively simple. It is usually composed of two metallic blocks (with high heat conductivity, preferably copper) with highly polished even surfaces between which a spacer is clamped. The actual dimensions of the metal block are usually 40–60 cm length, 3–6 cm width and a thickness of 2–3 cm. Electrolytic nickel and chromium plating increases the mechanical and corrosion resistance. In both blocks side holes are drilled into which thermistors, which serve for control and regulation of the temperature of both blocks and thus also of the temperature gradient between the two main channel walls, can be inserted.

One or both blocks are equipped with holes to which tubes are soldered for the solvent inlet, including sample injection and eluate outlet. Figure 17 illustrates the case in which inlet and outlet capillaries are placed in the upper heated block. It is, however, more advantageous to situate these capillaries in the lower cooled block for the reason that the lower wall is the accumulation wall of the channel so that the sample, after being injected, is transferred to the vicinity of this wall. In this way equilibration at the head of the channel is facilitated and the time required for primary relaxation is reduced. At the channel end, the solute is concentrated at the accumulation wall, and its exit is easier if the capillary is situated in this block so that the sample does not have to overcome the field strength.

The channel shape is properly cut into a spacer foil of low thermal conductive material which is inserted between the metal blocks. The material of the foil must be resistant to the solvents used within the range of operating tempera-

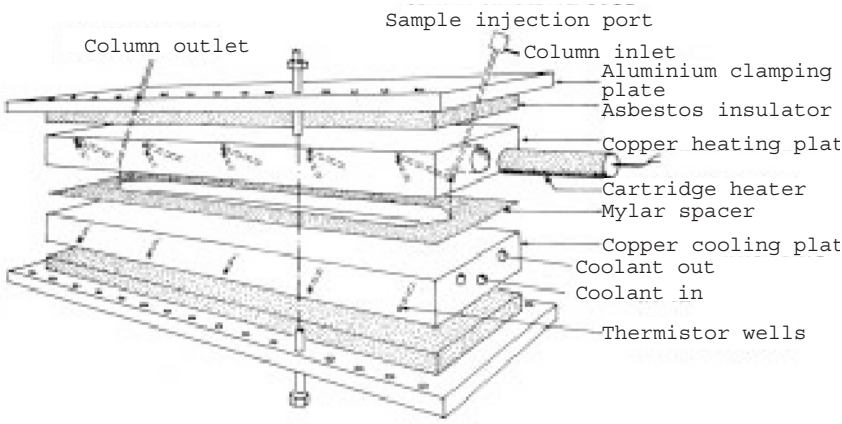

Fig. 17. Schematic representation of a Th-FFF channel. Reproduced from [175] with kind permission of John Wiley and Sons

tures, and the mechanical properties of the material must provide perfect sealing when the entire system is clamped. The channel is cut out of commercially available polymer foils made of engineering plastics (e.g., Mylar, Kevlar) which have proved best for these purposes. Channel shapes can be altered as required. In addition to the shape illustrated in Fig. 17, hairpin-shaped channels [198,199] with a higher channel length have been used. This geometry provides a more effective separation for the rather compact dimensions of the setup, but also restricts the experiment to lower loads.

This system of metal blocks and spacer is then layered between two heat-insulating plates of low-thermal-conductivity material and another two plates with high mechanical rigidity (e.g. of light aluminum alloy). The overall system is fixed with a system of torque-controlled screws, the balanced pressure providing channel sealing.

The applied field is a temperature gradient perpendicular to the solvent flow in a thin (≈100 μm) channel between a hot (upper) and cold (lower) metal block. The upper block is heated with electric cartridges; the lower one is cooled. A regulating transformer or controllable thyristor power supply can be used to feed the heating elements. Common thyristors combined with simple power supply regulators are sufficient to maintain the desired experimental parameters ΔT and T_c. The cold block temperature is kept constant by a circulating liquid with the aid of a thermostat with the same strength as the heating cartridges. This can lead to very high temperature gradients, exceeding 10,000 K/cm, as the temperature differences between the hot and the cold wall are up to 100 K in normal operation and even up to 150 K in extreme cases [200]. A typical Th-FFF channel is shown in Fig. 17.

From the theoretical viewpoint, Th-FFF is the most complicated of the FFF techniques suffering from numerous assumptions and approximations, al-

though the effective driving force $|F|$ per polymer molecule can be defined by a quite simple relationship:

$$|F| = kT\frac{D_T}{D}\frac{dT}{dx} \tag{36}$$

where D_T is the coefficient of thermal diffusion. Combining this equation with Eq. (6) yields a simple dependence of t_r on the molecular weight with $D \cong AM^{-b}$ ($b \approx 0.6$ for random coils):

$$\frac{t_r}{t_0} \cong (D_T / A)\Delta T M^b \tag{37}$$

in which ΔT has replaced $w \times dT/dx$.

However, such treatment neglects the numerous deviations from the assumed ideal behavior so that significant errors can occur. Therefore, possible deviations from ideal behavior, as well as the appropriate corrections, are treated below.

The movement of macromolecules in a temperature gradient is always in the direction from the hot to the cold region [43,197]. This movement is caused by thermal diffusion, exploited as the driving force in Th-FFF, and called the Soret effect, known already for over 50 years [201–203]. The transport (Eq. (1)) has to be extended by a term taking the thermal diffusion into account. Thus the flux density J_x can be expressed by [34,194]:

$$J_x = -D\left[\frac{dc}{dx} + c\left(\frac{\alpha}{T} + \gamma\right)\frac{dT}{dx}\right] \tag{38}$$

where γ is the thermal expansion coefficient and α the thermal diffusion factor $\alpha = (D_T/D)T$. The thermal diffusion factor α can be maximized through solvent adjustment, although a poor understanding of thermal diffusion limits the ability to predict this factor from polymer and solvent parameters. However, certain trends have been established. For example, thermal diffusion appears to increase with polymer density and the thermal conductivity difference of the polymer and carrier liquid [110]. Thermal diffusion also correlates inversely with the solvating power of the carrier liquid.

As already stated in Sect. 1.4.1, the resulting flux vanishes after the steady state has been established so that Eq. (38) can be rearranged:

$$\frac{1}{c}\frac{dc}{dx} = -\left(\frac{\alpha}{T} + \gamma\right)\frac{dT}{dx} \tag{39}$$

The bracketed term can be simplified, since the γ of liquids is usually in the range of $0.2–1.5 \times 10^{-3}$ and negligible compared to the values of α/T which can be up to 1000-fold [34]. The temperature dependence of the remaining terms $-(\alpha/T) \times (dT/dx)$ partially cancel each other out, since α/T decreases with in-

creasing temperature, whereas dT/dx increases [204,205]. The weak influence of temperature has been empirically explored for different conditions [109]. In the case of a weakly retained sample (R=0.5) in ethylbenzene using ΔT=100 K (T_c= 20 °C, with T_c=temperature of the cold wall), 85% of the solute molecules are distributed in temperature regions with ΔT=24.6 K which results in a difference of 17% in the $-(\alpha/T)\times(dT/dx)$ term. In the case of a strongly retained sample (R= 0.1) under the same conditions but with T_c=45 °C, 85% of the solute molecules are distributed in a range <1 K resulting in a difference in the $-(\alpha/T)\times(dT/dx)$ term of only 0.75%. Hence, $(\alpha/T)\times(dT/dx)$ can be considered as temperature independent for strongly retained samples ($R\leq 0.1$).

Equation (39) may be integrated:

$$c(x) = c_0 \exp\left(\frac{-x}{l}\right) \text{ with } \frac{1}{l} = \left(\frac{\alpha}{T} + \gamma\right)\frac{dT}{dx} \tag{40}$$

Applying the definition of the retention parameter λ (see Sect. 1.4.1), one can define the average concentration $\langle c(x)\rangle$ over the channel width as:

$$\langle c(x)\rangle = c_0\lambda(1-\exp(-1/\lambda)) \tag{41}$$

The average drift velocity of molecules in a region in the channel is determined by the magnitude of the temperature gradient at the distance l from the accumulation wall $(dT/dx)_{x=l}$. As l varies very slightly, only some microns even in the case of strong retention, the relevant temperature gradient for the separation is usually determined at the cold wall [206]. In the case of relatively small temperature gradients (ΔT<40 K), (dT/dx) can be approximated by $\Delta T/w$. With the above-discussed neglection of γ and inserting $\alpha=(D_T/D)T$, one obtains for λ:

$$\lambda = \left[\left(\frac{w \cdot D_T}{D}\right)\frac{dT}{dx}\right]^{-1} \approx \frac{D}{D_T \cdot \Delta T} \tag{42}$$

In Th-FFF the field strength is determined by the temperature difference ΔT between the channel walls. According to Eq. (42), the value of λ is a linear function of $1/\Delta T$. This fact was verified experimentally for a wide range of ΔT values for polystyrene samples of various molar masses [109,194]. It also follows from Eq. (42) that if the channel thickness w changes and ΔT remains constant, retention will not change, since the temperature gradient dT/dx will change accordingly. Furthermore, the ratio of D/D_T, the Soret coefficient, is important for the separation in Th-FFF. Janca and Klepárník [199] discussed the interchange of Th-FFF and the Soret effect (thermal diffusion) [207] and the possibility of fractionating polyelectrolytes [208].

Equation (42) shows that Th-FFF can be used to measure thermal diffusion coefficients [209] by plotting, for example, the elution volume vs. 1/D for a set of narrow standards with known D. However, only a few polymer/solvent combinations have been evaluated this way. Recently, Beckett has shown that excellent

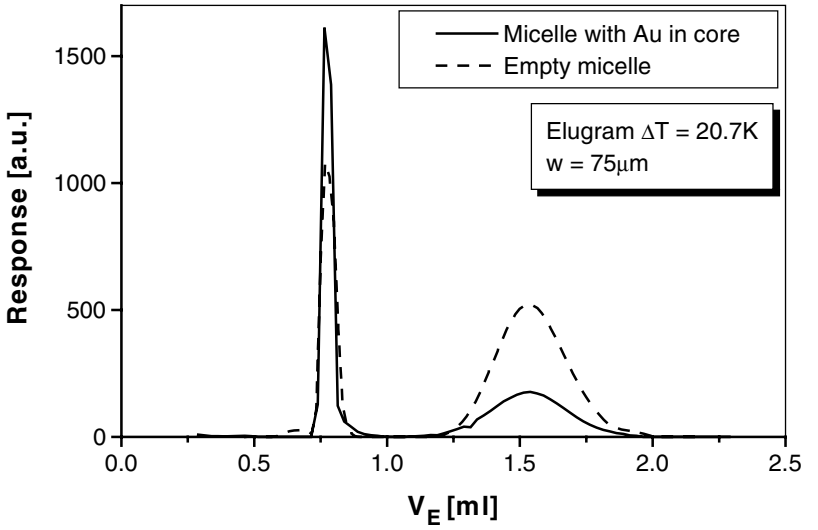

Fig. 18. Th-FFF measurements of polystyrene-poly-4-vinylpyridine (PS_{123}-b-$P4VP_{118}$) micelles in toluene [216]. The core consists of poly(4-vinylpyridine) which can be used as a nanoreactor for Au synthesis to generate a significantly different D_T of the core. However, the detected D_T is that of polystyrene

calibration curves can be obtained using four well-characterized (in terms of M_w) broad standards [210–212].

Experimental evidence was obtained showing that D_T itself may be temperature dependent [109]. Another method to determine D_T is the measurement of thermodiffusion in polymer solutions by "forced Rayleigh" light scattering [213]. This technique has the advantage that the employed temperature gradients are very small so that the coefficients are determined close to thermal equilibrium.

For polymers, D_T is found to be virtually independent of chain length and chain branching, but it is strongly dependent on polymer and solvent composition [84]. For random copolymers, D_T varies linearly with monomer composition; block copolymers display more complex behavior [111,214]. For segregated block copolymers like micelles, D_T seems to be determined by the monomers located in the outer region (see Fig. 18). For particles, D_T appears to be both composition and size dependent [215].

The two factors (D and D_T) controlling polymer retention are strictly orthogonal: D depends only on the size and geometry, whereas D_T depends on chemical composition. Th-FFF has been used mainly to discriminate between chain length differences (reflected in D) within polymer families, yielding molecular weight distributions (MWDs) [15,168]. The promise of compositional differentiation and measurement based on D_T has been little exploited but certainly has future potential as illustrated by the example in Fig. 10.

Complications in the theoretical description of retention in Th-FFF arise from deviation from isoviscous flow due to the temperature gradient resulting in a non-parabolic flow profile [194,217]. An exact analysis of the flow profile of a non-isothermal and thus non-isoviscous flow was published by Westerman-Clark [218]. The consequences of a temperature gradient on the form of the flow profile as well as on retention and peak broadening have been published by Gunderson et. al. [205].

A further source of complications is the assumption of solvent incompressibility, which is a severe simplification for any organic solvent. Using this simplification, Westerman-Clark defined the flow of an incompressible Newtonian fluid between two parallel plates in dependence of the distance from the accumulation wall x as [218]:

$$\frac{d}{dx}\left(\eta\frac{dv(x)}{dx}\right)=-\frac{\Delta p}{L} \tag{43}$$

where $\Delta p/L$ is the pressure drop over the channel length L. This equation can be solved when it is assumed that the flow velocities at both walls are zero ($v(o)=v(w)=0$) resulting in an expression for the flow velocity profile which is much more complicated than the general expression for v(x) in Eq. (9) in Sect. 1.4.1:

$$v(x)=-\frac{\Delta p}{L}\left[\int_0^x\frac{x}{\eta(x)}dx-\frac{\int_0^w\frac{x}{\eta(x)}dx}{\int_0^w\frac{1}{\eta(x)}dx}\int_0^x\frac{1}{\eta(x)}dx\right] \tag{44}$$

Considering the applied high temperature gradients of up to 10000 K/cm, the proper calculation of v(x) very much depends on the proper description of the temperature dependence of the viscosity $\eta(x,T)$. This dependence can be described by a virial expansion of the form:

$$\frac{1}{\eta}=a_0+a_1T+a_2T^2+a_3T^3 \tag{45}$$

The temperature coefficients a_x are solvent-specific thus complicating a universal description of flow properties in a Th-FFF channel.

The temperature gradient across the channel is only in a first approximation a linear function of x, because dT/dx is a function of the thermal conductivity κ which again depends on the temperature:

$$\kappa=\kappa_c+\frac{d\kappa}{dT}\left(T-T_c\right) \tag{46}$$

Equation (45) describes the situation at a defined T and T_c where κ_c is the thermal conductivity at T_c. If $d\kappa/dT$ is taken as constant in the applied ΔT, the

temperature profile across the channel can be described as a complicated function of x [205]:

$$T(x) = T_c + \frac{-1 + \sqrt{1 + \frac{2x}{w}\frac{1}{\kappa_c}\frac{d\kappa}{dT}\Delta T + \frac{x\Delta T^2}{w}\left(\frac{1}{\kappa_c}\frac{d\kappa}{dT}\right)^2}}{\frac{1}{\kappa_c}\frac{d\kappa}{dT}} \tag{47}$$

It is very difficult to determine $\eta(x)$ by substituting Eq. (47) into Eq. (45). Expansion into Taylor series simplifies further calculations and differs by only 0.25% from the exact solution [109]:

$$T(x) = T_c + x\left(\frac{dT}{dx}\right)_c + \frac{x^2}{2!}\left(\frac{d^2T}{dx^2}\right)_c + \frac{x^3}{3!}\left(\frac{d^3T}{dx^3}\right)_c + \ldots\ldots \tag{48}$$

Finally, using Eqs. (44), (45) and (48) yields the flow profile in the channel of Th-FFF:

$$v(x) = -\frac{\Delta p}{L}\sum_{i=1}^{5} h_i \left(\frac{x}{w}\right)^i \tag{49}$$

where h_i is a calculated polynomial coefficient. The average flow velocity $<v(x)>$ is:

$$< v(x) >= -\frac{\Delta p}{L}\sum_{i=1}^{5} h_i \frac{h_i}{(i+1)} \tag{50}$$

Now, the retention ratio R can be calculated using Eqs. (40), (41), (49) and (50) according to the general equation in Sect. 1.4.1, Eq. (7):

$$R = \frac{1}{\sum_{i=1}^{5} h_i \frac{h_i}{(i+1)}}\left\{\frac{1}{\left(1-\exp(-1/\lambda)\right)}\left[\sum_{i=1}^{5} h_i \sum_{j=1}^{i-1}\frac{i!}{(i-j)!}\lambda^j\right] + \sum_{i=1}^{5} i! h_i \lambda^i\right\} \tag{51}$$

For very high retention ($R \rightarrow 0$), the limiting value of Eq. (51) becomes:

$$R = \frac{\lambda}{\sum_{i=1}^{5} \frac{h_i / h_1}{(i+1)}} \tag{52}$$

The retention, which is determined via Eqs. (51) and (52), is larger than the value which would result from the corresponding simplified treatment in Sect. 1.4.1 using a parabolic flow profile which is explained by the reduced flow velocity near the cold wall. Exact velocity profiles in Th-FFF were numerically

computed for several solvents and ΔT-values increasing the accuracy of the retention prediction by two orders of magnitude compared to the parabolic flow profile [219].

Th-FFF can be applied to almost all kinds of synthetic polymers, like polystyrene, polyolefins, polybutadiene, poly(methyl methacrylate), polyisoprene, polysulfone, polycarbonate, nitrocelluloses and even block copolymers [114,194,220]. For some polymers like polyolefins, with a small thermal diffusion coefficient, high temperature Th-FFF has to be applied [221]. Similarly, hydrophilic polymers in water are rarely characterized by Th-FFF, due to the lack of a significant thermal diffusion (exceptions so far: poly(ethylene oxide), poly(vinyl pyrrolidone) and poly(styrene sulfonate)) [222]. Thus Th-FFF has evolved as a technique for separating synthetic polymers in organic solvents [194]. More recently, both aqueous and non-aqueous particle suspensions, along with mixtures of polymers and particles, have been shown to be separable [215].

Th-FFF, like S-FFF, is an FFF technique which takes significant advantage of field programming [164]. As already discussed, field programming is especially advantageous for solutes with a very broad molar mass distribution beginning with high ΔT for small solutes continuously decreasing to low ΔT for the high molecular polymers. Usually, significant separation problems occur for polymers with $M<10^4$ g/mol [200]. These restrictions were partially circumvented by the use of a pressurized system operating at elevated temperatures. This provided an effective fractionation of low molar mass PS [200]. The potential of this technique was shown for the fractionation of polymers with an extremely wide range of molar masses, from 4×10^3 to 7×10^6 g/mol in a single experiment [39]. A big advantage of Th-FFF is that ultrahigh molecular mass polymers can be separated in the absence of shear degradation. Velocity gradients are expected to be an order of magnitude less than those in SEC, and extentional shear is virtually absent. The ability of Th-FFF to maintain the integrity of the polymer has been clearly demonstrated by reinjecting well-retained fractions of a polymer standard having a molecular weight of 20.6×10^6 g/mol [126]. Miniaturization of the channel for Th-FFF and some other design modifications made it possible to reduce the time of analysis to several minutes and even down to several tens of seconds [118], and to increase the resolution [198].

Subsequent studies were oriented towards an explanation of the factors that cause and affect zone spreading in Th-FFF [223] as well as the determination of the precise polydispersity of polymer samples [224] by measuring at various carrier solvent velocities and extrapolating to zero velocity. Improved separation can be obtained by using a thermogravitational effect, that is, by using thermal convection in a non-horizontal channel [43]. The resulting velocity profile formed under such conditions has a more complicated non-parabolic shape [43]. Martin and Hes [134] demonstrated the advantage of coupling the Th-FFF channel with low-angle laser light scattering for the analysis of polymers.

To summarize, Th-FFF is especially well suited for the precise analysis of very high molecular weight macromolecules, macromolecular assemblies or species subject to shear degradation [125], copolymers, polymers prone to surface interaction,

polymers needing corrosive solvents, high-temperature polymer solutions, and narrow polymer samples requiring an accurate determination of polydispersity.

2.4 Flow-FFF (Fl-FFF)

Fl-FFF is the most universally applicable FFF technique as the separation only relies on differences in the diffusion coefficients. Thus, it nicely complements S-FFF or Th-FFF with respect to size distribution analysis [225]. Fl-FFF is capable of separating almost all particles (up to ≈50 μm [226] or even much larger) and colloids and polymers down to ≈2 nm [17] or 10^3 g/mol [227]. The lower limit is determined by the pore size of the membrane material. The need for such membrane covering the accumulation wall is the principle disadvantage of Fl-FFF due to possible interactions with the solute and the danger of a membrane-induced non-uniformity in the channel thickness, especially since thinner channels are highly favored for faster separations. However, the advantages of Fl-FFF usually more than balance the potential pitfalls and sources of error. Consequently, Fl-FFF is the FFF technique which has been developed the most in recent years in instrumentation [48] and has found the most widespread distribution.

Fl-FFF is flexible in channel design and each of the different existing variants has its merits. A secondary cross-flow of the solvent, perpendicular to the flow of the solvent in the channel, creates the external field [41,228–230] while the channel design is flexible. The channel can be set up either by two permeable walls (S-Fl-FFF), only one permeable wall (A-Fl-FFF) [231–233], or in a hollow fiber which may serve as the channel [234]. For S-Fl-FFF, the setup for the channel flow and cross-flow is simple and straightforward [41,228] so that thinner channels can be used leading to a faster separation and a distinct fractionation in the steric hyperlayer mode. A-Fl-FFF on the other hand has the advantage of a simpler construction of the fractionation channel itself and the possibility to focus the sample prior to elution to minimize zone broadening complications. A third Fl-FFF arrangement, of elution though a hollow ultrafiltration fiber, has been demonstrated [234–239] but this technique will not be discussed in detail here as the system properties depend almost exclusively on the characteristics of the hollow fiber and thus any improvement in this system relies on the availability of high quality hollow fibers.

2.4.1 *Symmetrical Flow-FFF (S-Fl-FFF)*

The design of a S-Fl-FFF channel is shown in Fig. 19. Both cross- and longitudinal-flows are provided by separate pumps. To provide the required ratio of cross- and longitudinal-flow rates, the exits of cross- and longitudinal-flows are equipped with metering valves. The metering valve on the longitudinal-flow exit should be placed after the detector in order to prevent higher extra-channel zone broadening.

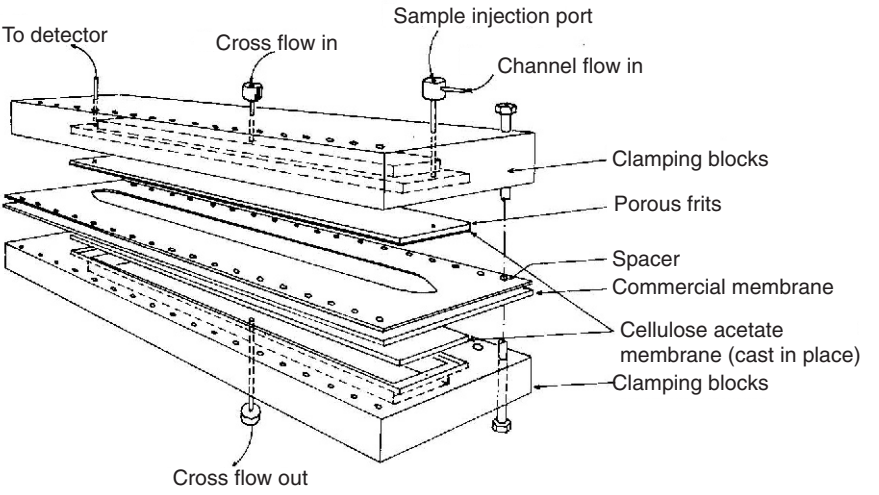

Fig. 19. Schematic presentation of an S-Fl-FFF channel. Reproduced from [175] with kind permission of John Wiley and Sons

Lee and Lightfoot [229] developed the theoretical basis of Fl-FFF. This theory has been confirmed by numerous works on the fractionation of model systems, including monodisperse spherical polystyrene latexes and a number of proteins [41,228,229,240], some polydextrans [229], viruses [241], and other spherical particles and macromolecules [242,243].

The driving force $|F|$ in Fl-FFF is the viscous force exerted on a particle by the cross-flow stream. Application of Stokes law gives for $|F|$ [17]:

$$|F| = fU = 3\pi\eta U d_H \tag{53}$$

where d_H is the hydrodynamic diameter of the particle, η the viscosity of the carrier liquid, and U is the velocity of the cross-flow stream. The quantity U is related to the experimentally accessible flow rate $\dot{V}_c$ of the cross-flow stream by [41]:

$$U = \frac{\dot{V}_c}{bL} \tag{54}$$

where b is the breadth and L the length of the channel. The substitution of Eqs. (53) and (54) into Eq. (6) shows that λ is inversely proportional to d_H:

$$\lambda = \frac{kTbL}{3\pi\eta\dot{V}_c w}\frac{1}{d_H} \tag{55}$$

Flow-FFF provides the best resolution and speed when $\lambda << 1$ which is achieved by a high $\dot{V}_c$ so that validity of Eq. (13) can be assumed under usual Fl-FFF operating conditions [41,244]. When Eq. (55) is substituted into Eq. (13), the retention time t_r is found to be directly proportional to d_H:

$$t_r = \frac{\pi\eta t_0 \dot{V}_c w d_H}{2kTbL} \tag{56}$$

The void time t_0 is by definition equal to the void or channel volume, V_0=bLw, divided by the channel flow rate V, which leads to:

$$t_r = \frac{\pi\eta w^2}{2kT}\frac{\dot{V}_c}{V}d_H \text{ or } \lambda = \frac{2kTV}{\pi\eta\dot{V}_c w^2 d_H} \tag{57}$$

This expression relates the experimental quantity t_r directly to d_H provided that all other parameters are known. Alternate expressions can be obtained relating t_r to the friction coefficient f or to D through use of the Stokes–Einstein equation D=kT/f giving:

$$t_r = \frac{w^2}{6kT}\frac{\dot{V}_c}{V}f \text{ or } \lambda = \frac{6kTbL}{w\dot{V}_c f} \tag{58}$$

and

$$t_r = \frac{w^2}{6D}\frac{\dot{V}_c}{V} \text{ or } \lambda = \frac{6bLD}{w\dot{V}_c} \tag{59}$$

The above equations are applicable when the two flow rates are held constant throughout the run. In some cases it is desirable to program $\dot{V}_c$ in order to expand the range of applicability [165,233]. This programmed field technique, however, complicates the above derived equations and results obtained in a way that is beyond the scope of this review; the interested reader is referred to the original literature here.

The first part of Eq. (11), respectively Eq. (13), yields that the product $t_r R$ is proportional to t_0. Using this and employing Eq. (56) to get t_r, the resolution expression is obtained:

$$R_s = \frac{\pi}{8}\left(\frac{3}{2}\frac{\dot{V}_c^3}{V}\right)^{1/2}\frac{\eta w^2}{kTV_0}\Delta d_H \tag{60}$$

where Δd_H is the difference in hydrodynamic diameters between the two species being fractionated. Equation (60) shows that the resolution R_s can be enhanced by increasing the cross-flow rate $\dot{V}_c$ or decreasing the channel flow rate V. As $\dot{V}_c$ affects R_s to the 3/2 power, it is, like the decrease in w, a major parameter for the optimization of R_s. However, the resulting gain in resolution is in turn achieved by longer run times. This is confirmed by Eq. (57) which shows that t_r has a similar dependence on $\dot{V}_c$ and V as R_s does.

Several modifications to the Fl-FFF method have been developed to enhance operation. Shortly after the introduction of Fl-FFF, the effect of relaxation on the retention and resolution was studied [245]. A substantial improvement in the

fractionation of viruses was achieved using the stop-flow technique [245]. A further improvement was the introduction of the outlet stream splitter which enables the sample stream near the accumulation wall to be led to the detector and thus enhance the concentration of the detected material for a better detector response [165,246]. This outlet stream splitter can, in principle, be applied to the other FFF techniques as well. Frit inlet Fl-FFF [52] allows the system to reach the steady-state more quickly thus eliminating the necessity for the stop-flow step [49]. This is achieved by utilizing a very high cross-flow in the first centimeter as the sample enters the channel to force the sample close to the accumulation wall. Furthermore, if a frit is applied as a channel outlet (frit outlet Fl-FFF) eluted samples can be concentrated by approximately five times which is a clear advantage if detector sensitivity is a problem. An extremely useful combination for a number of analyses has been frit outlet Fl-FFF and MALLS.

If the channel for Fl-FFF is utilized such that cross-flow is due to a solvent of different composition that has the solvent flowing in an axial direction, continuous separation of high-molar-mass components from low-molar-mass contaminants, migrating through the accumulation membrane, can be achieved. The ratio of cross-flow rate to axial-flow rate must be suitably adjusted. The function of a continuous Fl-FFF channel as a dialysis or ultrafiltration cell was described theoretically and demonstrated in practice for the separation of bovine serum albumin from low-molar-mass methylene blue [247].

2.4.2
Asymmetrical Flow-FFF (A-Fl-FFF)

Asymmetrical flow-FFFA (A-Fl-FFF) was introduced by Wahlund and Giddings in 1987 [47]. The same system was independently suggested slightly earlier by Granger et al. [237,248], but their application of the technique suffered from a lack of a primary relaxation step preceding separation [47]. A-Fl-FFF is notable for a channel which has only one permeable wall so that the solvent can leave the channel only via the accumulation wall and thus generates a cross-flow. The permeable wall is usually a sintered metal plate or ceramic frit covered by an ultrafiltration membrane (see Fig. 20).

The channels are initially of the same rectangular geometry as the symmetrical variant and the breadth remains constant along the channel length. The continuous loss of carrier fluid through the membrane as it flows down the channel leads to a gradual fall in volumetric flow rate between the inlet and outlet leading to a gradient in the mean channel flow velocity in channels with constant breadth. This variation of flow velocity must be taken into account in the determination of sample component properties from observed elution times, but poses no great difficulty. There is also an unavoidable gradient in the cross-flow velocity across the channel thickness, but this gradient is negligible for strongly retained material [47]. To compensate for these undesired effects, a trapezoidal channel [249] was introduced, and is almost exclusively applied now. In a recent paper, Williams proposed a theoretical channel which exponentially decreases

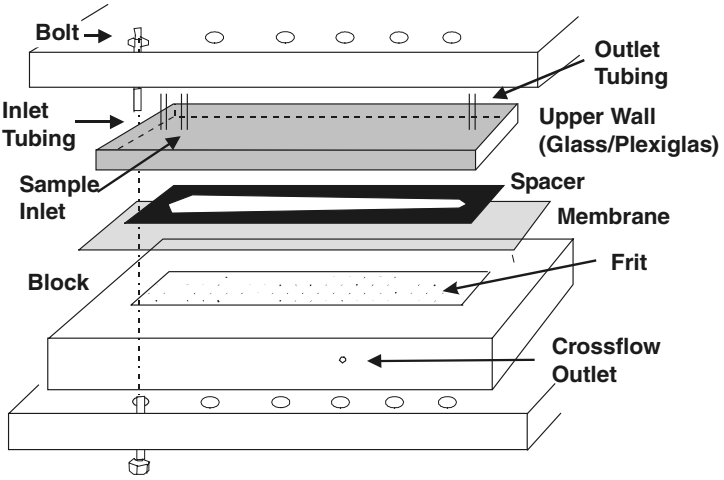

Fig. 20. Schematical presentation of an A-Fl-FFF channel

in breath along its length so that a constant flow velocity can be achieved throughout the channel length under certain flow conditions [250].

Due to the differences in the cross-flow generation compared with S-Fl-FFF, and the possibility of sample focusing, the experimental methodology differs from that applied for most other FFF techniques (stop-flow for sample relaxation). Thus, a short description of an A-Fl-FFF experiment as well as the whole experimental setup is necessary to understand its merits.

The A-Fl-FFF experiment is based on three different phases: (1) relaxation/focusing; (2) elution, and (3) backflushing. During the first phase, the flow is directed to enter the channel from the inlet and the outlet only exiting through the membrane. At a certain position in the channel determined by the counteracting flows, termed the focusing point, the axial velocity will be zero. The focusing point is made visible by a colored substance, e.g. bromophenol blue, which is injected into the channel during the relaxation/focusing mode. A sample, which is injected during this phase, is focused at this point, the exponential profile of the concentration distribution being established. Some samples can show altered retention behavior at different focusing times due to a pronounced interaction tendency with either themselves or with the ultrafiltration membrane [251,252]. After determination of the focusing point, the channel thickness needs to be calibrated using a protein with a well-known diffusion coefficient [253].

The next phase is the elution phase, where the flow enters the channel from the inlet end and exits, both through the membrane (cross-flow) and through the channel outlet end (outlet flow). The balance between the cross-flow rate $\dot{V}_c$ and the outlet flowrate $\dot{V}_{out}$ according to Eq. (69) can be adjusted by needle valves. V_{out} is measured by a flowmeter, the value of $\dot{V}_c$ is either measured directly by a

second flowmeter or simply calculated from the known V_{in} and V_{out} according to $\dot{V}_c = \dot{V}_{in} - \dot{V}_{out}$. Accurate knowledge of $\dot{V}_{out}$ is necessary. The elution phase is followed then by the third phase, backflushing, the flow entering the channel from the outlet end and flushing retained materials out of the channel [253].

A specific advantage of the asymmetrical channel design in A-Fl-FFF is the possibility to focus the sample into a very sharp band prior to separation resulting in higher separation resolution and improved accuracy of particle size measurements. Further advantages are that the construction of A-Fl-FFF channels is technically simple compared with S-Fl-FFF; the effects of heterogeneity and uneven permeability of the upper frit and unevenness of its surface are eliminated; and the glass/PMMA wall allows visual observation of the migration of suitable samples. The ability to observe the flow pattern of an injected dye aids in troubleshooting non-uniform flows that can occur with membranes that become uneven with deterioration or poor installation. Later, it was pointed out [249] that A-Fl-FFF channels also have an advantage in terms of reduced dilution of sample components during elution. Early studies indicate greater efficiency of the A-Fl-FFF channels compared to S-Fl-FFF [231,232], possibly because of irregular cross-flow in early S-Fl-FFF channels associated with an non-homogeneous upper frit. However, with good frits now available for S-Fl-FFF, there is no difference between these two geometries concerning the regularity of the cross-flow.

Drawbacks of the asymmetrical design associated with the non-uniform flow velocities are being reduced with innovative channel designs and continued theoretical development [249]. Due to the different generation of the cross-flow, the theoretical description of the flows acting in A-Fl-FFF and thus the whole retention theory is more difficult. Instead of the simple Eq. (54) for S-Fl-FFF, the following relationship is obtained for the cross-flow velocity U in the x-direction:

$$U = -|u_0|\left(1 - \frac{3x^2}{w^2} + \frac{2x^3}{w^3}\right) \tag{61}$$

where $|u_0|$ is the cross-flow velocity at the accumulation wall. Assuming a constant cross-flow, the average flow velocity in the z-direction $\langle v \rangle$ can be expressed by:

$$\langle v \rangle = \langle v \rangle_0 - \frac{|u_0|}{w} z \tag{62}$$

where $\langle v \rangle_0$ is the flow velocity at the channel inlet.

In a trapezoidal channel, the expression is more complicated.

$$\langle v \rangle = \frac{\dot{V}_{in} - |u_0| A(z)}{w b(z)} \tag{63}$$

where A(z) is the area of the accumulation wall from the inlet up to z and b(z) the width of the channel at z:

$$b(z) = b_0 - \frac{z(b_0 - b_L)}{L} \tag{64}$$

where b_0 and b_L are the channel widths at 0 and L. A(z) is given by:

$$A(z) = \int_0^z b(z)d(z) = b_0 z - \frac{z^2\left(b_0 - b_L\right)}{2L} \tag{65}$$

Combining Eqs. (63) and (65), the average flow velocity can be calculated by:

$$< v >= \frac{\dot{V}_{in} - |u_0|\left(b_0 z - \frac{z^2\left(b_0 - b_L\right)}{2L}\right)}{w\left(b_0 - \left(b_0 - b_L\right)\frac{z}{L}\right)} \tag{66}$$

The concentration profile in the x-direction c(x) can be obtained by combining Eqs. (1) and (61) and integration (see Eq. 2):

$$c(x) = c_0 \exp\left(\frac{-|u_0|x}{D}\left[1 - \frac{x^2}{w^2} + \frac{x^3}{2w^3}\right]\right) \tag{67}$$

To calculate the retention ratio R, one needs to know the void time t_0 (See Eq. (7)) which for an asymmetrical channel is given by [249]:

$$t_0 = \frac{V_0}{\dot{V}_c} \ln\left(1 + \frac{\dot{V}_c}{\dot{V}_{Out}}\left[1 - \frac{w\left(b_0 z' - \frac{b_0 - b_L}{2L} z'^2 - y\right)}{V}\right]\right) \tag{68}$$

where z' is the distance from the inlet to the focusing point, $\dot{V}_c$ and $\dot{V}_{out}$ the cross-flow, respectively, outlet flow rate, V_0 is the void volume and y the area excluded by the tapered inlet end. Using Eq. (65), Eq. (68) simplifies to:

$$t_0 = \frac{V_0}{\dot{V}_c} \ln\left(1 + \frac{\dot{V}_c}{\dot{V}_{Out}}\left[1 - \frac{A(z') - y}{A_{tot}}\right]\right) \tag{69}$$

where A(z') is the area from the inlet to the focusing point and A_{tot} is the area of the accumulation wall. For asymmetrical channels, the retention parameter λ is given by:

$$\lambda = \frac{DV_0}{\dot{V}_c w^2} \tag{70}$$

λ can be related to R by the simple approximation R=6λ (see also Sect. 1.4.1). The error is usually ≤5% for λ for sufficiently high retention (t_r/t_0)≥5.3 [47,254]. In the latter reference, a more detailed consideration of the relative errors caused by the approximation R=6λ is given for different levels of retention.

If R=6λ is assumed, Eq. (70) can be expressed as:

$$t_r = \frac{t_0 \dot{V}_c w^2}{6DV_0} \tag{71}$$

which shows that the diffusion coefficient can be determined directly and in an absolute fashion by measurement of t_r in A-Fl-FFF. Combining Eq. (70) with the Stokes–Einstein relationship and assuming R=6λ gives the relation of t_r to the hydrodynamic diameter d_H:

$$d_H = \frac{2kTV_0}{\pi\eta \dot{V}_c w^2 t_0} t_r \tag{72}$$

2.5 Electrical-FFF (El-FFF)

Electrical field-flow fractionation belongs to the most sophisticated experimental techniques of FFF although the schematical setup looks quite simple (see Fig. 21). However, the electrical fields are difficult to implement in practice and extensive problems, discussed below, can occur. Therefore, relatively few papers on El-FFF exist even though the first publication appeared as early as 1972 [35], and the high intensity and manipulability (such as through pH changes) of electrical forces principally promise a high potential of El-FFF [35,255].

The experimental setup is shown in Fig. 21. Two PMMA blocks with chambers that enable buffer solution to flow through are the main parts of the channel. The channel walls consisting of semipermeable flexible membranes of wet regenerated cellulose permit the passage of small ions and separate the channel volume from the electrode compartments in the blocks [175]. This layered setup is necessary because the applied high voltages needed to achieve highly selective separations even of small proteins and nucleic acids lead to the electrolysis of solutes and solvent. Placing the electrodes outside the channel ensures the generated gas bubbles do not perturb the desired flow profile The two membranes

are separated by the spacer foil, into which the channel is cut. Channel dimensions, as well as solvent transport, is similar to Fl-FFF. The entire channel is clamped together by a system of screws. Circulation of the buffer electrolyte prevents an accumulation of electrolysis products in both chambers. A channel designed in this manner has a very low electrical resistance but is very sensitive to even slight fluctuations of the flow inside, resulting in deflection of membranes leading to deformation of the channel shape and volume changes. A channel with walls composed of membranes of cellulose acetate cast on the surface of plastic frits is more mechanically resistant [256] but suffers from increased electrical resistance.

Recently, an improved channel design has been described, which makes use of solid electrodes as channel walls instead of the former applied membrane system [257–259]. The applied voltages are also much lower and beneath the electrolysis limit (ca. 1–2 V across the channel). Although such a setup was expected to generate fields of sufficient strength to separate colloidal particles, the inevitable electrode polarization limits the working field in the channel to a small fraction of the nominal field. The exact magnitude of the field responsible for retention in El-FFF must therefore be determined by calibration.

A third channel design has been reported [37,229,260–262] where the channel is composed of a circular semipermeable tube, and the electrical field is applied perpendicularly to the central axis of the channel. As with the corresponding circular Fl-FFF channel, such a system relies on the availability of suitable hollow fiber material.

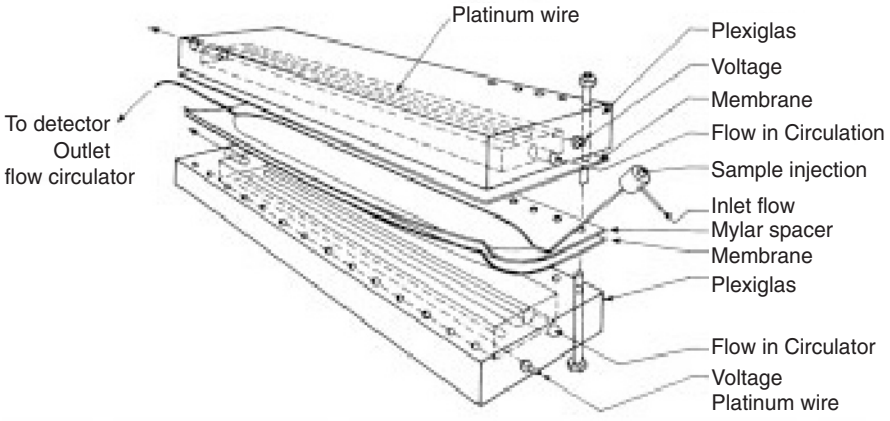

Fig. 21. Schematic representation of an El-FFF System. Reproduced from [175] with kind permission of John Wiley and Sons

El-FFF uses an electrical field E across the channel as the driving force for the particle separation. As the drift velocity U of a macromolecule with electrophoretic mobility μ_e is defined by:

$$U=\mu_e E \tag{73}$$

the force F acting on the sample according to Eq. (4) is $F=f\mu_e E$, finally leading to the expression for λ [36]:

$$\lambda = \frac{D}{\mu_e E w} \tag{74}$$

Kesner et al. [36] indicated a discrepancy between the theoretical retention and experimental values for some proteins in a channel with flexible membrane walls. These deviations were probably caused by the flexible membrane walls as such effects were not observed for a channel with rigid walls [256]. Nevertheless, the experimental data of Kesner et al. [36] was in reasonable agreement with the El-FFF theory [87,263] with respect to both retention and dispersion. Deviations were attributed to an electrical field gradient in the vicinity of the membrane interface [263]. Calculation of the dependence of λ on 1/E from literature data on electrophoretic mobilities and diffusion coefficients confirmed the validity of the retention theory in El-FFF.

For particles, the electrophoretic mobility μ_e is related to their surface charge density, which is best expressed in terms of the ζ-potential. For moderately charged particles (ζ-potential $<\pm 25$ mV), this relationship is given by Eq. (75), where the function $f(\kappa_D d_H)$ varies smoothly between 1.0 and 1.5 as κ_D varies between very small and very large values [264]:

$$\mu_e=\zeta(2\varepsilon/3\eta)f(\kappa_D d_H) \tag{75}$$

Here, κ_D is the inverse of the Debye length. Even though the ζ-potentials for latex spheres may exceed ± 25 mV and, therefore, require a more complex equation to relate to mobility (as per O'Brien and White [265]), the low ionic strength (small κ_D) of El-FFF measurements should still ensure a proportionality between μ_e and ζ. From the retention data, it is possible to obtain quantitative information regarding either the ζ-potential of samples with known particle size eluting from the channel or the particle size, if the electrophoretic mobility is known.

Despite the potential advantages that El-FFF offers, there are a number of serious drawbacks and limitations which restrict its use. First, the processes involved in the separation are much more complex than is assumed in the theory of El-FFF as pointed out by studies of the influence of experimental parameters on the retention of proteins [260,266–268], underlining the importance of solvent parameters and solute–solute interactions.

In two papers, Palkar and Schure studied the mechanism of electrical field-flow fractionation in detail [269,270]. An electrical circuit of the channel was

presented, discussing potential problems including voltage drops in the channel as well as their sources and suggesting an explanation as to why the electrical field in the channel differs from the calculated field. It was pointed out that it is of crucial importance to understand the internal electrical field in El-FFF which depends on the electrode material and electrode geometry, as well as the carrier liquid composition and even flow rate. In the second paper, the effect of the sample conductivity on the retention was studied, which results in a very strong concentration dependence of the retention, even at very low solute concentrations. Due to the conductivity differences between the sample and the carrier liquid, the electrical field in the channel is locally dependent. All these problems are true also for the newer El-FFF channel designs [257–259] such that El-FFF still has definite limitations.

2.6 Other Experimentally Tested FFF Techniques

The FFF techniques described in this section are already more or less specialities developed or suitable only for a limited amount of samples. Some of them have only been used a few times and are yet only poorly understood. However, they are presented here because they may be the technique of choice for special applications.

2.6.1 *Magnetic-FFF*

Magnetic-FFF is the obvious choice for ferromagnetic particles. In addition, it was theoretically proposed that various dia- and paramagnetic biological samples could also be separated by magnetic-FFF though requiring long separation times [271,272].

In magnetic-FFF, a magnetic field supplies the force for the separation of the sample:

$$F = \frac{M\chi_m H_m dH_m}{dx} \tag{76}$$

where χ_m is the molar magnetic susceptibility, H_m the intensity of the magnetic field, and ΔH_m the gradient of the intensity of the magnetic field dH_m/dx. If Eqs. (76) and (6) are combined, one obtains for λ:

$$\lambda = \frac{RT}{Mw\chi_m H_m \Delta H_m} \tag{77}$$

One possible magnetic-FFF channel arrangement is the classical FFF setup of a channel clamped between two glass plates [273]. The channel is then placed in the center of an electromagnet with a maximal magnetic field of approx. 300 to

450 G. The second arrangement was described by Vickrey and Garcia-Ramirez [45] who used a Teflon capillary of 1.5 mm diameter and 3040 mm length for separation. The capillary was coiled (coil diameter 5.6 cm) around an electromagnet (400 G).

Magnetic-FFF has been studied in only a few works [45,273,274] dealing with the separation and retention of BSA in the presence of Ni(II) ions and retention of metal oxides. The comparison of experimental retentions with the theoretical model indicated [45] that in addition to the effect of the magnetic field on the macromolecules, other yet unknown parameters seem to be present. Furthermore, the investigation of metal oxide particles in magnetic-FFF indicated that the slow velocity of relaxation processes probably influences the quality of the separation [273]. Even the surface nature of particles plays a role in retention [274]. In summary, magnetic-FFF remains an immature technique.

2.6.2 *Dielectrophoresis-FFF (DEP-FFF)*

Separation is not only obtained by a homogeneous electrical field (as applied in El-FFF) but the field can also be of an nonhomogeneous nature, leading to dielectrophoresis (DEP). Dielectrophoresis is the movement of particles in non-uniform electrical fields [275,276]. Here, the separation force F_{dep} is the result of the interaction between the dipole induced in the particle by the field and the field gradient over the particle. DEP is observed for charged and uncharged particles as well as in AC or DC electrical fields. The magnitude of the DEP force F_{dep} is described by:

$$F_{dep} = 0.25\pi\varepsilon_0\varepsilon_m d_H^3 \left(\frac{\sigma_p^* - \sigma_m^*}{\sigma_p^* + 2\sigma_m^*} \right) \nabla E^2(\text{rms}) \tag{78}$$

in which ε_0 is the permittivity of free space (8.854×10^{-12} F m^{-1}), ε_m the relative permittivity of the suspending medium, d_H the (hydrodynamic) diameter of the particle, σ^*_p and σ^*_m the complex conductivity of the particle and the medium, and ∇E the field gradient.

The combination of dielectrophoresis with field-flow fractionation (DEP-FFF) is potentially a very gentle and selective method for the separation of cells and other large particles. A large number of different designs of DEP channels has been used and proposed for the separation of particles [104,275,276]. However, the most successful designs [276–281] employ the typical FFF channel geometry containing large arrays of microelectrodes so that relatively small voltages can be used to generate the high field gradients needed to induce DEP. Microelectrodes not only simplify the equipment needed to generate the electrical fields, but also reduce secondary effects such as heating.

The solute particles are held at the accumulation wall by a DEP force which depends on the dielectric properties of the particles and the surrounding medium, the frequency and magnitude of the electrical field, and the electrode geometry. DEP-FFF is an unconventional FFF technique in that the DEP force is inherently non-uniformly distributed over the channel, not only in the plane of the electrodes/channel wall, but also across the channel above the electrodes [282]. Since solute particles themselves are a source of local field non-uniformities, mutual attraction occurs due to DEP forces between the particles which in extreme cases can lead to what is called pearl-chain formation. As a consequence, DEP-FFF can be considerably disturbed by interparticular interactions [57].

Most dielectrophoretic separations of cells to date have used steric-DEP-FFF. The cells are usually effectively immobilized in potential energy minima [282] near the electrodes by a combination of gravity and electrical field forces. Afterwards, the applied hydrodynamic flow forces transport those particles that are held less strongly at the electrodes.

Hyperlayer-DEP-FFF has the advantage of making better use of the parabolic velocity profile of the fluid since flow at different heights in the channel is exploited; as in steric-DEP-FFF the particles essentially stay in the layer near the channel wall. In addition, the hyperlayer mode minimizes the adhesion of the particles to the channel wall, which also suppresses the aggregation of cells into pearl-chains.

2.6.3 *Pressure-FFF*

Pressure-FFF is similar to Fl-FFF. In fact, some of the channel designs described for Fl-FFF can also be used for pressure-FFF. The difference between the two techniques is that in Fl-FFF, the flow field is applied externally, whereas in pressure-FFF the lateral flow across the channel wall(s) is initiated by an internal pressure drop in a liquid pumped along the channel with semipermeable walls on two sides of a hollow fiber membrane. Pressure-FFF has the advantage of increased solute concentration relative to Fl-FFF because of solvent leakage through the semipermeable walls during elution. In the case of the S-Fl-FFF channel, the cross-flow through both walls is oriented outwards from the channel and the membranes are sufficiently fixed on a porous, mechanically rigid support by the pressure so that the channel dimensions are well defined. Adjustment of the ratio of the transverse and longitudinal flows is also simplified analogous to A-Fl-FFF. The combination of a single pump and a metering valve on the cross-flow exit is already sufficient to operate a S-Fl-FFF channel for pressure-FFF. The arrangement of pressure-FFF with a hollow fiber serving as membrane is also straightforward [37]. To the exit of the circular tube, a metering valve is connected so that the required portion of the solvent passes through the capillary wall.

Although pressure-FFF was described as early as 1974, extensive examination was performed much later [234]. In the first work on pressure-FFF, the ba-

sic theoretical model of the separation in circular semipermeable tubes was developed, and blue dextran and human plasma were fractionated [37]. Later, the theory of pressure-FFF was improved on the basis of the general dispersion theory for a circular tube [283] and the description of the pressurized flow in a circular tube or a rectangular channel [44]. However, some complications arising from the transport phenomena in a pressure-FFF channel have yet to be solved.

2.6.4
Three-Dimensional Fl-FFF (Helical-Fl-FFF)

Helical-Fl-FFF belongs to a set of multidimensional FFF techniques where separating forces and flows operate in three dimensions. The separation occurs in the annular space between two rotating concentric circular cylinders ("Taylor-Couette device"). The inner cylinder is fixed, while the outer rotates at a constant angular velocity (Fig. 22A). A pressure gradient drives the carrier flow along the axis of rotation to elute for detection, so that a helical flow is generated. The helical flow multiplies migration differences in a radial direction for a large separation (Fig. 22B). It has recently been suggested theoretically that the separation mechanism could be refined further by applying a radial field, for example, a thermal, electrical or sedimentation field or other driving force used in normal FFF [284]. During a helical-Fl-FFF separation the solutes travel simultaneously in the direction of the outer cylinder which is the accumulation wall with linearly increasing azimuthal velocity by virtue of the applied field, and along the cylinder axis with the carrier liquid. As soon as the solutes have passed the region of the maximum axial flow velocity, their velocity in the axial flow di-

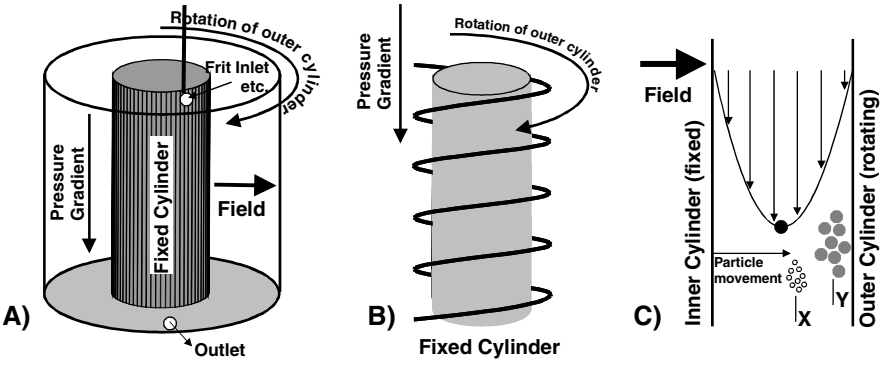

Fig. 22. Schematic presentation of a helical-Fl-FFF device (**A**), the generation of a helical flow in the annular space between a fixed and a constantly rotating cylinder (**B**) and the separation mechanism (**C**). The larger particles *Y* migrate faster towards the outer cylinder and are thus located in regions with lower axial velocity than the slower migrating ones

rection will decrease, although their azimuthal velocity increases. This has the consequence that the solutes which interact less with the field are located in the region of higher axial flow velocities as in classical FFF and thus elute first (Fig. 22C).

The two advantages of helical-Fl-FFF are (1) the amplification of the separation compared to a parallel plane FFF arrangement with concurrent improved resolution, and (2) that the fractionator body is smaller. Experimental verification of the helical-Fl-FFF concept was attempted using an electrical field across the concentric cylinders [285].

2.6.5 *Acoustic-FFF*

Acoustic-FFF was proposed and experimentally verified by preliminary measurements by Semyonov and Maslow applying a standing acoustic wave field as external force [286]. The particles can be pressed against the wall or be focused within the channel depending on the sign of the adiabatic compressibility difference between sample and solvent. The difference between the sample adiabatic compressibilities or alternatively the particle size can be determined from this FFF technique.

2.6.6 *Photophoretic-FFF*

Recently, Kononenko et al. proposed particle photophoresis (particle movement under the action of light) as a suitable field for FFF [287,288] as already suggested by Giddings in 1988 [77]. Initial experiments with carbon black showed that the elution curve changed when light was applied. These results indicate some potential for the practical introduction of photophoretic-FFF to the family of FFF techniques.

2.7 Theoretically Proposed FFF Techniques

In theory, almost any kind of physical effect may lead to a separation of a sample, and is thus suitable as the driving force in FFF. Therefore, the list of FFF techniques in this chapter is by no means complete. Here, then, are a few examples of FFF techniques provided which have been theoretically proposed but not yet demonstrated due to experimental difficulties, if not impossibilities.

2.7.1 *Concentration-FFF*

The separation force in concentration-FFF is a chemical potential field established by a concentration gradient of a mixed solvent across the channel in order

to induce effective chemical forces [42]. This technique is very difficult to realize experimentally.

The solute concentration distribution across the channel is determined by the chemical potential gradient caused by the varying solvent composition. For the chemical potential gradient dμ*/dx, the value of λ is determined by

$$\lambda = \frac{RT}{\Delta\mu_c^*} = \frac{1}{\ln c_0 / c_w} \tag{79}$$

where $\Delta\mu^* = (d\mu^*/dx)w$ is the total increment of the chemical potential across the channel and c_0 and c_w the concentrations near both walls (0 and w), respectively. The $\alpha_c = c_0/c_w$ required for an effective separation was calculated to exceed at least 10 to 100 which means the establishment of very large concentration gradients across the channel.

Substituting Eq. (79) into Eq. (11) yields the retention ratio [27]:

$$R = \frac{6}{\ln\alpha_c}\left(\frac{\alpha_c + 1}{\alpha_c - 1} - \frac{2}{\ln\alpha_c}\right) \tag{80}$$

Hence, it should be possible to measure differences in the chemical potential for the solute. The proposed channel for concentration-FFF is placed between two semipermeable membranes like in S-Fl-FFF permitting lateral flux of the binary solvent components. The reservoirs of the mixed solvent at various concentrations of active components are in contact with these membranes from opposite sides so that the solute should concentrate at the wall, displaying the minimum chemical potential.

2.7.2 *Shear-FFF*

Shear-FFF utilizes shear forces to drive a separation [46]. Such shear can be induced in the annular space between two concentric cylinders that are in relative rotational motion. This technique is in parts similar to helical-Fl-FFF (see Sect. 2.6.4) and is intended for the separation of large macromolecules and globular particles. The fluid flow in the axial direction is superposed over the angular flow caused by relative rotation [46] such that the shear flow generated causes the inward migration of solute macromolecules and particles. Two limiting cases differing in the freedom of fluid flow through random coil macromolecules were considered theoretically with several simplifications. The scope and limitations of shear-FFF have been discussed by Giddings [46].

2.8 Steric-FFF

Unlike the preceding FFF techniques, steric-FFF invokes a new mechanism but not a new field. Steric-FFF is a mechanism applicable to larger particles (~0.5 to 200 μm) and can be applied with any FFF technique provided that the acting forces are high enough to force the particles against the accumulation wall. The mechanism of steric-FFF has already been discussed in Sect. 1.2. In contrast to the normal mode, in steric-FFF larger particles elute first. An advantage of steric-FFF is the separation speed. Figure 23 shows an example of a separation of seven latexes within 3 min.

On the other hand, the mechanism of steric-FFF is complicated by a number of hydrodynamic phenomena [79]. The most important are the hydrodynamic lift forces that drive particles away from the wall and thus counteract the physical field [289–291]. This effect can even lead to an increase in the separation

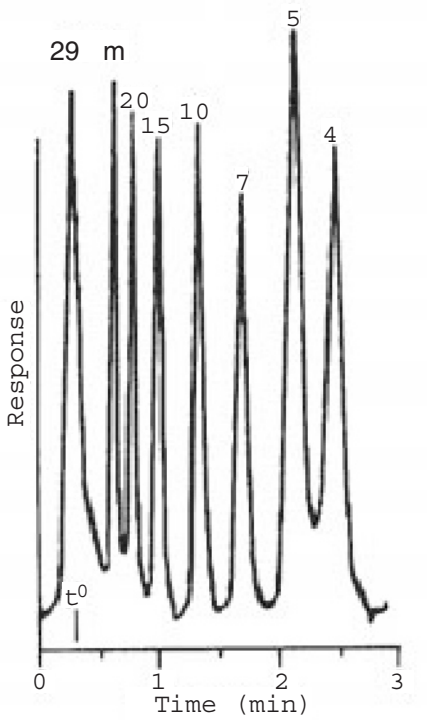

Fig. 23. High-speed separation of seven polystyrene latex beads by steric-S-FFF. Reproduced from [14] with kind permission of the American Association for the Advancement of Science

speed, as shown for the high-speed focusing-FFF of polystyrene latex particles [292].

The occurrence of hydrodynamic lift forces principally leaves two options to perform the FFF experiment: either the field force is increased to offset the lift forces and confine the particles close to the wall [226], or they can be adjusted to allow the particles to gain a significant elevation above the wall, where they form hyperlayers. The first mechanism preserves the steric mechanism, whereas the latter is the mechanism of lift-hyperlayer FFF (see Sect. 2.8.2). From these considerations, it becomes clear that the mechanism of steric-FFF is more complicated than the normal mode operation, necessarily requiring a calibration prior to measurement. This calibration is performed using a double logarithmic plot of the retention time t_r vs. the known hydrodynamic diameter d_H of a standard particle. From the slope and intercept, one can obtain the calibration constants S_d and t_{r1} by using the equation [293]:

$$\log t_r = -S_d \log d_H + \log t_{r1} \tag{81}$$

where S_d is the diameter-based selectivity and t_{r1} is a constant representing the retention time of a particle of unit diameter. The value of t_{r1} depends on the field strength and, for S-FFF, also on the particle density which enables density determinations from steric-S-FFF measurements. Using the calibration parameters S_d and t_{r1}, the particle size weight distribution, m(d) can be obtained directly from the elugram using:

$$m(d) = c(t_r)\langle v\rangle S_d t_{r1}\left(\frac{t_r}{t_{r1}}\right)^{(s_d+1)/s_d} \tag{82}$$

where $c(t_r)$ is the fractogram signal at retention time t_r and <v> is the flow rate through the channel.

Although steric-FFF can in principle be performed with any FFF technique, it was most successfully carried out with sedimentation forces which allowed the possibility to offset hydrodynamic lift forces (see Fig. 23). The calibration of steric-S-FFF is complicated because the sedimentation force depends on the density difference against the solvent, unless performed with standards which have the same density as the sample. This makes it difficult to use a simple diameter-based calibration method as indicated by Eq. (81). The approach towards a successful calibration in such cases is the density compensation principle [293] in which particles of an identical diameter but different densities can be eluted at the same retention time by adjusting the field strengths to compensate for the density difference between the particles [293,294]. This can be done by adjusting the field strength of a steric-S-FFF run inversely proportionally to the change in density difference by using the relationship:

$$(\mathrm{rpm})_{\mathrm{sample}} = \left\{\frac{\Delta\rho_{\mathrm{std}}}{\Delta\rho_{\mathrm{sample}}}\right\}^{1/2} (\mathrm{rpm})_{\mathrm{std}} \tag{83}$$

where $(rpm)_{sample}$ represents the rotational speed for a run with the sample, $(rpm)_{std}$ is the corresponding speed of the standard run, $\Delta\rho_{std}$ is the density difference between the standards and the carrier liquid, and $\Delta\rho_{sample}$ is that between the sample and the carrier.

However, even sophisticated calibration procedures cannot account for wall effects of the sample which might be absent for the calibration standard. The term "wall effects" summarizes all kinds of forces, both attractive and repulsive, which can become significant as the colloidal particles are usually forced to be in direct contact with the accumulation wall. Therefore, any information from such experiments can become error prone, so it is recommended to reduce the field or to alter the carrier flow rate in order to switch from the steric to the hyperlayer mode.

In addition, quantitative evaluation of steric-FFF experiments usually relies on special detectors, since the particles being separated are very large. A standard UV-detector, for instance, cannot be used, unless it accounts for the Mie scattering or Fraunhofer diffraction. A special photometric detector has been designed especially for steric-FFF [295].

2.8.1 *Hydrodynamic Lift Forces*

In contrast to the simple retention theory of steric-FFF, the retention ratios were found to depend experimentally not only on size but also on flow rate [296] and particle density. In 1979 Caldwell et al. [297] attributed this observation to flow-dependent hydrodynamic lift forces that elevate the particles away from the wall. These forces have the same origin as the forces governing the separation mechanism in hydrodynamic chromatography and were theoretically described prior to their observation in steric-FFF measurements [289–291]. Hydrodynamic lift forces increase with the carrier liquid flow rate and keep the particles a short distance from the accumulation wall and thus into regions with a higher flow velocity in the parabolic flow profile [79,298]. These lift forces decrease with higher field strengths and increasing particle size [299] and, in certain cases, they can also cause the loss of resolution [300]. Hydrodynamic lift forces have also been observed in other FFF techniques than S-FFF or Gr-FFF, for instance, A-Fl-FFF [231]. The action of hydrodynamic lift forces is outlined in Fig. 8.

As hydrodynamic lift forces are as yet only very poorly understood [79], they cannot yet be incorporated into a closed retention theory. However, early studies suggest that the retention ratio R in steric-FFF can be expressed by a quite simple relationship [294]:

$$R = \frac{t_0}{t_r} = \frac{3\gamma_S d_H}{w} \tag{84}$$

where γ_S is the steric correction factor which is related to the hydrodynamic lift forces. According to Eq. (84), it is shown that the prediction of particle retention

in steric-FFF requires a clear understanding of this steric correction factor. Therefore, attempts were made to quantitatively express the hydrodynamic lift forces. Different relationships were used over the years, the first originating from Caldwell et al. where the lift force $F_L(x)$ was described as [297]:

$$F_L(x) = 20.3(\eta\rho)^{0.5} \frac{d_H^2}{R_c} \left[3 < v(x) > x\right]^{0.5} \Delta v(x) \tag{85}$$

with x=0 in the center of the channel differing from the normal convention, R_c is the radius of the circular S-FFF channel, and $\Delta v(x)$ is the difference between the particle and the fluid velocity at the position of the particle center of gravity.

Recent systematic studies used steric-S-FFF with well-characterized latex beads of diameters 2–50 μm where the sedimentation force was adjusted to exactly counterbalance the lift force F_L [79,301] to provide a measure of F_L. This has led to a more subtle view of the hydrodynamic lift forces than expressed by Eq. (85). There are indications that the hydrodynamic lift force is presumably composed of two different contributions: (a) the lift force due to the fluid inertial effect F_{L_i}, which may be described by the theory of hydrodynamic lift forces [289–291], and (b) the hydrodynamic lift force by a near-wall effect F_{L_w} [61,62,79,301,302]. The latter was experimentally found to be a function of particle diameter d_H, the distance of the particle bottom from the wall δ, the fluid shear rate s_0, and the fluid viscosity η by:

$$F_{L_w} = C \frac{d_H^3 \eta s_0}{8\delta} \tag{86}$$

with C being a dimensionless coefficient. The origin of this incremental force is unclear but may be related to lubrication phenomena.

If the external field strength is kept so low that the particles are significantly elevated from the wall by the action of the hydrodynamic lift forces, the fluid inertial contribution of the hydrodynamic lift force F_{L_i} can be investigated [289–291,301]. Observed inertial lift forces were in reasonable agreement with values predicted by the inertial lift force theory expressed by:

$$F_{L_i} = 13.5\pi \frac{\langle v \rangle^2 d_H^4 \rho}{16 w^2} g(x/w) \tag{87}$$

where <v> is the mean flow velocity and g(x/w) is a function of (x/w) [302]. Combining Eqs. (86) and (87), a general expression of the overall active hydrodynamic lift force F_L is obtained [301]:

$$F_L = \underbrace{C\frac{d_H^3 \eta s_0}{8\delta}}_{\text{Near wall contribution}} + \underbrace{13.5\pi \frac{\langle v \rangle^2 d_H^4 \rho}{16 w^2} g(x/w)}_{\text{Inertial contribution}} \quad (88)$$

When particles are close to the channel wall, the first term dominates whereas the second does when particles are at some distance from the accumulation wall. Thus, steric-FFF is also a very promising technique to study particle hydrodynamics in the vicinity of the wall.

The behavior of particles under the simultaneous effect of field forces and lift forces can vary with the nature of different applied primary field forces [298]. The force acting on the particles is proportional to the third power of the particle diameter in S-FFF, but only to the first power of the particle diameter in Fl-FFF thus indicating that S-FFF is probably best suited for a fine balance between the external field and hydrodynamic lift forces.

On the other hand, retention in lift-hyperlayer FFF only depends on the particle size and is independent of density which makes the calibration easier. Lift-hyperlayer FFF is a very fast technique applicable to a particle size range from 0.5–50 μm if cross-flow forces are applied [226,303]. A further advantage of lift-hyperlayer FFF is that the particles are held well away from the wall during separation and thus particle–wall interactions are omitted.

2.8.2 *Capillary Hydrodynamic Fractionation (CHDF)*

CHDF is similar to steric-FFF in respect to the elution mode (larger particles elute more rapidly) but the separation characteristics are different. In CHDF, long capillaries (ca. 100 m) with internal diameters as small as only a few microns are used for the separation of particles and polymers in the size range of 30 nm up to several μm, depending on the capillary used. The underlying principle of hydrodynamic chromatography had already been put forward in 1970 [304], before the first experiments using non-porous silica columns were performed [63]. By 1974 the first separation of macromolecules in a capillary was reported [305]. There are only a few papers dealing with CHDF separations (for an example, see [306]), nevertheless, the setup is commercially available and has found application in several laboratories.

Advantages of CHDF include fast separations in a matter of minutes, easy handling and a very good reproducibility of the measurements. A problem of CHDF is the necessarily long capillary length required for a successful separation because the effectivity of the separation can be described by:

$$\Delta r = 3.039 \left(\frac{R_{cap.}^3}{L_{cap.}} \right)^{1/2} \left(1 - \frac{d_H}{2 R_{cap.}} \right)^{3/2} \quad (89)$$

where d_H is the hydrodynamic particle diameter, $R_{cap.}$ the internal radius of the capillary, and $L_{cap.}$ the length of the capillary. Thus the resolution of the measurement (small Δr) can be enhanced by the choice of long capillaries of small internal radii. On the other hand, such conditions promote the influence of diffusion in the flow direction resulting in band broadening. Furthermore, the influence of ill-defined colloidal forces (the "wall-forces") become more important for long capillaries and are often the dominant source of the separation. Therefore, the elution behavior cannot be predicted and relies at least on the calibration with standard samples. For all these reasons, CHDF can be regarded as a limiting case of steric-FFF separation but without the corresponding resolution or versatility.

2.9 Focusing-FFF

Focusing-FFF is a special mode of FFF where a gradient of a physicochemical quantity like density in S-FFF in the channel balances the external force. This leads to a focusing of the sample band at a defined position above the accumulation wall, where the external force is exactly counterbalanced. In the case of focusing S-FFF, the focusing would be at the position where the sample density is equal to the local density in the gradient, analogous to isopycnic ultracentrifugation. This principle has recently been generalized to demonstrate that other perichoric gradients and a variety of the fields could be combined to produce a focusing effect [18]. The principle of focusing-FFF is illustrated in Fig. 9. In the FFF literature, the term hyperlayer-FFF instead of focusing-FFF was suggested by Giddings and is also used.

The retention theory for focusing-FFF was developed for focusing-S-FFF but can be transferred to other focusing mechanisms [72,73]. Janca and Chmelik developed this theory for several shapes of fractionation channels [74] and found that it is advantageous to form axially asymmetrical velocity profiles in channels with modulated cross-sectional permeability [83].

2.9.1 *Focusing-S-FFF*

Focusing-S-FFF is based on the isopycnic centrifugation principle where a substance bands in a density gradient at a position where its density is equal to the local gradient density. The density gradient can be created by centrifugal forces acting on a liquid composed of two or more components differing in their effective densities. Diffusion processes disperse the formed zone of the banded solute so that a Gaussian concentration distribution is obtained with a width depending on the diffusion coefficient. For detailed reference about the underlying principles refer to the literature of isopycnic ultracentrifugation [307]. When the parabolic flow profile in the FFF channel is formed, the solute zone moves with a velocity of the streamline at the altitude corresponding to the coordinate of

equal densities [72,73]. Therefore, retention in focusing-S-FFF is just determined by the solute density whereas in normal S-FFF, it also depends on the size. In contrast to isopycnic sedimentation in an ultracentrifuge, the focused zone is laterally transported which improves the resolution. Furthermore, the migration distance in the thin FFF channel is magnitudes smaller than in an ultracentrifuge and, thus, the time for solute equilibration is shorter reducing the experimental time.

The density gradient, $d\rho/dx$, formed by the action of a centrifugal force can be calculated neglecting the pressure gradient according to [307]:

$$\frac{d\rho}{dx} = \frac{\partial\rho}{\partial c_i}\left(\frac{\partial c_i}{\partial a_i}\right)\frac{a_i M_i\left[1-\bar{v}_i\rho(x)\right]\omega^2 x}{RT} \tag{90}$$

where a_i or $\bar{v}_i$ is the activity, respectively, the partial specific volume of the i^{th} component of the density gradient. The force acting on the solute particles or macromolecules can be defined with knowledge of $d\rho/dx$ as:

$$F(x) = \bar{v}\omega^2 x_0 \frac{d\rho}{dx}(x_0 - x) \tag{91}$$

where $\bar{v}$ is the partial specific volume of the solute species and x_0 the coordinate where the force onto the solute is 0. F(x) has the meaning of a force per mass unit of the solute. Hence, the general equation for the Gaussian concentration distribution function c(x) of the sample in the direction of the focusing forces becomes for S-FFF [72, 73]:

$$c(x) = c_{max}\exp\left[\frac{-\bar{v}\omega^2 x_0(d\rho/dx)(x_0 - x)^2}{2RT}\right] \tag{92}$$

Experimentally, focusing-S-FFF can be carried out with the normal S-FFF equipment. The carrier liquid contains both components for the density gradient which is is established under the influence of the centrifugal forces.

There are two different philosophies about the optimum channel design for focusing-S-FFF reported in the literature. Whereas Janca et al. utilized channels with trapezoidal or parabolic cross sections [83,308–315], resulting in a variation of the fluid flow velocity across the channel width, Giddings [316] favored the classical rectangular cross section with a parabolic fluid velocity profile.

Focusing S-FFF suffers from the problem that the density gradient has to be formed instantaneously which is not the case in practice even for thin channels [107]. This may be the reason why published results obtained with focusing S-FFF are rare [27,74,83,308–315].

Focusing- S-FFF seems promising especially for the separation of samples due to structural changes. For example, polymers can be analyzed in terms of

tacticity or degree of branching due to the density differences for chains having the same molar mass but different structures. Also for biopolymers, the fractionation due only to density differences is advantageous as these substances are very often monodisperse with respect to molar mass, but exhibit differences in structure and the related density.

2.9.2 *Isoelectric-Focusing-FFF*

Isoelectric focusing-FFF is appropriate for the separation of amphoteric particles, since their electrophoretic mobility depends on pH and is zero at the isoelectric point. If a stable pH gradient is formed in the FFF channel due to an applied electrical field [317], the amphoteric solute will be focused into the position of its isoelectric point. Isoelectric-focusing-FFF was first proposed as a concept and experimentally verified five years later [314,315,318–321].

2.10 Adhesion-FFF/Potential-Barrier FFF

Adhesion-FFF is a very interesting FFF mode for colloidal samples which addresses colloidal forces. So far it has only been applied with Gr-FFF and S-FFF but can, in principle, be generalized. Adhesion-FFF makes use of the variation of colloidal forces by pH, surface tension, ionic strength, temperature or dielectric constant of the suspending medium of the carrier liquid and thus affects the Hamaker constant, surface potential and Debye–Hückel length [57,322–326]. If these parameters are properly adjusted, colloids adhere or detach from a solid surface. Thus it is possible to totally absorb or desorb colloidal particles onto or from the accumulation wall. This FFF variant is named potential-barrier FFF [269,270,322–325,327]. The total release of adherent particles is accomplished either by reducing the field strength, increasing the solvent velocity, or by varying the potential energy of interaction between the colloidal particles and the column material, for instance, by changing the ionic strength of the carrier solution. Adhesion-FFF is very useful for the study of possible aggregation processes as the particle size distributions prior and after adhesion to the accumulation wall can be compared [284]. This is illustrated in Fig. 24 by means of a typical experimental elution profile.

Unless aggregation is studied, potential-barrier FFF is restricted only to particles which fully adsorb in a reversible way on the channel wall. Thus, the material of the channel walls needs to be properly selected which is a difficult task. One major advantage of potential-barrier FFF is the possibility to separate and characterize dilute colloidal samples of the same size but differing surface potentials or Hamaker constants.

Another variant of adhesion-FFF is cellular adhesion chromatography (AC) which can be used to separate cells in a preparative manner. It utilizes selective

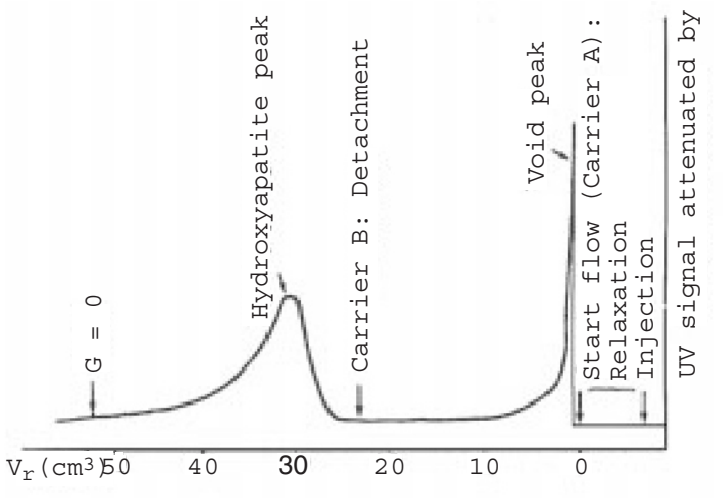

Fig. 24. Attachment and detachment of hydroxyapatite particles from a Hastelloy C surface in an S-FFF channel in carrier A: 10^{-3} M KNO_3 (pH 6.8) and carrier B: 0.5% v/v Fl-70+0.02% w/w NaN_3 (pH 9.4). Reproduced from [328] with kind permission of John Wiley and Sons

adhesion of cell groups to an FFF accumulation wall for separation which requires chemical surface modifications or even surface design [329–331].

Cellular adhesion FFF combines the controllable hydrodynamic shear forces of FFF and the selective adhesion of AC. The hydrodynamic shear is used to detach selectively and evenly adhered cells or particles from the surface and allows an estimation of the differences in cell/surface adhesion forces. The channel for cellular adhesion FFF is constructed in the same way as that used for Gr-FFF but is smaller in size and with the modification that the accumulation wall consists of either bare or polymer-coated surfaces. After the cell suspension is filled into the channel allowing sufficient time for cell adhesion, the flow is applied and fractions are collected. Despite the collection of fractions, cellular adhesion FFF can also be used as a tool to study rapid kinetics of cell surface adhesion, a largely unexamined area [332].

2.11 Preparative and Micropreparative FFF

Considering the mass of injected sample of some micrograms and the danger of solute–solute interactions, it is obvious that FFF is in general only an analytical method. However, some strategies have been employed to apply FFF principles for preparative separations as well.

Repeated sample injections allow at least micropreparative fractionation, which was described for polymer latex particles by S-FFF [333]. Preparative separations can however also be achieved by applying continuous sample feed. One possibility is to use SPLITT channels (see Sect. 2.12) but classical FFF methods

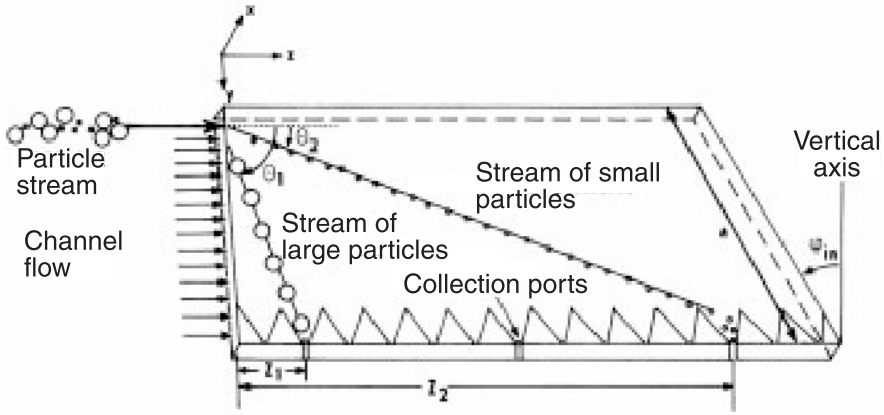

Fig. 25. Schematic representation of an inclined channel for continuous steric-Gr-FFF. Reproduced from [334] with kind permission of Elsevier Science Publishers

have also been described that work with continuous sample feed. For example, continuous steric-Gr-FFF was performed by inclining the transversal axis of the channel and by injecting the sample into the upper part [334]. The separated particles are carried by the flow and slide towards the lower regions of the channel into collectors situated along the channel (see Fig. 25), where the particles are trapped according to their size: larger particles are trapped in a shorter distance.

The distance from the injection point Z where the particles are trapped in the pocket can be calculated from:

$$Z = \frac{54\langle v \rangle \eta}{w^2 d_H \Delta\rho \, G \cos\varphi_{in}} \tag{93}$$

where <v>is the fluid flow rate, G the gravitational acceleration, and ϕ_{in} the inclination angle. This continuous fractionation was used for the separation of coal fly ash [335].

A continuous Fl-FFF channel analogous to a dialysis cell or ultrafiltration cell [247] was described theoretically and later demonstrated in practice for the separation of bovine serum albumin from methylene blue, various viruses, proteins, and colloidal silica particles.

Focusing-FFF can be applied as a preparative separation technique if the channel is equipped with several outlet capillaries situated at various heights above the accumulation wall of the focused samples, and the sample is fed continuously [74].

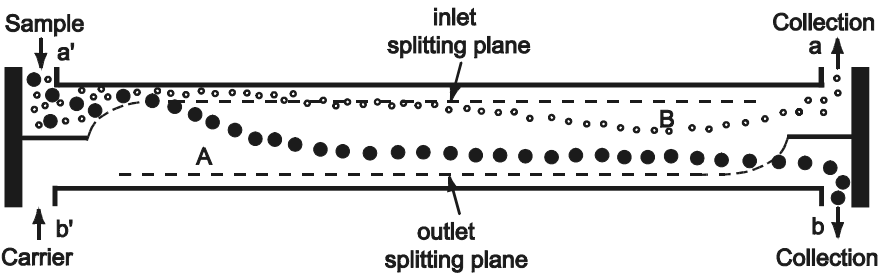

Fig. 26. Schematic representation of Gr-SPLITT-FFF

2.12 SPLITT-FFF

SPLITT-FFF uses stream splitters at the channel inlet and outlet which enables the separation of a mixture into two fractions. Although the separation of the sample is also achieved by the action of an external field, the mechanism of separation is different from FFF. The separation in FFF is along the flow axis of the channel because of the different flow velocities of each component, whereas in SPLITT separation is over the thinnest dimension of the channel. While conventional FFF is an analytical tool requiring operation with very small samples, SPLITT is a preparative tool which can be operated with continuous sample feed [336,337]. SPLITT channels are similar to FFF channels but with two carrier inlet streams a' and b' and two outflow streams a and b as illustrated in Fig. 26.

Control of the inlet and outlet flow rates determines the positions of the inlet and outlet splitting planes and allows the adjustment of the cut-off point between the two fractions and enhancement of the efficiency of the separation [338,339]. The feed stream enters through a', while the flow from b' compresses the sample feed flow upward into a band sometimes only 10 or 20 μm thick. This compression is determined by the flow rate ratio. Similarly, the outlet splitting is controlled by the ratio of flow rates from a and b. Conditions for successful separations in SPLITT channels by modifications to the inlet and outlet splits has been discussed in detail by Giddings [340].

Although SPLITT has the advantage of being a very rapid preparative fractionating technique due to the short transport paths of only a few hundred μm needed to achieve separation, the disadvantage is that only two fractions smaller or larger than a given cut size can be collected depending on the conditions used. Thus, only subsequent treatment of the fractions under different flow conditions can yield a narrow distribution of particles. Applying this procedure, SPLITT can also be used as an analytical tool to reconstruct the particle size distribution, although this is a very tedious method [69].

2.12.1 *Gravitational-SPLITT-FFF (Gr-SPLITT-FFF)*

Gr-SPLITT-FFF is the most simple design of a SPLITT channel and the most widely used among the different SPLITT techniques. The function of a Gr-SPLITT-FFF channel is illustrated in Fig. 26. Here, the fractionation is achieved according to the particle size and density analogous to Gr-FFF so that the smaller particles emerge through the upper outlet a while the larger ones leave at the lower outlet b.

2.12.2 *Electrical- and Magnetic-SPLITT-FFF*

In an electrical-SPLITT-FFF channel, an electrical field is applied which consequently leads to a SPLITT separation of differently charged particles or molecules [341]. The separation mechanism, however, is more similar to that of electrophoresis than El-FFF. Components with high mobility are driven through the outlet splitting plane and emerge through the outlet splitter. Adjustment of both the electrical field strength and the outlet stream splitting ratio tunes the cut point between the collected species. The electrical SPLITT cell can also be operated in the equilibrium mode by adjusting the pH such that some species go to the anodic wall and others to the cathodic wall. This is most useful for amphoteric samples with different isoelectric points, like proteins.

A magnetic SPLITT fractionation system extends the merits of SPLITT-FFF to magnetic samples [342]. Here, permanent magnets act as the driving force perpendicular to the solvent flow for the separation in the SPLITT channel. The system was experimentally tested using mixtures of silica particles, labelled silica particles and magnetic particles leading to a complete separation of particle mixtures with high and low magnetic susceptibilities. In the continuous mode, the throughput was around 0.1 g/h with a sample recovery of nearly 99%.

2.12.3 *Diffusion-SPLITT-FFF*

Diffusion can also be used as a driving force in SPLITT channels. If one uses a SPLITT channel analogous to a gravitational-SPLITT-FFF channel where the sample is injected into inlet a' (Fig. 26), the higher diffusion of smaller molecules allows them to cross the outlet splitting plane and thus to exit the lower outlet b, whereas larger molecules have a lower diffusion coefficient and exit from the upper outlet a. This method has been applied for continuous separations and diffusion coefficient determinations of a number of proteins [343,344].

3 Selected Applications of FFF

This section lists selected applications of the various FFF techniques demonstrating the possibilities of FFF for various samples. For simplicity, the section is structured into the major substance classes which are suitable for analysis by FFF distinguishing between samples of synthetic or natural origin.

3.1 Polymers

3.1.1 *Synthetic Polymers*

3.1.1.1 S-FFF

Although S-FFF is usually applied to particles or large biopolymers, its use for the analysis of synthetic polymers with high molecular weight (M) was demonstrated for polyacrylamide [176]. This is, however, a rare application.

3.1.1.2 Th-FFF

As Th-FFF is the technique of choice for synthetic polymers in organic solvents, there are many studies reported in the literature. Th-FFF has been found applicable to virtually every type of lipophilic polymer in the range $M=10^4$–10^7 g/mol using ΔT~10–100 K, but only to a very limited amount of hydrophilic polymers where Fl-FFF has its traditional strengths. Exceptions include poly(vinyl pyrrolidone) and poly(ethylene glycol) [222].

The list of examples of successful Th-FFF separations of lipophilic polymers is extensive and includes polystyrene [29,34,76,118,144,164,165,168,196,200,345–350], polyisoprene [55,110,144,196,349,350], polytetrahydrofuran [144,196,349,350] and poly(methyl methacrylate) [55,110,144,196,349,350], polybutadiene [349], poly(ethyl methacrylate), poly(*n*-butyl methacrylate), poly(octadecyl methacrylate), poly(α-methylstyrene), poly(dimethylsiloxane), poly(vinyl acetate), poly(vinyl chloride) and poly(vinyl carbazole) [144], polyethylene [351] and other polyolefins [221]. The polyolefin separations were achieved in a special high temperature channel [15,351]. Asphaltenes have also been separated with Th-FFF [352].

From the Th-FFF retention data, it is possible to obtain a molar mass distribution after a suitable calibration for the determination of the Mark–Houwink constants (straight-line plot of $\log(D/D_T)$ vs. $\log M$ [15]). Another possibility is to couple an absolute molar mass detector like MALLS (see Sect. 4.3.2) or a suitable detector combination such as an on-line viscometer coupled with a refractive index detector. This possibility does not require prior knowledge of D_T

[144]. A large variety of samples was investigated with the latter technique including polystyrene, poly(methyl methacrylate), poly(ethyl methacrylate), poly(*n*-butyl methacrylate), poly(octadecyl methacrylate), polyisoprene, poly(α-methylstyrene), poly(dimethylsiloxane), poly(vinyl acetate), poly(vinyl chloride) and poly(vinyl carbazole). Another advantage of coupling a continuous viscosity detector to the Th-FFF channel is that viscosity distributions can be measured resulting in a measurement of absolute intrinsic viscosities without the need for calibration [76]. If copolymer samples are investigated in Th-FFF coupled with a viscometer, both the average molecular weight and the average composition are accessible [142].

Th-FFF is also a good technique if polydispersities of very narrow samples from anionic polymerization need to be determined. This was demonstrated for polystyrene from band broadening data in Th-FFF with a higher accuracy than the results from SEC on the same samples [123].

Whereas polymers in the range $M=10^4$–10^7 g/mol are well resolved by Th-FFF, polymers of lower molecular weight (~10^3 g/mol) need an inconveniently high ΔT (~150 K) for retention, and problems of boiling solvent, etc. arise. However, successful separations of polystyrene down to 600 g/mol have been described using very high temperature gradients in a pressurized Th-FFF channel [200].

On the other hand, the upper end of accessible molar masses $M\approx10^7$ g/mol [126] can be significantly shifted to higher values if more compact structures such as branched, cross-linked, or particulate samples are investigated since the D_T of the sample is low. The fractionation of ultrahigh molar mass samples is a very promising application for Th-FFF as these polymers are often fragile and thus sensitive to shear degradation which can be mainly circumvented in the open FFF channel. Consequently, this type of application is on the rise [126].

Janca and Martin [353] studied the influence of various operational parameters on the retention of ultrahigh molecular weight polystyrenes (0.6–30×10^6 g/mol) in Th-FFF, finding that at high flow rates (1.5 ml/min) the retention was not strictly proportional to the molecular weight for polymers with $M>3\times10^6$ g/mol, although the samples did not suffer from shear degradation as demonstrated by reinjection. Such reversal in the M-dependence of retention at high flow rates had already been observed for high molar mass polymers [354], and can be explained by shear-induced entropic effects. By the action of such effects, the high molecular weight components are transported into the center of the channel where the velocity gradient across the polymer coil is reduced.

Another promising field of application of Th-FFF is the investigation of gel/microgel mixtures with polymers as pioneered by Lee et al. [355,356]. A major advantage is that for the Th-FFF experiment no filtration is required to endanger material loss. For example, microgels or particles which are problematic for SEC separations can be separated from a polymer, so that the major constituents of composites such as acrylonitrile-butadiene-styrene (ABS) rubber are quantitatively accessible.

Other examples include the monitoring of the degradation of poly(methyl methacrylate) (PMMA) by an electron beam [355] or the investigation of the

physicochemical difference between two acrylate elastomers that have been manufactured by the same procedure but show different mechanical properties [355]. These differences are not distinguished by SEC, even in combination with viscometry or light scattering. Composite polymers where particles are mixed with a polymer have also been examined [357].

The dependence of retention in Th-FFF on chemical composition of the polymers and solvent [84] also opens a wide field of application for Th-FFF, especially for copolymers. According to Eq. (42), retention in Th-FFF can be used to determine the thermal diffusion factor α_T which was demonstrated for polystyrene in toluene [209]. Later, this study was extended to other solvents (ethyl acetate, 2-butanone, *p*-dioxane, cyclohexane, dimethylformamide, chloroform, and ethylbenzene) [204].

The ability of Th-FFF to separate polymers by chemical composition [2] was demonstrated in the separation of polystyrene, polyisoprene and polybutadiene polymers of similar molecular weight [349] and extended to polytetrahydrofuran [350]. An impressive example of the ability to separate according to chemical composition was reported for two polymers indistinguishable by SEC (See Fig. 10).

Recent studies [111,214] indicate that Th-FFF can even be used to determine the relative chemical composition of two components in random copolymer and linear block copolymers whose monomers do not segregate due to solvent effects. However, this application is limited by the unpredictable nature of thermal diffusion. Nevertheless, combining information from Th-FFF with those derived on fractions by independent detectors selective to composition (such as an IR spectrometer) can yield further insight into the dependence of D_T on the chemical composition. Even more powerful is the combination of Th-FFF with SEC as, here, the chemical composition (from Th-FFF) can be studied as a function of the molar mass (from SEC). This was demonstrated by van Asten et al. by cross fractionating copolymers and polymer blends with SEC and Th-FFF [358].

Kirkland et al. [359] reported the possibility of varying the retention behavior in Th-FFF by the application of a solvent mixture, later supported by other workers [58,360]. The retention enhancement so achieved was attributed to a synergistic effect involving the thermal diffusion of both polymer and solvent.

Of all solvent mixtures examined thus far, the retention of polystyrene is highest in mixtures of THF and dodecane. This is illustrated in Fig. 27 where the separation of five polystyrene standards ranging in molecular weight from 2.5×10^3–17.9×10^4 g/mol in a mixture of 45 vol% THF in dodecane is shown [360]. This fractogram represents the lowest molecular weight polymer ever resolved from the void peak with a standard Th-FFF channel.

The extension of the application range of Th-FFF using exponential temperature programming was described by Kirkland, Yau et al. for the fractionation of polystyrene and poly(methyl methacrylate) and standard mixtures [164,168], whereas Giddings separated mixtures of polystyrene standards in ethylbenzene over a wide range of molar masses (9×10^3–1.97×10^6 g/mol) using high speed power programming with various field profiles of Th-FFF [54].

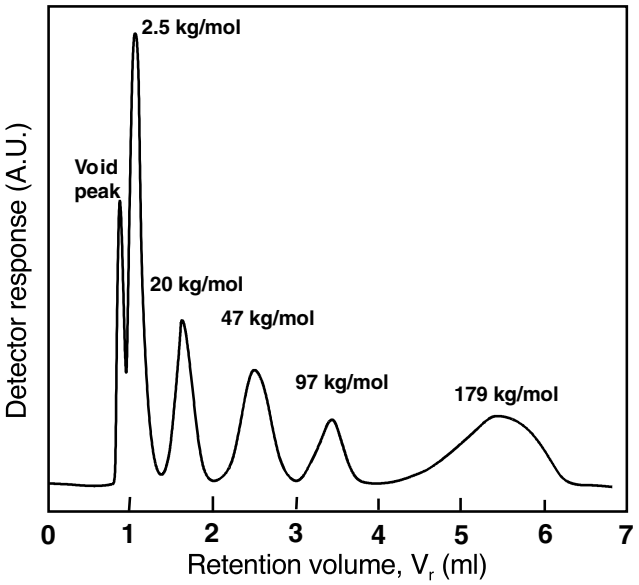

Fig. 27. Separation of polystyrene standards using a mixture of 45 vol% THF in dodecane as carrier liquid. Reproduced from [360] with kind permission of the American Chemical Society

The use of ultrathin (50 μm) channels for high speed separation by Th-FFF was demonstrated by Giddings [118] who separated mixtures of polystyrene standards in experimental times of less than a minute.

3.1.1.3 Fl-FFF

Fl-FFF is most attractive for water-soluble polymers [59] and can directly deliver the diffusion coefficient distribution and also a molar mass distribution via the relationship $D=AM^{-b}$. This was exploited for poly(ethylene oxide), poly(styrene sulfonate) and poly(vinyl pyrrolidone) and other polymers using published Mark–Houwink constants [361]. Many papers just report on the fractionation of polymers or the determination of the hydrodynamic size distribution of polymers. Examples include poly(styrene sulfonates) [59,165,243], poly(acrylic acid) [243] and poly(2-vinylpyridine) [59].

Polyelectrolytes are a substance class notoriously difficult to analyze. This problem also exists for Fl-FFF due to polymer–polymer or polymer–wall/membrane interactions. Benincasa and Giddings [59] completed a systematic study of ionic-strength effects in the application of Fl-FFF to both cationic and anionic polyelectrolytes over a broad molecular weight range. Poly(2-vinylpyridine) was effectively characterized in a 20 mM solution of nitric acid (pH 2), while the best results on poly(styrene sulfonate) were obtained in a dilute (6.5 mM) solution of

sodium sulfate. With tris(hydroxymethylaminomethane) buffer, anomalous behavior was observed. Thus, it becomes clear that a suitable carrier liquid is vital for the investigation of polyelectrolytes. Tank and Antonietti described a universal carrier fluid for Fl-FFF (deionized water containing 0.02% NaN_3 and 0.01% Tween 20) which simplifies the experimental conditions if large varieties of samples are to be investigated spanning from cationic to anionic polyelectrolytes [362]. With this solvent, polycations as poly(1-vinyl-2-pyrrolidone) and polyanions as poly(styrene sulfonates) were successfully fractionated. The results for an industrial poly(1-vinyl-2-pyrrolidone) sample agreed very well with the results from other absolute techniques like analytical ultracentrifugation on the same sample although an indication of absorption of high molar mass polymers to the membrane was reported. Other reports dealt with the aggregation behavior of charged amphiphilic graft copolymers in dependence on pH or of different salt concentrations as studied by A-Fl-FFF [251,252,363]. Shear sensitive commercial ultrahigh molar mass polyacrylamides in the range $0.35–9\times10^6$ g/mol were characterized in terms of molar mass distributions, shear effects, alteration of the solvent, degradation, and agglomeration and their effects on mineral flocculation [166,364]. These polymers, though industrially important as flocculants, are very difficult to characterize due to their polydispersity, high molar mass and shear sensitivity.

Although most applications of Fl-FFF have been reported for aqueous carrier liquids, a few studies have been carried out in organic liquids as well (for a more detailed discussion see also Sect. 4.3.1). Brimhall et al. [365,366] were the first to report non-aqueous polymer separations by Fl-FFF by separating polystyrene in ethylbenzene. Poly(ethylene oxide) and poly(methyl methacrylate) were characterized in THF [367] and, recently, a so-called universal fractionater also capable of high-temperature fractionations has been reported and applied to the separation of a variety of polymers and particles by Fl-FFF in non-aqueous carrier liquids, including the separation of polyethylene [368].

3.1.2 *Biopolymers*

3.1.2.1 S-FFF

S-FFF has successfully been applied to separate and characterize a number of biopolymers, including DNA [176,369], proteoglycans [370], cartilage proteoglycans [371], dextrans [141] and fibrinogen [176]. Further applications concerned preparative S-FFF of DNA-plasmid from crude cellular lysates [372].

3.1.2.2 Th-FFF

Th-FFF is also suitable for the separation of biomolecules, although the use of organic solvents restricts statements about the native state of aqueous-based

buffer. Also, extensive conformational changes and even denaturation can occur which significantly restrict the range of applicable samples. Nevertheless, dextrans, ficolls, pullulans, cellulose and the starch polymers amylose and amylopectin have been separated by Th-FFF using DMSO as a solvent [373]. These polysaccharide samples have a wide range of industrial applications. Examples include pullulans: coating materials, packaging agents, plasma additives and gelling agents; dextrans: blood substitutes, chromatographic media and immunological testing equipment, etc. Nevertheless, these samples are difficult to separate by SEC without complications of sample adsorption, shear degradation and clogging of the column.

Although thermal diffusion is weak in aqueous systems, mixtures of water and dimethyl sulfoxide can be used to fractionate dextrans by Th-FFF [204]. The retention was found to increase linearly with the dimethyl sulfoxide (DMSO) content which again underlines that D_T depends on the solvent composition.

Th-FFF was also applied for the characterization of natural rubber to avoid shear degradation and allow full characterization of the gel phases present [356]. More recently, similar studies applied Th-FFF/MALLS for the determination of the molar mass distribution of microgel ($M=10^{10}$ g/mol) containing natural rubber without filtering prior to the measurement. The largest molecules detected in the sample were found to be more than three orders of magnitude greater than indicated by SEC [374].

3.1.2.3 Fl-FFF

The most commonly biopolymers separated by Fl-FFF are proteins [49]. Fl-FFF is capable of separating proteins differing by just 15% in size within 3 to 10 min. S-Fl-FFF has been applied to a variety of proteins, including albumin, ovalbumin, γ-globulin, hemoglobin, ferritin, lysozyme, β-casein, apoferritin, human and rat blood plasmas and elastin [41,240,247]. Fl-FFF was also used to investigate the structural transformations of proteins [240].

More recently, A-Fl-FFF was used for highly efficient protein separations [231,249] and for the high-speed separation of biopolymers [232]. Other biopolymers and mixtures thereof were fractionated and characterized by Fl-FFF including bovine serum albumin, albumin, γ-globulin, thyroglobulin, protein conjugates, lipoproteins from blood plasma and DNA [60,232,233], nucleic acids [231], dextrans [237], ferritin and aldolase [109,362], molar mass distributions of dextrans and pullulans [361] as well as diffusion coefficients of linear and circular DNAs [375]. Protein complexes also exhibit baseline resolution by Fl-FFF. Figure 28 shows an example of such a separation. Protein dimers elute as satellite peaks at ~1.4 t_r and monoclonal antibody aggregates can also be resolved.

Humic acids, a mixture of amphiphilic heterogeneous macromolecules from soil which vary widely in composition and molecular weight, are soluble in neutral or alkaline water – distinct from fulvic acids. They are usually quite small macromolecules, but they heavily interact with any column material, thus re-

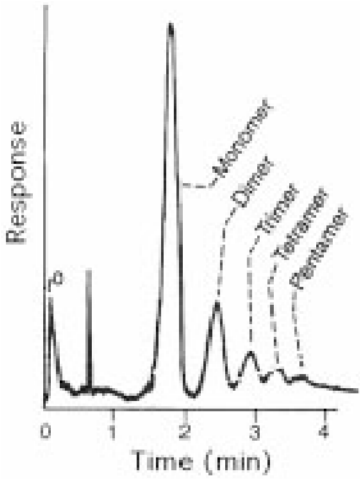

Fig. 28. Separation of a monoclonal antibody from its higher oligomers showing separable peaks up to pentamer aggregation. Reproduced from [14] with kind permission of the American Association for the Advancement of Science

stricting the use of SEC. Humic acids have been successfully studied by Fl-FFF [376]. Beckett et al. characterized humic and fulmic acids in terms of molar mass distributions [11,227,377]. Schimpf and Wahlund investigated the influence of pH, ionic strength, humic acid concentration and bridging by Ca^{2+} addition on the molar mass and size distribution of humic acids [378], whereas the complexation ability of humic acids was studied by van den Hoop and van Leeuwen [379]. In a related study, Beckett et al. studied the size and molar mass distribution of pulp and paper mill effluents by Fl-FFF [380,381].

3.1.2.4 Other FFF Techniques

El-FFF is a technique devoted to the fractionation of proteins which is reflected in the number of papers applying this technique to protein separations. The possibilities of El-FFF were first demonstrated by Caldwell for the separation of albumin, lysozyme, hemoglobin, and γ-globulin in two different buffer solutions (pH 4.5 and 8.0) [35]. Later, the performance of an El-FFF channel with flexible membranes [36], a channel with rigid membranes [256], or a circular channel [260] for the separation of proteins were described. In these studies, human and bovine serum albumin, γ-globulin (bovine), cytochrome C (horse heart), lysozyme (egg white) and soluble ribonucleic acid (t-RNA), as well as denaturated proteins, were successfully separated.

Dielectrophoresis in combination with fluid flow through an open chamber with interdigitated sinusoidally corrugated electrodes was used for the separation of proteins and DNA [382].

Pressure-FFF was found to be suitable for the fractionation of blue dextran and human plasma in a circular semipermeable capillary, 0.2 cm in diameter [37], whereas magnetic-FFF was applied to the study of the retention behavior of bovine serum albumin in the presence and absence of nickel nitrate [45]. In the presence of nickel(II) ions, the retention time of the BSA sample was 6% higher with the magnetic field than it was without the field while the retention times reported for BSA samples both with and without a magnetic field in action did not differ in the absence of nickel(II) ions.

3.2 Colloids

3.2.1 *Synthetic Colloids*

3.2.1.1 S-FFF

S-FFF can be most advantageously applied to address questions related to colloids. The fractionation according to the particle size and particle density is not necessarily problematic but can be turned into an advantage either by seeking independent size information or by a proper design of the experimental conditions. In a trilogy of papers from 1983, Giddings et al. explored the capabilities and methodology of colloid characterization by S-FFF for the investigation of monodisperse samples [81], particles having size distributions [130] and emulsions [383]. Apart from polystyrene latexes, which are the most common standards for particle sizing techniques, polymerized serum albumin microspheres. [183,384], polychloroprene [6,384], poly(methyl methacrylate) [6], poly(vinyl chloride) [130,190], poly(glycidyl methacrylate) [131], poly(vinyl chloride) [130] and polychloroprene [6] latexes have been fractionated.

Apart from latexes, S-FFF has been used to fractionate and determine the size distribution of numerous industrial colloids including water-based titanium dioxide dispersions [6,171], carbon black dispersions [6], phthalocyanine blue [6], various silica sols [141,171,176], gold and silver sols [385], pigments, metal and ceramic particles, clay and a host of latexes [294]. Gold, palladium, silver and copper particles in the size range 0.3–15 μm were separated by steric-S-FFF and their size distributions determined in less than 12 min [69].

Similar studies which adress colloidal phenomena like aggregation were reported [386]. For a partially aggregated poly(methyl methacrylate) latex, singlet, doublet and triplet particle clusters could be cleanly resolved. Remarkably, there were two detected doublet peaks that differed by ~10% in mass suggesting a two-stage latex growth process, the lighter doublets forming after first-stage growth and the heavier doublets after the second stage (see Fig. 29). These observations were confirmed by electron microscopy. Other studies on aggregated PMMA latexes [387] and other colloids have also been reported [16,251,388,389].

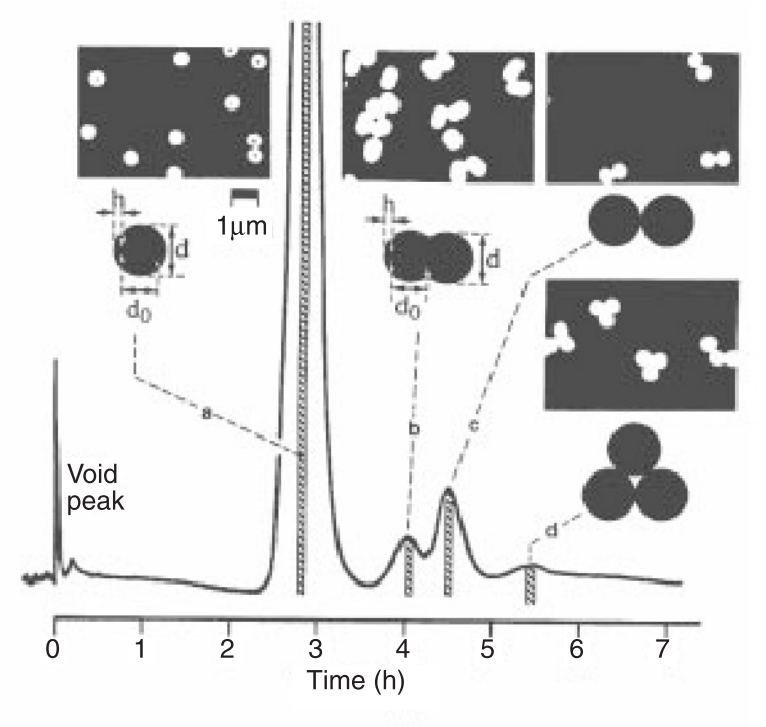

Fig. 29. Separation of components of partially aggregated latex by S-FFF. Reproduced from [386] with kind permission of the American Chemical Society

Li and Caldwell used S-FFF to determine the mass and surface concentration of absorbed PEO-PPO-PEO triblock copolymers (Pluronics) onto PS latex standards [185]. Fl-FFF was found to work equally well for this problem. As experimental absorption problems are widespread and extremely relevant, it is expected that FFF will play an important future role in such studies, as long as the mass of the absorbed layer is sufficiently high.

Another promising application of S-FFF is the characterization of emulsions and S-FFF is used as the standard technique for emulsion characterization in some laboratories [390]. Manifold emulsions or organelles have been fractionated with S-FFF [75,383,391–396] including perfluorocarbon blood substitutes [391].

Other reported applications of S-FFF include the characterization of samples of environmental samples like diesel exhaust soot [384]. The first successful experimental implementation of focusing-S-FFF fractionated a mixture of polystyrene latex with poly(glycidyl methacrylate) latex differing in density which was eluted with Percoll as the carrier fluid [309].

3.2.1.2 Th-FFF

Colloid characterization is not the classical application of Th-FFF. Nevertheless, Th-FFF was first applied to silica particles suspended in toluene testing a correlation between thermal diffusion and thermal conductivity [397]. Although a weak retention was achieved, no further studies were carried out until the work of Liu and Giddings [398] who fractionated polystyrene latex beads ranging from 90 to 430 nm in acetonitrile applying a low ΔT of only 17 K. More recently, polystyrene and polybutadiene latexes with particle sizes between 50 μm and 10 μm were also fractionated in aqueous suspensions despite the weak thermal diffusion [215] (see Fig. 30). Th-FFF is also sensitive to the surface composition of colloids (see the work on block copolymer micelles), recent effort in this area has been devoted to analyzing surfaces of colloidal particles [399,400].

3.2.1.3 Fl-FFF

Many papers report the fractionation of polystyrene latexes or mixtures thereof, as such commonly available spherical latex standards are an ideal system to test FFF setups or evaluations (for an example, see [362,401]). Recent coupling of Fl-FFF to MALLS enables a very high precision in particle size determinations. One example is shown in Fig. 31, where two Duke standard latex batches of a nominal size of 100 nm were investigated by Fl-FFF/MALLS, underlining both separation power and resolution. Using traditional techniques such as photon correlation spectroscopy (PCS) and classic Fl-FFF detection, these samples seem to be identical. However, with Fl-FFF/MALLS, the batches could be separated as two discrete size distributions with a peak size that differed by 3 nm. However, it is not stated if a precise temperature control was maintained so that, critically considered, the observed differences could also have their origin in slight temperature

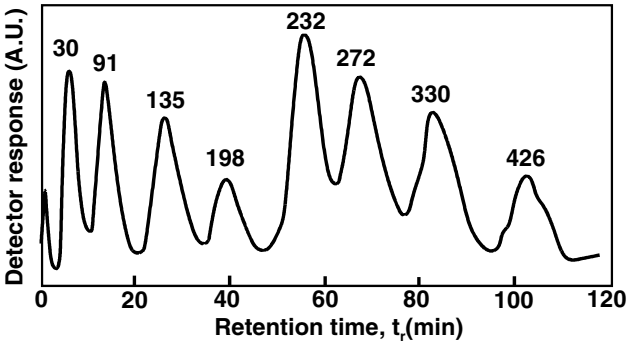

Fig. 30. Separation of eight polystyrene latex particles in aqueous suspension by Th-FFF. The numbers above each peak correspond to the particle diameter in nm. Reproduced from [215] with kind permission of Elsevier Science Publishers

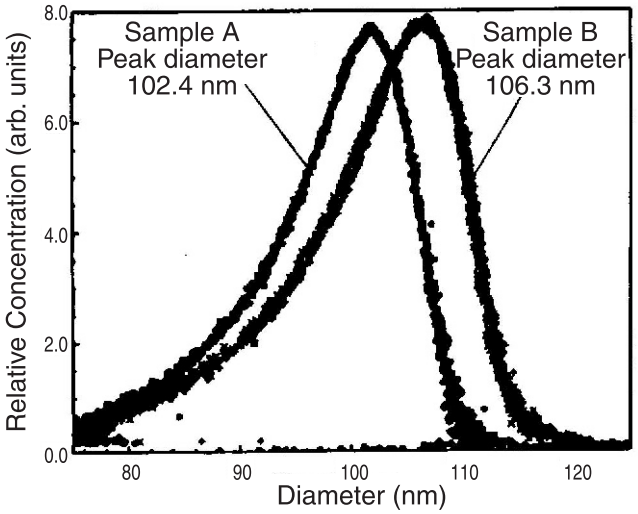

Fig. 31. Fl-FFF-MALLS particle size distribution for two Duke standard latexes of nominal size 100 nm but from two different batches. Reproduced from [374] with kind permission of John Wiley and Sons

differences between the measurements. Unfortunately, no information about the reproducibility of a measurement on an identical sample was given.

Other colloids which have been fractionated and characterized by Fl-FFF include colloidal silica of 10–130 nm diameter [242] or down to 2 nm [17], Xylophene (emulsion), Stabisol (silica sol), Ludox (colloidal silica) and emulsion paints [237].

Complex colloids can be characterized advantageously by a combination of Fl-FFF with different analytical or other FFF techniques, yielding supplemental information. Examples reported in the literature are combinations of Fl-FFF and S-FFF for size (Fl-FFF) and density (S-FFF) as well as the thickness and density of the shell of core shell latexes [402], El-FFF for the charge and composition of emulsions [403], Th-FFF for the characterization of the size and composition of core shell latexes [404] and, finally, with SEC for the particle size distribution and stoichiometry of gelatin complexes with poly(styrene sulfonate) and poly(2-acrylamido-2-methylpropane sulfonate) [405].

3.2.1.4 Other FFF Techniques

Colloid characterization by El-FFF has been attempted. First trials of the separation of polystyrene latexes were not successful as the samples were strongly adsorbed when an electrical field was applied, while the fraction of adsorbed particles increased at greater field intensity [36]. With the improved El-FFF channel working with lower electrical fields, uncoated and protein-coated poly-

styrene latexes and mixtures thereof could be characterized [257]. As the relaxation of the highly charged PS latex standards occurs rapidly (within minutes or less) in El-FFF, it was suggested that this method could be a convenient means to gain insight into the early phase of adsorption reactions which was later experimentally verified for absorption of Pluronic F108 onto a PS latex [406]. Even minor amounts of adsorbed polymer were found to significantly change the retention behavior of the particle in El-FFF.

Magnetic-FFF was applied for the fractionation of iron oxide particles (Fe_2O_3) suspended in acetonitrile [273,274] but only with poor resolution. The effect of the surface modification of Fe_2O_3 particles by the addition of a surfactant in a magnetic field has been studied [274].

3.2.2
Natural Colloids

3.2.2.1
S-FFF

One important application of S-FFF is the fractionation of natural colloids in river water which exhibit a very broad particle size distribution [407,408]. These studies show that different river sources exhibit different size and mineralogy distribution patterns, which are characteristic for the river source. For such investigations S-FFF is used to provide fractions, and these fractions are investigated by further techniques to yield the morphology by EM, elemental content by energy-dispersive X-ray analysis, and mineralogy by X-ray diffraction, to name just a few. By using S-FFF, twenty or more fractions in the size range 0.1–2 μm can be generated in 60 to 100 min, whereas traditional centrifugation or ultrafiltration procedures take days. Modern on-line coupling of FFF and inductively coupled plasma MS has simplified and improved the sensitivity of measuring elemental profiles for different particle sizes [150]. Despite the above characterizations, it is often important to address pollutant adsorption onto the colloids in the river water to understand the transport mechanisms of these pollutants. Colloids from soils, for example, are thought to play a major role in the transport of pollutants through soil profiles and ground waters [409]. Such questions can be addressed if the particle size distribution is known and, thus, S-FFF delivers the amount and surface density of adsorbed materials across the particle size range of colloids [410]. S-FFF has also been applied to the characterization of liposomes [184,384,411,412].

3.3
Particulate Matter

Due to the size of these particles (>1 μm) most applications described in this section apply steric- or hyperlayer-FFF if not stated otherwise. Furthermore, the transition between colloids and particles is not strictly defined so that some experiments are described in the section about colloids, others here in this section.

3.3.1 *Synthetic Particles*

3.3.1.1 S-FFF/Gr-FFF

For particle sizes >1 μm, natural gravitation suffices for separation. A simple Gr-FFF apparatus has been utilized for particles larger than 1 μm [413–422]. Steric-Gr-FFF was applied to separate large polystyrene latexes up to 100 μm in diameter [299], residues from coal liquefaction [423] and fine coal particles [424]. The Gr-FFF channel in combination with a standard HPLC setup is furthermore already being used for an effective determination of the particle size distribution of spherical and irregular chromatographic silica particles in the range 4–7 μm [422]. Information about the porosity of such chromatographic silicas can be obtained by coupling the information from S-FFF with an independent technique for particle size determination, such that the S-FFF data deliver the particle density and thus their porosity. This was demonstrated for a combination of S-FFF/steric-S-FFF and microscopy to evaluate the particle density of fractions of chromatographic supports (d=2–12 μm) [425].

Steric-S-FFF has also been used for numerous fast fractionations including gold, palladium, silver and copper particles in the size range 0.2–15 μm [69,294,385], alumina, low-porosity 7–65 μm poly(vinyl chloride) latex [426] or quartz [427]. Many of these samples were fractionated in times of only 1–5 min.

3.3.1.2 Fl-FFF

One important application of Fl-FFF is the determination of the particle size distribution of chromatographic silica for HPLC packings [226,428,429] which, in combination with S-FFF, allows characterization of the porosity of the samples and particle size distribution.

S-Fl-FFF and A-Fl-FFF were found to be suitable techniques for the characterization of paint components, namely pigments, binders and fillers with their very broad and overlapping size distributions [70]. Both normal FFF and the hyperlayer-FFF mode could be successfully applied.

3.3.2 *Natural Particles*

3.3.2.1 S-FFF

Many environmental samples are particularly well suited for S-FFF or Gr-FFF due to their large sizes, and many successful fractionations of such samples have been reported, including silt-sized particles and river-borne particulates [377], as already discussed in the section on colloids. Another promising application is

the fractionation of subcellular biological compartments. For example, streptococcal cell wall fragments were investigated [430], and the collected fractions were further investigated by PCS. However, differences between the results obtained by the two methods were observed and attributed to the sensitivity of the QELS method to the shape of particles measured. Other examples of successfully analyzed subcellular particles include mitochondria and microsomes [431] or cell wall fragments by coupling S-FFF to gas chromatography-mass spectrometry (GC-MS) [432].

Many samples of interest for medical applications can be fractionated and characterized by S-FFF. Reported examples include viral aggregates (singlets, doublets, and so forth) of the gypsy moth nuclear polyhedrosis virus [433], protein particles including those responsible for optical clouding in cataractous human lenses [434], and for the size determination of the Kreutzfeldt–Jakob disease agent [435]. Other successfully fractionated samples of natural origin are wheat, corn and oat starch granules [436], 2–70 μm starch granules [426] or clays [156].

3.3.2.2
Fl-FFF

Lipoproteins which are difficult to investigate by techniques relying on the particle density as well as on the particle size (S-FFF, ultracentrifugation, etc.) can be successfully separated by Fl-FFF which yields the particle size distribution of high, low and very low density lipoproteins [437,438]. Furthermore, Fl-FFF has been used to fractionate ground minerals by size [439].

3.4
Other Samples

3.4.1.1
S-FFF

S-FFF has been applied for the separation of living cells such as human, sheep, rabbit, and horse blood cells or HeLa cells [12,296,420,440–444] which, furthermore, could give insight into the growth and cell cycle distribution of cells in cultivation broths [444] or an estimation of the bacterial biomass in natural waters [445]. Blood components have been separated in the same apparatus [446]. Cardot, Martin, and co-workers have shown that abnormal blood cells (from anemia or transfusions) can be distinguished from healthy erythrocytes in Gr-FFF [413,415]. In such channels, a prevalent parasite can be isolated from blood, suggesting a possibility for rapid diagnosis [414].

Another sample class that is well separable by S-FFF are viruses [182,433]. Molar masses were determined [80,433,447] including T2 bacteriophage [80,171,174], R17 *E. coli* bacteriophage [31] and the T4D virus, for which it was shown that the infectivity of the virus remained essentially unaffected by its passage through the FFF channel and detector system.

Furthermore, S-FFF has been applied to nuclear-energy-related materials [448,449] and Gr-FFF for residues from coal liquefaction processes [423].

3.4.1.2 Th-FFF

Giddings et al. applied a pressurized Th-FFF channel to increase the temperature range of Th-FFF and used very high temperature gradients (up to $\Delta T = 158\ ^{\circ}C$) for the extension of this FFF technique to lower molar mass samples. This allowed the successful separation of several crude oils and asphalts [200] as well as asphaltenes [450].

3.4.1.3 Fl-FFF

Fl-FFF, in the lift-hyperlayer mode, was applied for the high-speed (2 to 3 min) fractionation of normal and abnormal erythrocytes from various species [12] as illustrated in Fig. 32. Furthermore, various viruses were successfully separated including bacteriophage Qβ, MS2, f2 and ϕx174 [231,241].

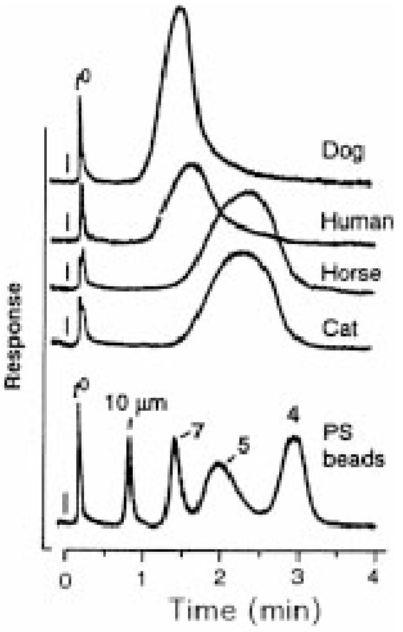

Fig. 32. Separation of different mammalian red blood cells and polystyrene latexes of the indicated diameters by hyperlayer-Fl-FFF. Reproduced from [12] with kind permission of the American Chemical Society

3.4.1.4 Other FFF Techniques

A hybrid technique of FFF and adhesion chromatography was used to study the rapid biological kinetics of cell surface adhesion of B and T lymphocytes to HA13 surfaces. Since cell adhesion is critical in many areas, including cancer metastasis and thrombosis research, a tool for the study of adhesion kinetics is highly desired [332]. Cells [281] and yeast cells [451] were successfully separated by DEP-FFF.

SPLITT-FFF has been applied in environmental studies and oceanography [452,453] for fractionating water samples into a number of fractions which were then analyzed by other methods.

Coal fly ash [335] was fractionated on a preparative scale by the technique of continuous steric-FFF.

4 Possibilities and Limits

In this section, recent developments of the FFF methodology are presented which might have a significant impact on the possibilities of FFF separations. On the other hand, problems which are associated with FFF measurements in general are discussed. These problems and possible artifacts have to be kept in mind when interpreting FFF results, regardless of the technique or detection system used.

4.1 Advantages of FFF

The main advantages of FFF measurements include: speed (from a few minutes to few hours); the small quantity of material required (typically: 10 μL of a 1 wt% solution corresponding to 100 μg sample) and the fractionating power which makes FFF suitable for impure and mixed species. Further advantages are the minimal effort needed for sample preparation and the possibility of sample recovery in order to take fractions after separation since FFF is generally a non-destructive method.

The application range of the FFF family is wider than that of any other analytical method for the characterization of particle sizes or molar masses and includes macromolecules in solutions, emulsions and particles in suspension: the accessible molar mass for macromolecules extends from 10^3 to 10^{18} g/mol, a size range for particles from 1 nm to 100 μm. Even very complex mixtures with components spanning many orders of magnitude of particle sizes and molar masses can be successfully characterized. A particular advantage, mainly exploited in Th-FFF and Fl-FFF, is the absence of shear degradation as ultrahigh molecular weight polymers are only exposed to gentle tangential shear forces with the possible exception of higher shear forces at the inlet valve which needs to be considered.

4.2
Problems and Potential Pitfalls

As in every analytical measurement, one must be aware of the problems or potential weaknesses of an FFF measurement as well as of sources of experimental artifacts. There are a number of studies which have investigated theoretical predictions and the experimental results and pointed out error sources which lead to deviations between experiment and theory.

4.2.1
Experimental Artifacts

The numerous reasons which can account for various deviations from the ideal FFF retention theory were discussed in the corresponding sections. Here, additional problems are treated which can complicate FFF measurements and significantly distort the results obtained. General requirements for a successful FFF measurement include precise flow control and flow rate; precise temperature measurement; precise determination of t_0 and t_r; correct relaxation procedure; control of sample overloading and integrity and control of mixed normal and steric retention effects as well as wall adsorption control. Some of these complications cannot be avoided so one must correct for these effects, usually in a semiempirical and partially very complicated fashion.

On the other hand, the average FFF experiments are not designed to vary the numerous parameters which detect deviations from the ideal behavior. Therefore, the user will often not be aware of the complicating phenomena and thus get erroneous results. Hence, it appears necessary to routinely run several experiments with the same sample under varying conditions to get correct physicochemical quantities. This is a severe disadvantage which spoils the picture of FFF being a very fast and convenient absolute technique.

4.2.1.1
Artifacts Due to Sample Non-idealities/Overloading

Transport properties like the diffusion coefficient of polymers and particles depend in part drastically on the sample concentration. For random-coil polymers, the effect of concentration is especially large near the critical overlap concentration c^* [454]. In the semidilute regime, polymer coils interact and tangle with one another so that their transport through a solution is limited and, consequently, the magnitude of the diffusion coefficient drops dramatically. The higher the molecular weight and the better the solvent quality, the lower is c^*. According to these considerations, it is important to keep the polymer concentration within the channel below c^* so that diffusion and thus retention is not influenced. Above c^* overloading effects occur, such as peak "fronting", and a shift towards higher retention volumes. Excessive overloading can even result in additional peaks at higher retention volumes, probably due to polymer entan-

glements and aggregation. To estimate if the applied polymer concentration is below c*, one can calculate the sample concentration c_0 at the accumulation wall which is the highest sample concentration in the channel. Practically, c_0 can be related to the injected concentration c_{inj} by [121]:

$$c_0 = \frac{c_{inj}}{\lambda\left(1-\exp\left(-1/\lambda\right)\right)} \cong \frac{c_{inj}}{\lambda} \tag{94}$$

Substituting c_0 by the critical concentration c* in Eq. (94) gives:

$$c_{inj,max} \cong c^{*}\lambda \tag{95}$$

The maximum injectable concentration will be somewhat higher than that predicted by Eq. (95) due to zone broadening which occurs immediately after injection with consequent dilution of the sample. If it is impossible to inject concentrations below $c_{inj,max}$ due to an inadequate detection limit, or if this value is unknown, the injected concentration must be varied and the elution profiles examined in order to trace indications of sample overloading. For example, in the analysis of high molecular weight polymers ($>1\times10^6$ g/mol), concentrations below 1 mg/ml are usually required to prevent overloading. In the case of detection problems at sample concentrations below the overload concentration, especially in the case of broad distributions, the outlet stream can be split by a stream splitter (see Fig. 12 for the inlet analogon) which concentrates the outlet stream and leads to improved detector response [165,246].

The effect of sample overloading is reported to be different for the various FFF techniques. In S-FFF, sample overloading leads to earlier elution with a tailing peak shape [57]; for polymers in organic solvents, the overloading effect is opposite [121] while, for Fl-FFF, overloading results in completely distorted peaks [232] or in later sample elution [231]. This effect, however, is strongly dependent on the ionic strength of the carrier liquid. At low ionic strengths, overloading results in earlier elution whereas, at high ionic strengths, the opposite is observed [455].

Beside overloading effects, charge interaction effects play an important role in the retention behavior of polyelectrolytes [243]. In such cases, a strong dependence of the retention data on the concentration and volume of the injected polymer sample can also be observed. This phenomenon related to intermolecular interactions complicates quantitative evaluation of distributions from FFF retention data. Such effects can be partly suppressed by the addition of an electrolyte but investigations of polyelectrolytes are still complicated. Other sample–sample interactions can significantly change the effective size of the polymer and thus also its retention behavior [456]. Such interactions are common with biopolymers as they are very often part of their biological function.

The three effects mentioned above, overloading, charge effects and solute–solute interactions, were observed experimentally for various FFF techniques

early on [171,194,241] but have not as yet been satisfactorily included in the retention theory of FFF.

4.2.1.2 Solvent Effects

The carrier liquid can also influence the FFF results as it can alter solute–solute or solute–wall interactions as well as the extension of a polymer in solution [266]. This in turn influences the diffusion and retention of the sample. Limited efforts have been made to describe these phenomena so that their influence still cannot be quantitatively treated. The practical importance of solvent effects becomes clear for the example of proteins which can be switched from positive to negative polyelectrolytes by pH variation. In any case, the pH should be chosen outside the range of the isoelectric point to avoid adsorption problems.

4.2.1.3 Sample–Wall Interactions

There are many forces which can account for the interaction of a sample with the accumulation wall. Numerous electrostatic, colloidal or other forces, both of attractive and repulsive nature, influence the interaction of the sample with the wall. These effects are summarized under the term "wall effects". Recently a correction for such wall effects was presented in terms of a semiempirical correction parameter [457]. It is however not easy to determine whether or not such effects disturb the results of a particular FFF measurement. Only measurements under different conditions and with different sample concentrations and solvent compositions can show an alteration of the retention behavior caused by such wall effects.

The other important class of solute–wall interactions are the repulsive forces which are generated when a particle is driven towards the accumulation wall equal to the particle radius. This "steric exclusion" effect leads to an earlier elution of the particle [67].

A third class of solute–wall interactions is the sample adsorption to the accumulation wall which may become particularly problematic in Fl-FFF since the accumulation wall consists of a membrane. The severity of adsorption differs significantly among the limited number of membranes that have been used in Fl-FFF, so that as additional membranes are explored, one can expect improvements. A number of membranes has been tested for use for Fl-FFF with respect to sample adsorption including polypropylene, polysulfone, several supported regenerated celluloses and their derivatives and polycarbonate membranes [166]. The extent of sample adsorption obtained with the wrong membrane material is demonstrated in Fig. 33.

Sample–wall interactions may also be encountered with all other FFF techniques. The sample interaction with the accumulation wall can become a problem especially if thin channels are used to shorten elution times and to improve efficiency. For such cases, a rinsing procedure has been suggested [455].

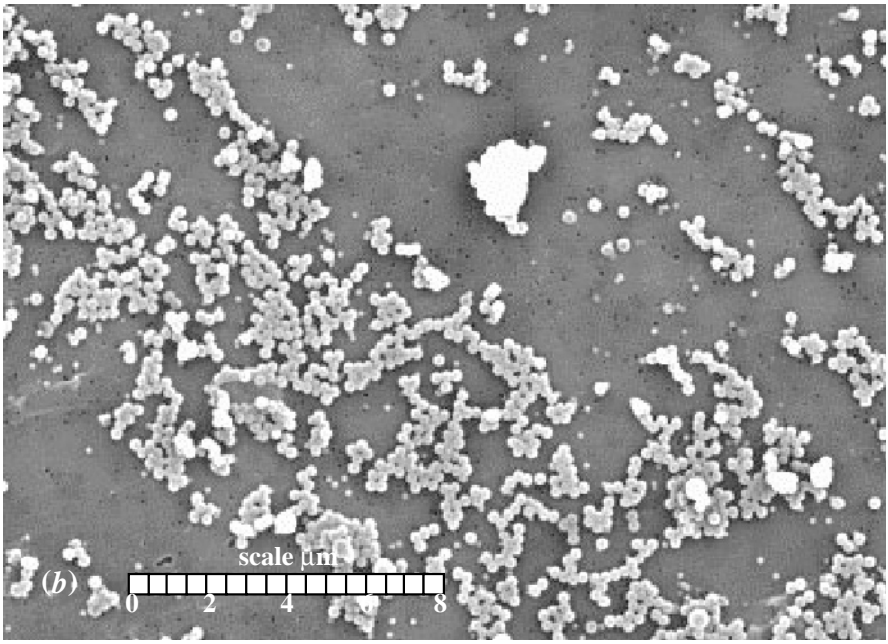

Fig. 33. SEM micrograph of a polycarbonate Fl-FFF membrane after the fractionation of a mixture of 121, 265 and 497 nm polystyrene standards. Reproduced from [166] with kind permission of the author

Another source of deviations to the ideal behavior is the smoothness of the channel surface which, in reality, is hardly perfect. The surface quality affects substantially both retention and zone dispersion. Smith et al. [223] illustrated this fact experimentally for Th-FFF. Dilks et al. [458] studied experimentally the effect of sample injection and flow pattern on the zone shape inside the channel by performing measurements in a transparent channel and photographing the colored zones formed under various conditions of injection, flow, and geometric channel irregularities. One important result was that even apparently minor channel irregularities can give rise to considerable distortion of the zone formed. In Fl-FFF, the membrane is the critical parameter as ideally it has to fulfill the requirements of pressure and mechanical stability, even surface, uniform pore size, inert behavior with respect to solvent and samples and sufficient counter pressure to achieve smooth and uniform flow rates. A membrane fulfilling all the above requirements does not exist so that the choice of a membrane for Fl-FFF is always a compromise and depends on the analytical problem. In addition, for all other FFF techniques, the surface quality, in particular the smoothness of the channel accumulation wall, substantially affects both retention and zone dispersion. Smith et al. [223] illustrated this fact experimentally for Th-FFF.

4.2.1.4 Field Programming

When using field programming, serious alterations to the retention behavior can be induced. For example, due to the initially strong fields used in programming, high molecular weight components are severely compressed early in the experiment, which can lead to chain entanglement. Therefore, when deriving quantitative information from the elution profile, it is important to change the field programme, sample concentration, or carrier flow to verify the derived distribution function of the measured quantity.

In the case of Fl-FFF, cross-flow programming may be accompanied by a "threshold" migration effect. This effect is represented by an abrupt and total cessation of zone migration when the cross-flow rate exceeds a certain threshold value, and is only poorly understood. However, the immobilization appears to reversible. In one such study [165], three poly(styrene sulfonate) standards ranging in molecular weight from 4×10^4 to 1.3×10^6 g/mol were immobilized in a Fl-FFF channel for 16 h. After the initiation of a field-decay program, the polymers were immediately released and eluted with near-baseline resolution.

4.2.1.5 Other Problems

Litzén and Wahlund systematically studied error sources like temperature effects, sample overloading, sample adsorption to the accumulation wall membrane and influences of the carrier liquid composition, that occur with Fl-FFF [455]; the latter has already been discussed above. It was shown that preservation of constant channel temperature is very important as repeated measurements of an identical sample resulted in gradually decreasing retention times due to increasing channel temperature caused by frictional heat, especially when using high flow rates. As constant channel temparature is usually not fulfilled with the standard Fl-FFF channels, which simply operate at room temperature without any temperature control, this is an important point to consider.

Non-uniform field strengths can also affect FFF results. For example in S-FFF, the centrifugal field strength inside the channel is heterogeneous due to finite channel thickness and thus different distance from the axis of rotation [105]. However, as the channel thickness is usually many times less than the radius of its coiling, this influence is negligible but will come into play if rotors with smaller diameter are designed. For El-FFF the generation of a uniform field can be a problem.

Another experimental artifact of FFF is the occurrence of "ghost peaks". Granger et al. speculated for the case of A-Fl-FFF that such peaks can occur if the sample does not reach its steady state concentration distribution and is thus transported by pure convection in the flow field which can occur at high flow rates [248]. The other peak is that for the separation by diffusion and fits well with theory.

A further experimental problem is caused by the action of hydrodynamic lift forces in A-Fl-FFF. As the mean carrier fluid velocity varies along the channel length in the rectangular channel geometries, the equilibrium positions of the particles also vary. Hence conditions may be encountered where the carrier velocity close to the outlet of a rectangular A-Fl-FFF channel falls to such a low level that lift forces are unable to counter the drag of the flow through the membrane. These particles then make contact with the membrane and do not elute [250].

4.2.2 Zone Spreading

As in every transport-based fractionating technique, zone spreading of the concentrated sample zone must occur in FFF due to the generated concentration gradient which causes diffusion according to Fick's law. Therefore, the width of a peak in an FFF fractogram consists both of the polydispersity of the sample and zone spreading due to diffusion. It is clear that significant overestimations of the sample polydispersity can be made especially if the samples are small and thus have high diffusion coefficients. In methods which study time-dependent transport processes via snapshots at a fixed time, like sedimentation in an analytical ultracentrifugation cell, a correction for zone broadening due to diffusion is possible.

In FFF, however, the fractogram is recorded in dependence of time so that a correction via extrapolation to infinite time in order to eliminate diffusion effects is not possible. A different strategy may be used for the correction of zone spreading which suffers from a number of assumptions and restrictions. A number of authors, reviewed by Janca [459], have dealt with the methods of correction for zone spreading which was found to be particularly extensive at high flow rates or low retentions. The results are summarized below.

An FFF fractogram represents the dependence of the detector response h(V) on the retention volume V. The value of h(V) at every point of the fractogram is the sum of the relative concentration of a fraction in this retention volume and of spreading contributions of the neighboring fractions of the separated solute. A relation between the experimental fractogram h(V) and the fractogram corrected for zone spreading g(Y) is given by Eq. (96).

$$h(V) = \int_{-\infty}^{+\infty} g(Y)G(V,Y)dY \tag{96}$$

where G(V,Y) is the spreading function, whose physical meaning can be explained as the zone broadening caused in the separation system and diffusion processes.

There are at least two significant contributions to the separation system: The first is the channel geometry which influences the flow patterns. Giddings et al. [89] reported, theoretically and experimentally, the intrachannel contributions to zone dispersion appearing in the triangular end pieces of an FFF channel re-

sulting in a process where parts of the solute zone follow flow paths of different lengths. The second contribution is caused by extra-channel elements of the separation system such as the injector, the detector cell, and the tubing connecting between the channel and the separation system. These contributions cannot be excluded but they must be minimized.

Equation (96) can analytically be solved only for a uniform spreading function which is a severe restriction. In such cases Eq. (96) becomes a convolution integral:

$$h(V) = \int_{-\infty}^{+\infty} g(Y) G(V - Y) dY \tag{97}$$

For many cases, especially if the spreading is small, the spreading function can be approximated by the normal Gaussian distribution function G in the form:

$$G = \left(\frac{1}{2\pi\sigma^2} \right)^{1/2} \exp\left[-\frac{(V - Y)^2}{2\sigma^2} \right] \tag{98}$$

where σ is the standard deviation of the spreading function. Its magnitude is very often considered to be constant within a very limited range of elution volumes meaning practically that Eq. (98) can be used for narrowly distributed samples only. For samples with wider distributions, a non-uniform spreading function can be used:

$$h(V) = \int_{-\infty}^{+\infty} g(Y) \left[\frac{1}{2\pi\sigma(Y)^2} \right]^{1/2} \exp\left[-\frac{(V - Y)^2}{2\sigma(Y)^2} \right] dY \tag{99}$$

which can be approximated and solved numerically by:

$$h(V) = \left[\frac{1}{2\pi\sigma(Y)^2} \right]^{1/2} \int_{V_i}^{V_f} g(Y) \exp\left[-\frac{(V - Y)^2}{2\sigma(Y)^2} \right] dY \tag{100}$$

V_I and V_f are the initial and final retention volumes between which the integration of experimental fractograms is performed.

The dependence of $\sigma(Y)$ for FFF can be calculated from the theoretical equation:

$$\sigma(Y) = \left[\frac{\chi(\lambda) w^2 < v(x) > L}{D} \right]^{1/2} \tag{101}$$

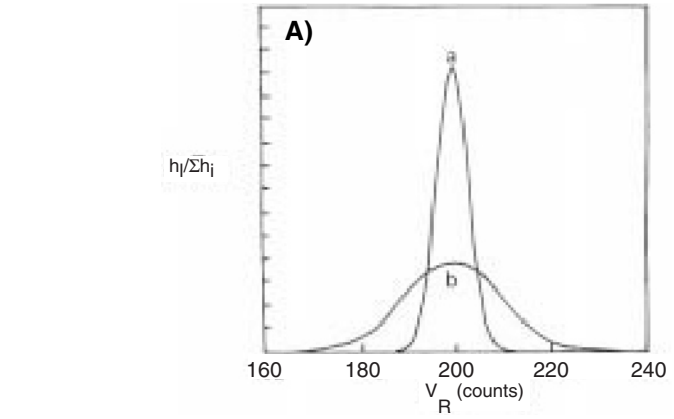

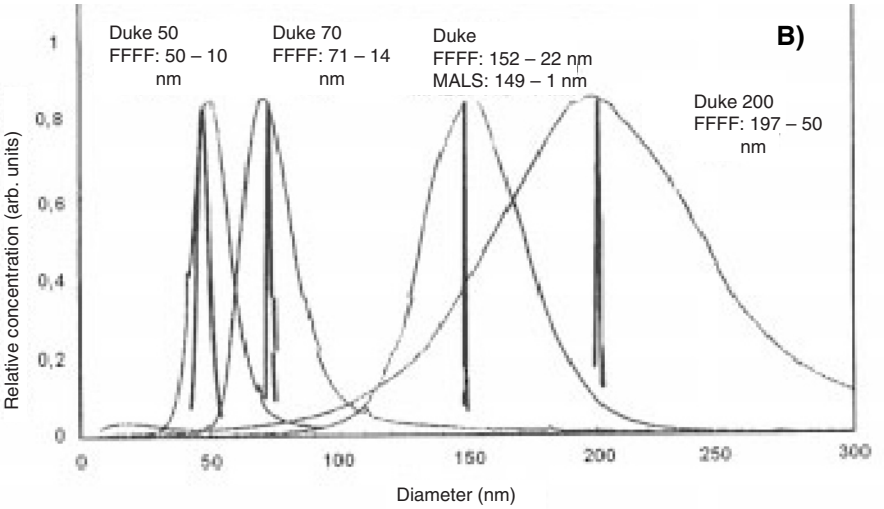

Fig. 34.A Correction for zone broadening of a model fractogram. *a* represents the original curve and the corrected one whereas *b* is the uncorrected fractogram. Reproduced from [460] with kind permission of the American Chemical Society. **B** Comparison of differential particle size distributions of narrowly distributed polystyrene latex standards derived by MALLS and Fl-FFF without correction for zone broadening. Reproduced from [461] with kind permission of Academic Press

where $\chi(\lambda)$ is a dimensionless parameter which depends on λ in a complex manner. If $\lambda \to 0$, then $\lim_{\lambda \to 0} \chi = 24\,\lambda^3$ [34] and if $\lambda \to \infty$, $\lim_{\lambda \to \infty} \chi = \frac{1}{105}$ [347].

The efficiency of the presented correction method was verified on model fractograms for different conditions. A very good correlation between the original distribution and the corrected fractogram was found for simulated data. The ne-

cessity of a correction for zone dispersion can be seen in Fig. 34 where corrected and uncorrected model fractograms are shown together with the known distribution. Figure 34B, in particular, shows the dramatic effect of band broadening.

4.2.3 *Elution of Non-Spherical Samples*

Steric hyperlayer-FFF is well established as a fast separation technique for micron-sized particles, although the hydrodynamic lift forces are not yet well understood. This is worse for the steric elution of non-spherical particles. Despite over thirty years of application of FFF techniques, only very little has been reported about the fractionation of non-spherical particles by any FFF mode. The few available studies so far reported are the investigation of coal particles [423,424], inorganic colloids [462], metal particles [69] and doublets of polystyrene beads, rod-shaped glass fibers, compressed latex discs and quartz particles with complex shape [427]. In the latter paper, systematic studies of particle shape on the retention behavior of non-spherical particles are reported with the result that the qualitative major retention behavior of spheres and other shapes is equal (e.g. response to increase in the field strength, etc.). However, the quantitative differences in the retention behavior were found to depend on numerous factors in a complex way so that no quantitative relation between the hydrodynamic radius and the retention ratio could be established.

In a recent paper, Beckett and Giddings have extended the general retention equation for the normal and steric FFF mode to include an entropy contribution associated with the orientation of non-spherical particles during the elution process [463]. The result is an increase in the mean cloud thickness l which results in an earlier elution of the sample. Interestingly, it was stated that the normal mode of S-FFF is thought to be independent of particle shape whereas some shape dependencies could be expected for Fl-FFF although the discussed entropic contributions on particle retention should be applicable to any FFF technique. Nevertheless, the independence of the normal S-FFF mode on the particle shape for moderately sized samples (axial ratio <10) was experimentally confirmed by results of Kirkland et al. [464]. They showed that for S-FFF, the shape of separated particles has only a negligible effect on retention and zone dispersion. Only with an extreme axial ratio does the dependence of retention on flow rate change. This was reported to be caused by the orientation of such particles in the flow gradient of the carrier liquid (e.g. rod-like λ-DNA [464]). As a convenient solution, a fractionation at low flow velocities was suggested at which no marked orientation of separated particles in the flow gradient should occur. Nevertheless, the entropic contributions are still likely to influence retention under these conditions as they are based on limited rotational freedom degrees near the accumulation wall [463].

Provided that the particle dimensions are known from other sources (microscopy etc.), equations were derived to correct the retention ratios for these entropic effects [463]. Nevertheless, the distortion of the elution of non-spherical

particles due to entropic contributions was also found for the normal mode in A-Fl-FFF [128]. Here, well-characterized proteins and polysaccharides of defined shapes ranging from spherical to highly elongated structures were examined by A-Fl-FFF and AUC. Whereas the shape was correctly obtained by AUC, A-Fl-FFF yielded significantly too high diffusion coefficients in the case of the elongated structures. The effect was found to increase with increasing elongation of the solute. These results confirmed the theoretical predictions of Gajdos and Brenner [88].

That no indication of the significant influence of particle shape on FFF elution behavior has been published until recently may be attributed to the fact that the majority of the approximately 500 papers so far published have reported on spherical or nearly spherical samples, and that the studies on the non-spherical samples focused only on sample fractionation rather than on a quantitative assessment of physicochemical quantities. This problem can be solved if fractions from FFF are further characterized, for example, by dynamic light scattering or if an independent detector for diffusion coefficients is available.

4.3 Recent Developments

The last few years have seen significant developments in the Fl-FFF technique with respect to increasing its application range for organic solvents, accessible physicochemical quantities (FFF/MALLS) or instrument design (frit inlet-outlet Fl-FFF). Parallel to these developments, the application of Fl-FFF as an analysis technique has increased, possibly catalyzed by the commercial availability of S-Fl-FFF as well as A-Fl-FFF channels of different designs. For other FFF techniques, instrumentation has been more or less unmodified with the exception of El-FFF so that, in the next section, only improvements to Fl-FFF are discussed. The development of the other FFF techniques is discussed in Sect. 2.

4.3.1 *Fl-FFF for Organic Solvents*

Fl-FFF is the most flexible of the FFF techniques as it is based only on the sample diffusion coefficient. Hence it was conclusive to optimize the materials used for the construction of Fl-FFF channels so that non-aqueous solvents could be applied as well. Here, the selection of a suitable membrane is the biggest problem. Brimhall et al. were the first to apply Fl-FFF for the separation of polymers in non-aqueous solvents [365]. They separated polystyrenes ($M=2.0\times10^4$–1.8×10^6 g/mol) in ethylbenzene using a cellulose nitrate membrane. Other papers on Fl-FFF using organic solvents followed from the Giddings group [121,465].

An A-Fl-FFF channel was described by Kirkland and Dilks [367] where the glass plate as the upper wall, in principle also suitable for organic solvents, was replaced by a stainless steel metal plate compatible with HPLC stainless steel connections/fittings which are better suited for organic solvents. Standard po-

ly(ethylene oxide) mixtures were fractionated in methanol with salt addition using regenerated cellulose membranes whereas polystyrenes and poly(methyl methacrylate) standards adhered to this membrane when non-protic solvents, such as toluene, were used. Hydrophobization of the membrane by silanes enabled the investigation of these samples in THF. However, the modified membranes were not optimal as the membrane dissolved in the mobile phase after three weeks of continuous use. Nonetheless, using published Mark–Houwink coefficients, molar mass distributions of the poly(ethylene oxide) samples were calculated.

In 1996, a paper was published which was dedicated to selecting suitable membranes for separations in organic solvents [466]. Membranes tested in an asymmetrical channel included polysulfone MWCO 20,000 g/mol, regenerated cellulose MWCO 20,000 g/mol, PTFE pore size 0.02 mm, polyaramide MWCO 50,000 g/mol, poly(vinylidene fluoride) MWCO 50,000 g/mol, poly(phenylene oxide) MWCO 20,000 g/mol and a DDS fluoro polymer MWCO 30,000 g/mol. The first membrane was tested with water, the others with THF or a THF/acetonitrile mixture. Numerous problems occurred with the different membranes. The best membrane for THF was found to be the DDS fluoro polymer membrane.

Recently, a "universal separator" has been developed which can be applied for aqueous and organic solvents at temperatures up to 140 °C [368]. This instrument is a specially designed Fl-FFF channel operating in an oven. Here, a PET ultrafiltration membrane with a high molar weight cut off of 30000 g/mol was applied. Solvents which were reported to be applicable were water, toluene, xylene, heptane, cyclohexane and THF.

4.3.2 *FFF Coupled with MALLS Detection*

By combining a mass-sensitive detector with multiangle laser light scattering (MALLS), both the size and molecular weight can be determined. MALLS has been used in several applications of SEC [467,468], but only recently been combined with FFF [140]. As in SEC, the FFF channel is used as a fractionating device producing almost monodisperse sample slices which are subsequently characterized by light scattering. The combination of Th-FFF with MALLS is particularly effective for ultrahigh molecular weight polymers, where high resolution and multiangle capability are critical factors. Although low molar masses are a problem for light scattering detection, molar mass distributions can still be obtained on an absolute basis by applying electrospray mass spectrometry, as has recently been suggested [152].

Lee compared the accuracy of SEC and Th-FFF with and without the use of a MALLS detector for such samples [140]. Without the MALLS detector, SEC consistently underestimated the molecular weight (M). But even with MALLS, the accuracy was limited by the resolution of SEC to achieve monodispersity in each data slice. In conclusion, Th-FFF was found to be better than SEC.

The FFF-MALLS hybrid proved to be a powerful analysis technique on an absolute basis [139,254,461]. In analogy to SEC-MALLS, the molar mass distribution as well as the radius of gyration r_G of the sample can be determined permitting the setting up of a double logarithmic plot of M vs. r_G. The slopes of these linear dependencies then provide information about the architecture and conformation of the sample. Further information about the sample can, in principle, also be derived by the determination of the hydrodynamic radius r_H via the D determination using the standard FFF evaluation from UV or RI detector responses. Then, the ratio r_G/r_H can be determined which also gives information about the particle shape, as was demonstrated and discussed in detail for different pullulan standards by Adolphi and Kulicke [469] and for bovine serum albumin (spherical) and tobacco mosaic virus (rod) by Thielking and Kulicke [470].

With respect to the virtually very low sample loads, one could argue that the determined diffusion coefficient is at infinite dilution. However, there is no possibility in FFF techniques to perform a safe extrapolation to infinite dilution as in analytical ultracentrifugation or dynamic light scattering. In addition there is a severe problem for all particles deviating from the spherical shape (see Sect. 4.2.3 for a detailed discussion), as the evaluation of D from the FFF experiments using the conventional theory is inappropriate.

In principle, every FFF technique is suitable for MALLS coupling. The first papers on an S-FFF-MALLS hybrid appeared as early as 1991 [53]. The coupling of Th-FFF to MALLS proved to be especially advantageous, as demonstrated for polystyrene polymers and microgels and poly(styrene sulfonates) [109,471] or, more recently, for polybutadienes or natural rubbers [374]. S-FFF-MALLS was applied for the characterization of starch polymers, a type of sample which is very sensitive to shear [137]. Many more applications have been reported for Fl-FFF-MALLS. S-Fl-FFF-MALLS was successfully used for the molar mass characterization of polystyrene latexes and dextran [135], size characterization of polystyrene standards 50–300 nm [136] and 50–500 nm [139], sulfonated poly(styrene sulfonate) standards (18×10^3–3×10^6 g/mol) [138], bovine serum albumin and size differences between different polystyrene standard latex batches of only 3% [374] (see also Fig. 31), and to characterize poly(diallyldimethylammonium chloride) (poly-DADMAC, a polycation) and pectin (complex system with aggregates) [470]. Recently, the advantages of the MALLS coupling to Fl-FFF for the measurement of particle size distributions of shear sensitive vesicles [472] or the molar mass distributions of shear sensitive commercial ultrahigh molar mass polyacrylamides in the range 0.35–9×10^6 g/mol [166,364] have been elucidated.

A-Fl-FFF/MALLS has been used for the determination of the molar mass and size distribution of dextrans and pullulans of various molar masses [473], hydroxypropylmethylcelluloses [474] and κ-carrageenan in different conformations and aggregation states [475].

Recently, the advantages of coupling FFF to MALLS with respect to the traditional evaluation of an identical FFF experiment with a UV or an RI detector have been pointed out by Wyatt, who demonstrated the tiny differences between

the apparent particle sizes derived from both evaluations for different PS latex standards [461]. In this paper, experimentally determined particle size distributions of polystyrene latex mixtures, emulsions and liposomes were presented, using S-Fl-FFF and El-FFF coupled with MALLS [461].

For more complex solute mixtures, it is obvious that the change of the light scattering regime from Rayleigh to Mie scattering is a problem if the particle size approaches the wavelength of the light.

4.3.3
Other Fl-FFF Improvements

Zahoransky et al. described an improved Fl-FFF channel which assures a uniform cross-flow in the whole channel [476]. This is achieved by a division of the hollow compartment under the membrane supporting frit into three separate chambers with an independent pressure control. By means of special spring-loaded clamping devices, the spacer and membrane change is reported to be simple, thus making the whole experimental handling with this new channel convenient.

Beside the frit inlets for Fl-FFF (see Fig. 12) which help to enhance the sample relaxation, Moon et al. have recently suggested a frit inlet which applies a small permeable frit near the injection point in the A-Fl-FFF channel [51,401]. As sample materials injected into the flow streams are hydrodynamically relaxed by the compressing action of high speed frit flow, the usual focusing relaxation procedure can be avoided which makes the experiment more reliable and faster.

Frit outlets which work in reverse to the frit inlets (see Fig. 12) have been constructed allowing a sample concentration due to the fact that the sample is compressed near the accumulation wall so that the majority of the solvent containing no sample can leave through the frit thus concentrating the sample at the outlet [52].

Such sample concentration procedures are very important, since one must often cope with a very poor detector response if the sample is not concentrated at the outlet. For very diluted analytes, a new on-line sample concentration method called "opposed flow sample concentration" (OFSC) has recently been proposed and tested for Fl-FFF [477]. This method applies two opposing flowstreams to focus sample into a narrow band near the inlet of the Fl-FFF channel which enables concentration factors up to 10^5 to be achieved. Such a concentration procedure appears particularly interesting for environmental samples. An example for the concentration of river water colloids was given.

4.4
Outlook to the Future

Looking at recent FFF developments, one can try to predict some future trends. One is certainly the on-line coupling of absolute techniques like MALLS to the fractionating FFF channel which can yield very fast determinations of the distribution of molar mass and other molecular properties. In this respect, the poten-

tial of other detection techniques like electrospray mass spectroscopy (molar mass) or ICP-MS (for chemical composition) is also promising. The better and smoother separation characteristics of an FFF channel compared to SEC or other chromatographic techniques with a stationary phase, combined with the very large application range, make FFF particularly well suited for such coupling.

Another important trend is focused on faster and more efficient analyses, requiring thinner channels and stronger, more uniform fields. Thinner channels enhance the separation speed of FFF dramatically due to the square dependence of the retention time on the channel thickness [118,478,479]. Applying stronger and more uniform fields definitely has its physical and/or experimental limits. For example, in Th-FFF, the field is limited by the cooling capacity at the cold wall. Regarding the uniformity of the field, Th-FFF separations have benefited greatly from improvements in the path of water flow through the cold wall.

In A-Fl-FFF, field-strength limitations are governed by the channel pressure required to drive carrier liquid through the small pore membrane, necessary to retain the analyte. The back pressure caused by the accumulation wall membrane keeps the field fairly uniform throughout the channel, so long as the pressures at the axial- and cross-flow outlets are equalized through the adjustment of the back-pressure valve. Future work may focus on a more automated method for controlling the back pressure, so that the field strength can be varied without operator assistance. Automated control of the back pressure will also make field programming more attractive for A-Fl-FFF.

Another development with much potential benefit is the design of new channels and membranes for Fl-FFF in order to make this technique truly universally applicable. However, at the moment, the design of these novel membranes which will fulfill all of the numerous requirements of Fl-FFF is proceeding only very slowly and may even be impossible.

A further interesting development is multidimensional FFF where several FFF separation mechanisms are coupled, like helical Fl-FFF. Such techniques certainly have much future potential as they combine the merits of two or maybe even more FFF methods with all the possible information of each of the combined FFF techniques. However, the effective practical realization is a current problem which deserves attention.

Applying FFF techniques for preparative separations in the form of SPLITT channels also seems to be very promising. Here, future developments must concentrate not only on the application of other physical fields for the separation in SPLITT but also on the coupling of various SPLITT channels with different cut off limits to design a preparative fractionator for broadly distributed samples.

Other future FFF developments may address the highly desired continuous preparative FFF fractionation apart from SPLITT channels. This requires the following experimental conditions:

– Very fast hydrodynamic relaxation as can be achieved by stream splitters or frit inlets (see Fig. 12) so that there is no need for a stop-flow or focusing period. It is important that the injection time can serve as a triggering pulse for an automated fractionator coupled to the FFF outlet.

- Sample concentration after the sample fractionation as can be achieved by stream splitters or frit outlets.
- Automated, computer-controlled fractionation from the FFF outlet coupled to the injection time.
- Automated repetition of the sample injection after one fractionation cycle which is indicated by a signal decrease of a concentration detector to the baseline signal. If samples with multimodal distributions are to be fractionated, the threshold logic for sample reinjection needs to be modified accordingly.
- Highly stable flow and field strength conditions.

Even then the fractionation of gram quantities will be tedious and time-consuming work if one considers that the typical amount per injection into an FFF channel is in the μg range. Nevertheless, the fractionation of mg amounts of samples is especially interesting for modern biopolymer samples, such as DNS fragments, or molecular factors which are produced in such amounts.

5 Conclusions

It is clear that FFF comprises a family of flexible analytical techniques which can supply a tremendous amount of physicochemical information when complimentary FFF methods are used. Also, the application range (1 nm–100 μm for colloids or 1000 g/mol up to more than 10^{18} g/mol for polymers) is larger than with any other analytical technique for particle size or molar mass measurement coupled with usually short measurement times.

There are, however, also some drawbacks to these techniques: The inversion of elution from the normal to the steric mode complicates measurements in the particle size range around 1 μm and, although this transition region can be shifted by experimental conditions, serious interpretation errors can occur if the particle size distribution spans this transition region.

In addition, quantitative evaluation of FFF experiments shows that the idealized FFF theory can only rarely be applied. Numerous corrections taking account of the various deviations from the idealized behavior may become necessary. On the other hand, qualitative information on a separation and the number of resolved components is often already sufficient. If an independent absolute detector like MALLS is coupled to the FFF channel, FFF can be operated as a relative separation device. Even in this restricted mode, FFF offers numerous advantages for polymer analysis over the dominant SEC (see Sect. 1.5.1).

FFF is therefore regarded as an extremely promising, but still underdeveloped, technique and many other experimental problems remain to be overcome, like sample adsorption to the walls and solute–solute interactions, etc., which keep FFF from being a "black box" universal laboratory analytical technique. The experimental conditions have to be optimized for the specific sample of interest. Nevertheless, in the hands of an expert, FFF shows a superb resolution

and is thus well suited for a large variety of problems in fundamental research, industrial production control, biotechnology or environmental analysis.

FFF is an analytical technique well deserving of a more widespread application at least in its most developed variants: Fl-FFF, Th-FFF and S-FFF. Especially for complex colloidal or particulate matter, emulsion and dispersion technology, there are many advantages of FFF which certainly justify the implementation and research in most analytical laboratories dealing with such problems.

6 FFF on the Internet

Currently, there are two Internet web sites which are devoted to FFF methods. The first is based at the University of Ferrara, Italy: http://dns.unife.it/~rsk/ and gives an introduction to various FFF techniques as well as a short literature review on Gr-FFF. Furthermore, a "Who is Who in the FFF World" library is found there which lists the expertises and experimental equipment of various workers in the FFF field.

The other server is an FFF literature database at Rohm & Haas: http://www.rohmhaas.com/fff/ which is updated frequently. It is possible to get e-mail notice on database updates. Furthermore, it is planned to install an FFF user discussion forum on this web site.

Acknowledgements. The authors thank A. Pape for substantial help with manuscript typing and U. Ziehut for large parts of the artwork. Dr. R. Hecker is acknowledged for careful proofreading of the manuscript and several useful suggestions towards the quality of the manuscript.

References

1. Giddings JC (1966) Sep Sci 1:123
2. Gunderson JJ, Giddings JC (1989) Field-flow fractionation. In: Booth C, Price C (eds) Polymer characterization. Pergamon, Oxford, pp 279–291
3. Caldwell KD (1988) Anal Chem 60:959A
4. Giddings JC (1981) Anal Chem 53:1170A
5. Lightfoot EN, Chiang AS, Noble PT (1981) Annu Rev Fluid Mech 13:351
6. Kirkland JJ, Rementer SW, Yau WW (1981) Anal Chem 53:1730
7. Giddings JC, Graff KA, Caldwell KD, Myers MN (1983) Adv Chem Ser 203:257
8. Janca J, Kleparnik K, Jahnova V, Chmelik J (1984) J Liq Chrom 7:1
9. Giddings JC, Caldwell KD, Jones HK (1987) Measuring particle size distribution of simple and complex colloids by sedimentation field-flow fractionation. In: Provder T (ed) Particle size distribution: assessment and characterization. American Chemical Society, Washington, DC, pp 215–230
10. Janca J (1987) Chem Listy 81:1034
11. Beckett R, Bigelow JC, Jue Z, Giddings JC (1989) Analysis of humic substances using flow field-flow fractionation. In: MacCarthy P, Suffet IH (eds) Influences of aquatic humic substances on fate and treatment of pollutants. American Chemical Society, Washington, DC, pp 65–80

12. Giddings JC, Barman BN, Liu MK (1991) Separation of cells by field-flow fractionation and related methods. In: Kompala DS, Todd P (eds) Cell separation science and technology. American Chemical Society, Washington, DC, pp 128–144
13. Levin S (1991) Biomed Chromatogr 5:133
14. Giddings JC (1993) Science 260:1456
15. Myers MN, Chen P, Giddings JC (1993) Polymer separation and molecular-weight distribution by thermal field-flow fractionation. In: Provder T (ed) Chromatography of polymers: characterization by SEC and FFF. American Chemical Society, Washington, DC, pp 47–62
16. Barman BN, Giddings JC (1993) Separation and characterization of polymer latex beads and aggregates by sedimentation field-flow fractionation. In: Provder T (ed) Chromatography of polymers: characterization by SEC and FFF. American Chemical Society, Washington, DC, pp 30–46
17. Ratanathanawongs SK, Giddings JC (1993) Particle size analysis using field-flow fractionation. In: Provder T (ed) Chromatography of polymers: characterization by SEC and FFF. American Chemical Society, Washington, DC, pp 13–29
18. Janca J (1993) Mikrochim Acta 111:135
19. Mori Y (1994) Adv Colloid Interf Sci 53:129
20. Giddings JC, Ratanathanawongs SK, Barman BN, Moon MH, Liu GY, Tjelta BL, Hansen ME (1994) Adv Chem Ser 234:309
21. Schimpf ME (1996) Trends Polym Sci 4:114
22. Myers MN (1997) J Microcolum Sep 9:151
23. Moon MH, Lee SH (1997) J Microcolum Sep 9:565
24. Janca J (1997) J Liq Chromatogr Rel Technol 20:2555
25. Martin M (1998) Theory of field-flow fractionation. In: Brown PR, Grushka E (eds) Advances in chromatography. Marcel Dekker, New York, pp 1–138
26. Janca J (1998) Chem Listy 92:449
27. Janca J (1988) Field-flow fractionation: analysis of macromolecules and particles. Marcel Dekker, New York
28. Giddings JC (1991) Unified separation science. John Wiley & Sons, New York
29. Thompson GH, Myers MN, Giddings JC (1967) Sep Sci 2:797
30. Berg HC, Purcell EM (1967) Proc Natl Acad Sci USA 58:862
31. Berg HC, Purcell EM (1967) Proc Natl Acad Sci USA 58:821
32. Berg HC, Purcell EM (1967) Proc Natl Acad Sci USA 58:1286
33. Giddings JC (1968) J Chem Phys 49:81
34. Hovingh ME, Thompson GH, Giddings JC (1970) Anal Chem 42:195
35. Caldwell KD, Kesner LF, Myers MN, Giddings JC (1972) Science 176:296
36. Kesner LF, Caldwell KD, Myers MN, Giddings JC (1976) Anal Chem 48:1834
37. Lee HL, Reis JFG, Dohner J, Lightfoot EN (1974) AIChE J 20:776
38. Yang FJF, Myers MN, Giddings JC (1974) Anal Chem 46:1924
39. Giddings JC, Smith LK, Myers MN (1976) Anal Chem 48:1587
40. Giddings JC, Caldwell KD, Moellmer JF, Dickinson TH, Myers MN, Martin M (1979) Anal Chem 48:30
41. Giddings JC, Yang FJF, Myers MN (1976) Anal Chem 48:1126
42. Giddings JC, Yang FJF, Myers MN (1977) Sep Sci Technol 12:381
43. Giddings JC, Martin M, Myers MN (1979) Sep Sci Technol 14:611
44. Doshi MR, Gill WN (1979) Chem Eng Sci 34:725
45. Vickrey TM, Garcia-Ramirez JA (1980) Sep Sci Technol 15:1297
46. Giddings JC, Brantley SL (1984) Sep Sci Technol 19:631
47. Wahlund KG, Giddings JC (1987) Anal Chem 59:1332
48. Liu M-K, Williams PS, Myers MN, Giddings JC (1991) Anal Chem 63:2115
49. Liu MK, Li P, Giddings JC (1993) Protein Sci 2:1520
50. Dean GA, Cardile CM, Stead RJ, Alecu ID (1994) J Mater Sci Lett 13:872
51. Moon MH, Kwon H, Park I (1997) J Liq Chrom Related Tech 20:2803

52. Li P, Hansen M, Giddings JC (1998) J Microcol Sep 10:7
53. Wyatt PJ (1991) Polym Mat Sci Eng 65:198
54. Giddings JC, Kumar V, Williams PS, Myers MN (1990) Polymer separation by thermal field-flow fractionation: high speed power programming. In: Craver CD, Provder T (eds) Polymer characterization: physical properties, spectroscopic, and chromatographic methods. American Chemical Society, Washington, DC, pp 1–21
55. Gunderson JJ, Giddings JC (1986) Macromolecules 19:2618
56. Mori Y, Scarlett B, Merkus HG (1990) J Chromatogr 515:27
57. Hansen ME, Giddings JC, Beckett R (1989) J Coll Interf Sci 132:300
58. Sisson R, Giddings JC (1994) Anal Chem 66:4043
59. Benincasa MA, Giddings JC (1992) Anal Chem 64:790
60. Giddings JC, Benincasa MA, Liu M-K, Li P (1992) J Liq Chromatogr 15:1729
61. Williams PS, Moon MH, Xu Y, Giddings JC (1996) Chem Eng Sci 51:4477
62. Williams PS, Moon MH, Giddings JC (1996) Colloids Surf A 113:215
63. Small H (1974) J Colloid Interface Sci 48:147
64. Husain A, Hamielec AE, Vlachopoulos J (1981) J Liq Chromatogr 4(S-2):295
65. Penlidis A, Hamielec AE, MacGregor JF (1983) J Liq Chromatogr 6:179
66. Jahnová V, Janca J (1984) Chem Listy 78:346
67. Giddings JC (1978) Sep Sci Technol 13:241
68. Myers MN, Giddings JC (1982) Anal Chem 54:2284
69. Moon MH, Giddings JC (1992) Anal Chem 64:3029
70. Schauer T (1995) Part Syst Charact 12:284
71. Giddings JC (1983) Sep Sci Technol 18:765
72. Janca J (1982) Makromol Chem Rapid Commun 3:887
73. Janca J (1983) Makromol Chem Rapid Commun 4:267
74. Janca J, Chmelik J (1984) Anal Chem 56:2481
75. Caldwell KD, Li J (1989) J Colloid Interface Sci 132:256
76. Kirkland JJ, Rementer SW, Yau WW (1989) J Appl Polym Sci 38:1383
77. Giddings JC (1988) Chem Eng News 66:34
78. Chase MW, Davies CA, Downey JR, Frurip DJ, McDonald RA, Syverud AN (1985) Janaf thermochemical tables, 3rd edn. 1. AL-CO. J Phys Chem Ref Data 14 (Suppl 1):1–926
79. Williams PS, Koch T, Giddings JC (1992) Chem Eng Comm 111:121
80. Giddings JC, Yang FJF, Myers MN (1975) Sep Sci 10:133
81. Giddings JC, G. Karaiskakis, Caldwell KD, Myers MN (1983) J Colloid Interface Sci 92:66
82. Giddings JC, Karaiskakis K, Caldwell KD (1981) Sep Sci Technol 16:607
83. Janca J, Jahnova V (1983) J Liq Chrom 6:1559
84. Schimpf ME, Giddings JC (1989) J Polym Sci Polym Phys Ed 27:1317
85. Giddings JC (1973) J Chem Educ 50:667
86. Giddings JC (1973) Sep Sci 8:567
87. Krishnamurthy S, Subramanian RS (1977) Sep Sci 12:347
88. Gajdos LJ, Brenner H (1978) Sep Sci Technol 13:215
89. Giddings JC, Schure MR, Myers MN, Velez GR (1984) Anal Chem 56:2099
90. Davis JM, Giddings JC (1985) J Phys Chem 89:3398
91. Giddings JC (1986) Anal Chem 58:735
92. Berthod A, Armstrong DW (1987) Anal Chem 59:2410
93. Andreev VP, Semenov SN, Kustensov AA, Reifman LS (1987) Zh Fiz Khim 61:1
94. Giddings JC, Schure MR (1987) Chem Eng Sci 42:1471
95. Ugrozov VV (1989) Zh Fiz Khim 62:89
96. Davis JM (1989) Sep Sci Technol 24:219
97. Martin M, Williams PS (1992) Theoretical basis of field-flow fractionation. In: Dondi F, Guichon G (eds) Theoretical advancement in chromatography and related separation techniques. Kluver, Dordrecht, pp 513–580
98. Andreev VP, Stefanovich LA (1993) Chromatographia 37:325

99. Giddings JC (1993) J Microcol Sep 5:497
100. Williams PS, Giddings JC (1994) Anal Chem 66:4215
101. Buffham BA (1996) J Colloid Interface Sci 181:490
102. Semenov SN (1996) Zh Fiz Khim 70:1674
103. Zolotarev PP, Ugrozov VV, Skornyakov EP (1988) Zh Fiz Khim 62:1896
104. Davis JM, Giddings JC (1986) Sep Sci Technol 21:969
105. Davis JM (1986) Anal Chem 58:161
106. Hoyos M, Martin M (1994) Anal Chem 66:1718
107. Schure MR, Caldwell KD, Giddings JC (1986) Anal Chem 58:1509
108. Janca J, Chmelik J, Jahnove V, Novekove N, Urbenkov E (1991) Chem Anal 36:657–666
109. Tank C (1995) Trennung und Charakterisierung komplexer Polymere und Kolloide durch Feld-Fluß Fraktionierung. PhD Thesis, Technische Universität Berlin, Germany
110. Schimpf ME, Giddings JC (1987) Macromolecules 20:1561
111. Schimpf ME, Giddings JC (1990) J Polym Sci Part B Polym Phys 28:2673
112. Ko G-H, Richards R, Schimpf ME (1996) Sep Sci Technol 31:1035
113. Giddings JC (1994) Anal Chem 66:2783
114. Schimpf ME (1990) J Chromatogr 517:405
115. Gunderson JJ, Giddings JC (1986) Anal Chim Acta 189:1
116. Stegemann G, van Asten AC, Kraak JC, Poppe H, Tijssen R (1994) Anal Chem 66:1147
117. van Asten AC, Stegemann G, Kok WT, Tjissen R, Poppe H (1994) Anal Chem 66:3073
118. Giddings JC, Martin M, Myers MN (1978) J Chromatogr 158:419
119. Schimpf ME (1993) Ind J Technol 31:443
120. Hellmann MY (1977) In: Cazes J (ed) Liquid chromatography of polymers and related materials. Marcel Dekker, New York, pp 29–39
121. Caldwell KD, Brimhall SL, Gao Y, Giddings JC (1988) J Appl Polym Sci 36:703
122. Schimpf ME, Williams PS, Giddings JC (1989) J Appl Polym Sci 37:2059
123. Schimpf ME, Myers MN, Giddings JC (1987) J Appl Polym Sci 33:117
124. Freifelder D (1982) Applications to biochemistry and molecular biology. In: Physical biochemistry. WH Freeman and Co., San Francisco, chap 13
125. Bird RB, Armstrong RC, Hassager O (1977) In: Dynamics of polymeric liquids. John Wiley, New York, pp 169–253
126. Gao YS, Caldwell KD, Myers MN, Giddings JC (1985) Macromolecules 18:1272
127. Li J, Caldwell KD, Mächtle W (1990) J Chromatogr 517:361
128. Pauck T, Cölfen H (1998) Anal Chem 70:3886
129. Yau WW, Kirkland JJ (1981) J Chromatogr 218:217
130. Yang FS, Caldwell KD, Giddings JC (1983) J Colloid Interface Sci 92:81
131. Janca J, Pribylova D, Bouchal K, Tyrackova V, Zurkova E (1986) J Liq Chromatogr 9:2059
132. Vickrey TM (1983) Liquid chromatography detectors. Chromatogr Sci Ser. Marcel Dekker, New York, chap 23, p 434
133. Ouano AC, Kaye W (1974) J Polym Sci Polym Chem Ed 12:1151
134. Martin M, Hes J (1984) Sep Sci Technol 19:685
135. Roessner D, Kulicke W-M (1994) J Chromatogr A 687:249
136. Thielking H, Roessner D, Kulicke WM (1995) Anal Chem 67:3229
137. Hanselmann R, Ehrat M, Widmer HM (1995) Starch/Stärke 46:345
138. Thielking H, Kulicke WM (1996) Anal Chem 68:1169
139. Shortt DW, Roessner D, Wyatt PJ (1996) Am Lab 28:21
140. Lee S, Kwon O-S (1995) Determination of molecular weight and size of ultrahigh molecular weight polymers using thermal field-flow fractionation and light scattering. In: Provder T, Barth HG, Urban MW (eds) Chromatographic characterization of polymers: hyphenated and multidimensional techniques. Amercian Chemical Society, Washington, DC, pp 93–107
141. Oppenheimer LE, Mourey TH (1984) J Chromatogr 298:217

142. Schimpf ME (1995) Determination of molecular weight and composition in copolymers using thermal field-flow fractionation combined with viscometry. In: Provder T, Barth HG, Urban MW (eds) Chromatographic characterization of polymers: hyphenated and multidimensional techniques. American Chemical Society, Washington, DC, pp 183–196
143. Caldwell KD, Jones HK, Giddings JC (1986) Colloids Surf 18:123
144. Kirkland JJ, Rementer SW (1992) Anal Chem 64:904
145. Kirkland JJ, Rementer SW, Yau WW (1991) J Appl Polym Sci Appl Polym Symp 48:39
146. Stabinger H, Leopold H, Kratky O (1967) Monatsh Chem 98:436
147. Trathnigg B, Jorde C (1984) J Liq Chromatogr 7:1789
148. Kirkland JJ, Yau WW (1991) J Chromatogr 550:799
149. Beckett R (1991) At Spectrosc 12 (special issue):228
150. Taylor HE, Garbarino JR, Murphy DM, Beckett R (1992) Anal Chem 64:2036
151. Murphy DM, Garbarino JR, Taylor HW, Hart BT, Beckett R (1993) J Chromatogr 642:459
152. Hassellöv M, Hulthe G, Lyven B, Stenhagen G (1997) J Liq Chromatgr Rel Technol 20:2843
153. Wyatt PJ (1993) Anal Chim Acta 272:1
154. Barth HG, Boyes BE, Jackson C (1996) Anal Chem 68:445R
155. Lee S, Rao SP, Moon MH, Giddings JC (1996) Anal Chem 68:1545
156. Blo G, Contado C, Fagioli F, Rodriguez MHB, Dondi F (1995) Chromatographia 41:715
157. Dondi F, Blo G, Martin M (1997) Annali di Chimica 87:113
158. Giddings JC (1985) Anal Chem 57:945
159. Lee S, Myers MN, Giddings JC (1989) Anal Chem 61:2439
160. Giddings JC (1990) Anal Chem 62:2306
161. Williams PS, Giddings JC, Beckett R (1987) J Liq Chromatogr 10:1961
162. Grushka E, Caldwell KD, Myers MN, Giddings JC (1973) Field-flow fractionation. In: Perry ES, Oss CJV, Grushka E (eds) Separation and purification methods. Marcel Dekker, New York, pp 127–151
163. Giddings JC, Caldwell KD (1984) Anal Chem 56:2093
164. Kirkland JJ, Yau WW (1985) Macromolecules 18:2305
165. Wahlund K-G, Winegarner HS, Caldwell KD, Giddings JC (1986) Anal Chem 58:573
166. Hecker R (1998) The characterization of polyacrylamide flocculants. PhD Thesis, Curtin University of Technology, Perth, Australia
167. Yau WW, Kirkland JJ (1981) Sep Sci Technol 16:577
168. Kirkland JJ, Rementer SW, Yau WW (1988) Anal Chem 60:610
169. Williams PS, Giddings JC (1987) Anal Chem 59:2038
170. Kirkland JJ, Yau WW (1990) J Chromatogr 499:655
171. Kirkland JJ, Yau WW, Doerner WA, Grant JW (1980) Anal Chem 52:1944
172. Yang FJ, Myers MN, Giddings JC (1977) J Colloid Interface Sci 60:574
173. Wyatt PJ, Villalpando D (1997) Langmuir 13:3913
174. Giddings JC, Yang FJF, Myers MN (1974) Anal Chem 46:1917
175. Giddings JC, Myers MN, Caldwell KD, Fisher SR (1980) Analysis of biological macromolecules and particles by field-flow fractionation. In: Glick D (ed) Methods of biochemical analysis. John Wiley, New York, pp 79–136
176. Kirkland JJ, Dilks CH Jr, Yau WW (1983) J Chromatogr 255:255
177. Mächtle W (1992) Analysis of polymer dispersions with an eight cell AUC-multiplexer: High resolution particle size distribution and density gradient techniques. In: Harding SE, Rowe AJR, Horton JC (eds) Analytical ultracentrifugation in biochemistry and polymer science. The Royal Society of Chemistry, Cambridge, pp 147–175
178. Cölfen H (1998) unpublished results
179. Kirkland JJ, Yau WW (1982) Science 218:121
180. Mächtle W (1984) Makromol Chem Macromol Chem Phys 185:1025
181. Müller HG, Herrmann F (1995) Progr Colloid Polym Sci 99:114

182. Yonker CR, Caldwell KD, Giddings JC, van Etten JL (1985) J Virol Methods 11:145
183. Caldwell KD, Karaiskakis G, Myers MN, Giddings JC (1981) J Pharm Sci 70:1350
184. Moon MH, Giddings JC (1993) J Pharm Biomed Anal 11:911
185. Li JT, Caldwell KD (1991) Langmuir 7:2034
186. Beckett R, Ho J, Jiang Y, Giddings JC (1991) Langmuir 7:2040
187. Langwost B, Caldwell KD (1992) Chromatographia 34:317
188. Caldwell KD, Li J, Li J-T, Dalgleish DG (1992) J Chromatogr 604:63
189. Giddings JC, Karaiskakis G, Caldwell KD (1981) Sep Sci Technol 16:725
190. Giddings JC, Yang FS (1985) J Colloid Interface Sci 105:55
191. Karaiskakis G, Myers MN, Caldwell KD, Giddings JC (1981) Anal Chem 53:1314
192. Giddings JC (1986) Anal Chem 58:2052
193. Thompson GH, Myers MN, Giddings JC (1969) Anal Chem 41:1219
194. Myers MN, Caldwell KD, Giddings JC (1974) J Sep Sci 9:47
195. Sanyal SK, Adhikari M (1981) J Indian Chem Soc 58:1055
196. Giddings JC, Myers MN, Janca J (1979) J Chromatogr 186:37
197. Martin M, Reynaud P (1980) Anal Chem 52:2293
198. Giddings JC, Martin M, Myers MN (1981) J Polym Sci Polym Phys Ed 19:815
199. Janca J, Klepárník K (1981) Sep Sci Technol 16:657
200. Giddings JC, Smith LK, Myers MN (1975) Anal Chem 47:2389
201. Emery AH, Drickamer HG (1955) J Chem Phys 23:2252
202. Bonner FJ (1967) Ark Kemi 27:19
203. Grew KE (1969) Transport phenomena in fluids. Marcel Dekker, New York
204. Giddings JC, Caldwell KD, Myers MN (1976) Macromolecules 9:106
205. Gunderson JJ, Caldwell KD, Giddings JC (1984) Sep Sci Technol 19:667
206. Giddings JC (1976) J Chromatogr 125:3
207. Brochard F, Martin M (1982) Bull Soc Fr Phys 46:17
208. Brochard-Wyart F (1983) Macromolecules 16:149
209. Giddings JC, Hovingh ME, Thompson GH (1970) J Phys Chem 74:4291
210. Ngyuen M, Beckett R (1993) Polym Int 30:337
211. Nguyen M, Beckett R (1996) Sep Sci Technol 31:291
212. Nguyen M, Beckett R (1996) Sep Sci Technol 31:453
213. Köhler W (1993) J Chem Phys 98:660
214. Schimpf ME, Wheeler LM, Romeo PF (1993) Copolymer retention in thermal field-flow fractionation: dependence on composition and conformation. In: Provder T (ed) Chromatography of polymers: characterization by SEC and FFF. American Chemical Society, Washington, DC, pp 63–76
215. Liu G, Giddings JC (1992) Chromatographia 34:483
216. Pauck T, Cölfen H, unpublished results
217. van Asten AC, Boelens HFM, Kok WT, Poppe H, Williams PS, Giddings JC (1994) Sep Sci Technol 29:513
218. Westerman-Clark G (1978) Sep Sci Technol 13:819
219. Belgaied JE, Hoyos M, Martin M (1994) J Chromatogr A 678:85
220. Giddings JC (1979) Pure Appl Chem 51:1459
221. Brimhall SL, Myers MN, Caldwell KD, Giddings JC (1981) Sep Sci Technol 16:671
222. Kirkland JJ, Yau WW (1986) J Chromatogr 353:95
223. Smith LK, Myers MN, Giddings JC (1977) Anal Chem 49:1750
224. Martin M, Myers MN, Giddings JC (1979) J Liq Chromatogr 2:147
225. Giddings JC, Myers MN, Moellmer JF (1978) J Chromatog 149:501
226. Ratanathanawongs SK, Lee I, Giddings JC (1991) Separation and characterization of 0.01–50 μm particles using flow field-flow fractionation. In: Provder T (ed) Particle size distribution II. American Chemical Society, Washington, DC, pp 229–246
227. Beckett R, Jue Z, Giddings JC (1987) Environ Sci Technol 21:289
228. Giddings JC, Yang FJ, Myers MN (1976) Science 193:1244
229. Lee HL, Lightfoot EN (1976) Sep Sci Technol 11:417

230. Davis JM (1991) Anal Chim Acta 246:161
231. Wahlund KG, Litzén A (1989) J Chromatogr 461:73
232. Litzén A, Wahlund KG (1989) J Chromatogr 476:413
233. Kirkland JJ, Dilks Jr CH, Rementer SW, Yau WW (1992) J Chromatogr 593:339
234. Joensson JA, Carlshaf A (1989) Anal Chem 61:11
235. Carlshaf A, Jönsson A (1989) J Chromatogr 461:89
236. Carlshaf A, Jonsson JA (1991) J Microcol Sep 3:411
237. Granger J, Dodds J (1992) Sep Sci Technol 27:1691
238. Carlshaf A, Jonsson JA (1993) Sep Sci Technol 28:1031
239. Wijnhoven JEGJ, Koorn JP, Poppe H, Kok WT (1995) J Chromatogr 699:119
240. Giddings JC, Yang FJ, Myers MN (1977) Anal Biochem 81:395
241. Giddings JC, Yang FJ, Myers MN (1977) J Virol 21:131
242. Giddings JC, Lin GC, Myers MN (1978) J Colloid Interface Sci 65:67
243. Giddings JC, Lin GC, Myers MN (1978) J Liq Chromatogr 1:1
244. Giddings JC (1984) Sep Sci Technol 19:831
245. Yang FJ, Myers MN, Giddings JC (1977) Anal Chem 49:659
246. Giddings JC, Lin HC, Caldwell KD, Myers MN (1983) Sep Sci Technol 18:293
247. Giddings JC, Yang FJ, Myers MN (1977) Sep Sci Technol 12:499
248. Granger J, Dodds J, Leclerc D, Midoux N (1986) Chem Eng Sci 41:3119
249. Litzén A, Wahlund KG (1991) Anal Chem 63:1001
250. Williams PS (1997) J Microcolumn Sep 9:459
251. Wittgren B, Wahlund KG, Dérand H, Wesslén B (1996) Macromolecules 29:268
252. Wittgren B, Wahlund KG, Dérand H, Wesslén B (1996) Langmuir 12:5999
253. Litzén A (1992) Asymmetrical flow field-flow fractionation. PhD Thesis, University of Uppsala, Sweden
254. Wittgren B (1997) Size characterization of water-soluble polymers using asymmetrical flow field-flow fractionation. PhD Thesis, Lund University, Sweden
255. Giddings JC (1989) J Chromatogr 480:21
256. Giddings JC, Lin GC, Myers MN (1976) Sep Sci Technol 11:553
257. Caldwell KD, Gao YS (1993) Anal Chem 65:1764
258. Schimpf ME, Russell DD, Lewis JK (1994) J Liq Chromatogr 17:3221
259. Schimpf ME, Caldwell KC (1995) Am Lab 27:64
260. Reis JFG, Lightfoot EN (1976) AIChE J 22:779
261. Reis JFG, Ramkrishna D, Lightfoot EN (1978) AIChE J 24:679
262. Davis JM, Fan FRF, Bard J (1987) Anal Chem 59:1339
263. Subramanian RS, Jayaraj K, Krishnamurthy S (1978) Sep Sci Technol 13:273
264. Hunter RJ (1993) Introduction to modern colloid science. Oxford University Press, Oxford
265. O'Brien RW, White LR (1978) J Chem Soc Faraday Trans 2 74:1607
266. Chiang AS, Kmiotek EH, Langan SM, Noble PT, Reis JFG, Lightfoot EN (1979) Sep Sci Technol 14:453
267. Shah AB, Reis JFG, Lightfoot EN, Moore RE (1979) Sep Sci Technol 14:475
268. Lightfoot EN, Noble PT, Chiang AS, Ugulini TA (1981) Sep Sci Technol 16:619
269. Palkar SA, Schure MR (1997) Anal Chem 69:3223
270. Palkar SA, Schure MR (1997) Anal Chem 69:3230
271. Semenov SN, Kuznetsov AA (1984) Zh Fiz Khim 60:424
272. Semenov SN (1986) Zh Fiz Khim 60:1231
273. Schunk TC, Gorse J, Burke MF (1984) Sep Sci Technol 19:653
274. Gorse J, Schunk TC, Burke MF (1984) Sep Sci Technol 19:1073
275. Pohl HA (1978) Dielectroporesis. Cambridge University Press, Cambridge
276. Pethig R (1991) Application of AC electrical fields to the manipulation and characterization of cells. In: Karube I (ed) Automation in biotechnology. Elsevier, Amsterdam, pp 159–185
277. Becker FF, Wang XB, Huang Y, Pethig R, Vykoukal J, Gascoyne PRC (1995) Proc Natl Acad Sci USA 92:860

278. Gascoyne PRC, Huang Y, Pethig R, Vykoukal J, Becker FF (1992) Meas Sci Technol 3:439
279. Talary MS, Mills KI, Hoy T, Burnett AK, Pethig R (1995) Med Biol Eng Comp 33:235
280. Markx GH, Talary MS, Pethig R (1994) J Biotechnol 32:29
281. Markx GH, Pethig R (1995) Biotechnol Bioeng 45:337
282. Wang XB, Huang Y, Burg JPH, Markx GH, Pethig R (1993) J Phys D: Appl Phys 26:1278
283. Doshi MR, Gill WN, Subramanian RS (1975) Chem Eng Sci 30:1467
284. Pearlstein J, Shiue MP (1995) Sep Sci Technol 30:2251
285. Shiue MP, Pearlstein AJ (1995) J Chromatogr A 707:87
286. Semyonov SN, Maslow KI (1988) J Chromatogr 446:151
287. Kononenko VL, Giddings JC, Myers MN (1997) J Microcolumn Sep 9:321
288. Kononenko VL, Shimkus JK, Giddings JC, Myers MN (1997) Feasibility studies on photophoretic effects in field-flow fractionation of particles. J Liq Chrom Rel Technol 20:2907
289. Cox RG, Brenner H (1968) Chem Eng Sci 23:147
290. Ho BP, Leal LG (1974) J Fluid Mech 65:365
291. Cox RG, Hsu SK (1977) Int J Multiphase Flow 3:201
292. Chen K, Wahlund KG, Giddings JC (1988) Anal Chem 60:362
293. Giddings JC, Moon MH, Williams PS, Myers MN (1991) Anal Chem 63:1366
294. Giddings JC, Myers MN, Moon MH, Barman BN (1991) Particle separation and size characterization by sedimentation field-flow fractionation. In: Provder T (ed) Particle size distribution. American Chemical Society, Washington, DC, pp 198–216
295. Compton BJ, Myers MN, Giddings JC (1983) Chem Biomed Environ Instrum 12:299
296. Caldwell KD, Cheng ZQ, Hradecky P, Giddings JC (1984) Cell Biophys 6:233
297. Caldwell KD, Nguyen TT, Myers MN, Giddings JC (1979) Sep Sci Technol 14:935
298. Giddings JC, Chen X, Wahlund KG, Myers MN (1987) Anal Chem 59:1957
299. Peterson RE, Myers MN, Giddings JC (1984) Sep Sci Technol 19:307
300. Koch T, Giddings JC (1986) Anal Chem 58:994
301. Williams PS, Lee S, Giddings JC (1994) Chem Eng Commun 130:143
302. Williams PS, Moon MH, Giddings JC (1992) Fast separation and characterization of micron size particles by sedimentation/steric field-flow fractionation: role of lift forces. In: Stanley-Wood NG, Lines RW (eds) Particle size analysis. Royal Society of Chemistry, Cambridge, pp 280–289
303. Ratanathanawongs SK, Giddings JC (1992) Anal Chem 64:6
304. DiMarzio EA, Guttman CM (1970) Macromolecules 3:131
305. Mori S, Porter RS, Johnson JF (1974) Anal Chem 46:1599
306. DosRamos JG, Silebi CA (1990) J Colloid Interface Sci 135:165
307. Meselson M, Stahl FW, Vinograd J (1957) Proc Natl Acad Sci USA 43:581
308. Janca J (1992) Am Lab 24:15
309. Chmelik J, Janca J (1986) J Liq Chromatogr 9:55
310. Janca J (1987) Makromol Chem Rapid Comm 8:233
311. Janca J, Novakova N (1987) J Liq Chromatogr 10:2869
312. Janca J, Novakova N (1988) J Chromatogr 452:549
313. Janca J (1991) J Liq Chromatogr 14:3317
314. Chmelik J, Thormann W (1992) J Chromatogr 600:305
315. Chmelik J, Deml M, Janca J (1989) Anal Chem 61:912
316. Giddings JC (1992) Am Lab 24:20D-M
317. Chmelik J (1991) J Chromatogr 539:111
318. Chmelik J, Janca J (1989) Chem Listy 83:321
319. Chmelik J (1991) J Chromatogr 545:349
320. Chmelik J, Thormann W (1992) J Chromatogr 600:297
321. Chmelik J, Thormann W (1993) J Chromatogr 632:229
322. Karaiskakis G, Koliadima A (1989) Chromatographia 28:31
323. Koliadima A, Karaiskakis G (1990) J Chromatogr 517:345
324. Koliadima A, Karaiskakis G (1994) Chromatographia 39:74

325. Athanasopoulou A, Karaiskakis G (1995) Chromatographia 40:734
326. Hansen ME, Giddings JC (1989) Anal Chem 61:811
327. Athanasopoulou A, Koliadima A, Karaiskakis G (1996) Instrum Sci Technol 24:79
328. Karaiskakis G, Athanasopoulou A, Koliadima A (1997) J Microcolumn Sep 9:275
329. Kataoka K, Okano T, Sakurai Y, Nishimura T, Maeda M, Inoue S, Watanabe T, Tsuruta T (1982) Makromol Chem Rapid Comm 3:275
330. Kataoka K, Okano T, Sakurai Y, Nishimura T, Inoue S, Watanabe T, Maruyama M, Tsuruta T (1983) Eur Polym J 19:979
331. Maruyama A, Tsuruta T, Kataoka K, Sakurai Y (1987) Makromol Chem Rapid Comm 8:27
332. Bigelow JC, Nabeshima Y, Kataoka K, Giddings JC (1991) Separation of cells and measurement of surface adhesion forces. In: Compala DS, Todd P (eds) ACS Symp Ser. American Chemical Society, Washington, DC, p 146
333. Janca J, Pribylova D, Konak C, Sedlacek B (1987) Anal Sci 3:297
334. Myers MN, Giddings JC (1979) Powder Technol 23:15
335. Schure MR, Myers MN, Caldwell KD, Byron C, Chan KP, Giddings JC (1985) Environ Sci Technol 19:686
336. Giddings JC (1985) Sep Sci Technol 20:749
337. Levin S, Giddings JC (1991) J Chem Tech Biotechnol 50:43
338. Giddings JC (1992) Sep Sci Technol 27:1489
339. Fuh CB, Trujillo EM, Giddings JC (1995) Sep Sci Technol 30:3861
340. Giddings JC (1988) Sep Sci Technol 23:119
341. Giddings JC (1985) Sep Sci Technol 20:749
342. Fuh CB, Chen SY (1998) J Chromatogr 813:313
343. Williams PS, Levin S, Lenczycki T, Giddings JC (1992) Ind Eng Chem Res 31:2172
344. Fuh CB, Levin S, Giddings JC (1993) Anal Biochem 208:80
345. Reid RC, Prausnitz JM, Sherwood TK (1977) The properties of gases and liquids; 3rd edn. MacGraw-Hill chemical engineering series. McGraw-Hill Book, New York, p 688
346. Morawetz H (1975) Macromolecules in solution. Wiley-Interscience, New York
347. Giddings JC, Yoon YH, Caldwell KD, Myers MN, Hovingh ME (1975) Sep Sci Technol 10:447
348. Giddings JC, Myers MN, Yang FJF, Smith LK (1976) Mass analysis of particles and macromolecules by field-flow fractionation. In: Kerker M (ed) Colloid and interface science. Academic Press, New York, pp 381–398
349. van Asten AC, Venema E, Kok WT, Poppe H (1993) J Chromatogr 644:83
350. van Asten AC, Kok WT, Tijssen R, Poppe H (1994) J Chromatogr A 676:361
351. Pasti L, Roccasalvo S, Dondi F, Reschiglian P (1995) J Polym Sci Part B: Polym Phys 33:1225
352. Martin M, Ignatiadis I, Reynaud R (1987) Fuel 66:1436
353. Janca J, Martin M (1992) Chromatographia 34:125
354. Giddings JC, Li S, Williams PS, Schimpf ME (1988) Makromol Chem Rapid Commun 9:817
355. Lee S (1993) Gel-content determination of polymers using thermal field-flow fractionation. In: Provder T (ed) Chromatography of polymers: characterization by SEC and FFF. American Chemical Society, Washington, DC, pp 77–88
356. Lee S, Molnar A (1995) Macromolecules 28:6354
357. Shiundu PM, Remsen EE, Giddings JC (1996) Appl Polym Sci 60:1695
358. van Asten AC, van Dam RJ, Kok WT, Tijssen R, Poppe H (1995) J Chromatogr A 703:245
359. Kirkland JJ, Boone LS, Yau WW (1990) J Chromatogr 517:377
360. Rue CA, Schimpf ME (1994) Anal Chem 66:4054
361. Kirkland JJ, Dilks CH Jr., Rementer SW (1992) Anal Chem 64:1295
362. Tank C, Antonietti M (1996) Macromol Chem Phys 197:2943
363. Derand H, Wesslen B, Wittgren B, Wahlund K-G (1996) Macromolecules 29:8770
364. Hecker R, Fawell PD, Jefferson A, Farrow JB (1999) J Chromatogr A 837:139

365. Brimhall SL, Myers MN, Caldwell KD, Giddings JC (1984) J Polym Sci Polym Lett Ed 22:339
366. Brimhall SL, Myers MN, Caldwell KD, Giddings JC (1984) Polym Mater Sci Eng 50:48
367. Kirkland JJ, Dilks CH (1992) Anal Chem 64:2836
368. Miller ME, Giddings JC (1998) J Microcolumn Sep 10:75
369. Schallinger LE, Yau WW, Kirkland JJ (1984) Science 225:434
370. Arner EC, Kirkland JJ (1989) Biochim Biophys Acta 993:100
371. Schallinger E, Arner EC, Kirkland JJ (1988) Biochim Biophys Acta 966:231
372. Schallinger LE, Gray JE, Wagner LW, Knowlton S, Kirkland JJ (1985) J Chromatogr 342:67
373. Lou J, Myers MN, Giddings JC (1994) J Liq Chromatogr 17:3239
374. White RJ (1997) Polym Int 43:373
375. Liu M-K, Giddings JC (1993) Macromolecules 26:3576
376. Dycus PJM, Healy KD, Stearman GK, Wells MJM (1995) Sep Sci Technol 30:1435
377. Beckett R (1987) Environ Technol Lett 9:339
378. Schimpf ME, Wahlund KG (1997) J Microcolumn Sep 9:535
379. van den Hoop MAGT, van Leeuwen HP(1997) Coll Surf A: Physicochem, Eng Aspects 120:235
380. Dixon DR, Wood FJ, Beckett R (1992) Environ Technol 13:1117
381. Beckett R, Wood FJ, Dixon DR (1992) Environ Technol 13:1129
382. Washizu M, Suzuki S, Nishizaka T, Shinohara T (1992) 1992 IEEE Ind Appl Soc Annu Meetings 1 and 2, pp 1446–1452
383. Yang FS, Caldwell KD, Myers MN, Giddings JC (1983) J Colloid Interface Sci 93:115
384. Kirkland JJ, Yau WW (1983) Anal Chem 55:2165
385. Oppenheimer LE, Smith GA (1988) Langmuir 4:144
386. Barman BN, Giddings JC (1992) Langmuir 8:51
387. Jones HK, Barman BH, Giddings JC (1988) J Chromatogr 455:1
388. Barman BN, Giddings JC (1991) Overview of colloidal aggregation by sedimentation field-flow fractionation. In: Provder T (ed) Particle size distribution II: Assessment and characterization. American Chemical Society, Washington, DC, pp 217–228
389. Barman BN, Giddings JC (1995) Anal Chem 67:3861
390. Arlauskas RA, Burtner DR, Klein DH (1993) Calibration of a photosedimeter using sedimentation field-flow fractionation and gas chromatography. In: Provder T (ed) Chromatography of polymers: characterization by SEC and FFF. American Chemical Society, Washington, DC, pp 2–12
391. Yang F-S, Caldwell KD, Giddings JC, Astle L (1984) Anal Biochem 138:488
392. Arlauskas RA, Weers JG (1996) Langmuir 12:1923
393. Hansen ME, Short DC (1990) J Chromatogr 517:333
394. Li J, Caldwell KD, Anderson BD (1993) Pharm Res 10:535
395. Weers JG, Arlauskas RA (1995) Langmuir 11:474
396. Levin S, Klausner E (1995) Pharm Res 12:1218
397. Schimpf ME (1987) Characterization of polymers and their thermal diffusion by thermal field-flow fractionation. PhD Thesis, University of Utah, USA
398. Liu G, Giddings JC (1991) Anal Chem 63:296
399. Shiundu PM, Liu G, Giddings JC (1995) Anal Chem 67:2705
400. Shiundu PM, Giddings JC (1995) J Chromatogr 715:117
401. Moon MH, Kwon H, Park I (1997) Anal Chem 69:1436
402. Ratanathanawongs SK, Giddings JC (1993) Polym Mater Sci Eng 70:26
403. Caldwell KD, Li J, Li J (1993) Polym Mater Sci Eng 69:404
404. Ratanathanawongs SK, Shiundu PM, Giddings JC (1995) Colloids Surf A: Physicochem Eng Aspects 105:243
405. Tan JS, Harrison CA, Li JT, Caldwell KD (1998) J Polym Sci B: Polym Phys 36:537
406. Dunkel M, Tri N, Beckett R, Caldwell KD (1997) J Microcolumn Sep 9:177
407. Karaiskakis G, Graff KA, Caldwell KD, Giddings JC (1982) Int J Environ Anal Chem 12:1

408. Beckett R, Nicholson G, Hart BT, Hansen M, Giddings JC (1988) Water Res 22:1535
409. McCarthy JF, Zachara JM (1989) Environ Sci Technol 23:496
410. Beckett R, Hotchin DM, Hart BT (1990) J Chromatogr 517:435
411. Caldwell KD, Karaiskakis G, Giddings JC (1981) Colloids Surf 3:233
412. Kirkland JJ, Yau WW, Szoka FC (1982) Science 215:296
413. Cardot PJP, Gerota J, Martin M (1991) J Chromatogr 568:93
414. Merino A, Bories C, Gantier J-C, Cardot PJP (1991) J Chromatogr 572:291
415. Merino-Dugay A, Cardot PJP, Czok M, Guernet M, Andreux AP (1992) J Chromatogr 579:73
416. Bories C, Cardot PJP, Abramowski V, Poüs C, Merino-Dugay A, Baron B (1992) J Chromatogr 579:143
417. Urbánková E, Vacek A, Nováková N, Matulík F, Chmelík J (1992) J Chromatogr 583:27
418. Pazourek J, Chmelík J (1993) Chromatographia 35:591
419. Pazourek J, Urbánková E, Chmelík J (1994) J Chromatogr A 660:113
420. Cardot PJP, Elgéa C, Guernet M, Godet D, Andreux JP (1994) J Chromatogr B 654:193
421. Bernard A, Bories C, Loiseau PM, Cardot PJP (1995) J Chromatogr B 664:444
422. Reschiglian P, Torsi G (1995) Chromatographia 40:467
423. Meng H, Caldwell KD, Giddings JC (1984) Fuel ProcessTechnol 8:313
424. Graff KA, Caldwell KD, Myers MN, Giddings JC (1984) Fuel 63:621
425. Giddings JC, Moon MH (1991) Anal Chem 63:2869
426. Giddings JC, Ratanathanawongs SK, Moon MH (1991) KONA: Powder Particle 9:200
427. Beckett R, Jiang Y, Liu G, Moon MH, Giddings JC (1994) Part Sci Technol 12:89
428. Ratanathanawongs SK, Giddings JC (1989) J Chromatogr 467:341
429. Ratanathanawongs SK, Giddings JC (1994) Chromatographia 38:545
430. Fox A, Schallinger LE, Kirkland JJ (1985) J Microbiol Methods 3:273
431. Mozersky SM, Caldwell KD, Jones SB, Maleeff BE, Barford RA (1988) Anal Biochem 172:113
432. Gilbart J, Wells AF, Hoe MH, Fox A (1987) J Chromatogr 387:428
433. Caldwell KD, Nguyen TT, Giddings JC, Mazzone HM (1980) J Virol Methods 1:241
434. Caldwell KD, Compton BJ, Giddings JC, Olson RJ (1984) Invest Ophthalmol Visual Sci 25:153
435. Sklaviadis T, Dreyer R, Manuelidis L (1992) Virus Res 26:241
436. Moon MH, Giddings JC (1993) J Food Sci 58:1166
437. Li P, Giddings JC (1996) J Pharm Sci 85:895
438. Li P, Hansen M, Giddings JC (1997) J Liq Chromatogr Rel Tech 20:2777
439. Barman BN, Myers MN, Giddings JC (1989) Powder Technol 59:53
440. Barman BN, Ashwood ER, Giddings JC (1993) Anal Biochem 212:35
441. Barman BN (1994) J Colloid Interf Sci 167:467
442. Yue V, Kowal R, Neargarder L, Bond L, Muetterties A, Parsons R (1994) Clin Chem 40:1810
443. Tong X, Caldwell KD (1995) J Chromatogr B 674:39
444. Hoffstetter-Kuhn S, Rösler T, Ehrat M, Widmer HM (1992) Anal Biochem 206:300
445. Sharma RV, Edwards RT, Beckett R (1993) Appl Environ Microbiol 1864
446. Fuh CB, Giddings JC (1995) Biotechnol Prog 11:14
447. Caldwell KD, Karaiskakis G, Giddings JC (1981) J Chromatogr 215:323
448. Myers MN, Graff KA, Giddings JC (1980) Nucl Technol 51:147
449. Giddings JC, Graff KA, Myers MN, Caldwell KD (1980) Sep Sci Technol 15:615
450. Martin M, Reynaud R (1984) Collect Colloq Semin Inst Fr Pet 40:263
451. Markx GH, Rousselet J, Pethig R (1997) J Liq Chromatogr Rel Tech 20:2857
452. Keil RG, Tsamakis E, Fuh CB, Giddings JC, Hedges JI (1994) Geochim Cosmochim Acta 58:879
453. Contado C, Dondi F, Beckett R, Giddings JC (1997) Anal Chim Acta 345:99
454. DeGennes PG (1976) Macromolecules 9:594
455. Litzén A, Wahlund K-G (1991) J Chromatogr 548:393

456. Inagaki H, Tanaka T (1980) Anal Chem 52:201
457. Williams PS, Xu Y, Reschiglian P, Giddings JC (1997) Anal Chem 69:349
458. Dilks CH Jr., Yau WW, Kirkland JJ (1984) J Chromatogr 315:45
459. Janca J (1984) Steric exclusion liquid chromatography of polymers. Chromatogr Sci Ser. Marcel Dekker, New York, chap 25, p 329
460. Jahnova V, Matulik F, Janca J (1987) Anal Chem 59:1039
461. Wyatt PJ (1998) J Colloid Interface Sci 197:9
462. Dalas E, Karaiskakis G (1987) Colloids Surf 28:169
463. Beckett R, Giddings JC (1997) J Colloid Interf Sci 186:53
464. Kirkland JJ, Schallinger LE, Yau WW (1985) Anal Chem 57:2271
465. Miller ME, Lee H, Li X, Szentirmay R, Giddings JC (1994) Polym Prepr (ACS Div Polym Chem) 35:764
466. Wijnhoven JEGJ, van Bommel MR, Poppe H, Kok WT (1996) Chromatographia 42:409
467. Johann C, Kilz PJ (1991) J Appl Polym Sci: Appl Polym Symp 48:111
468. Wyatt PJ (1991) J Liq Chromatogr 14:2351
469. Adolphi U, Kulicke WM (1997) Polymer 38:1513
470. Thielking H, Kulicke WM (1998) J Microcolumn Sep 10:51
471. Antonietti M, Briel A, Tank C (1995) Acta Polymer 46:254
472. Korgel BA, Vanzanten JH, Monbouquette HG (1998) Biophys J 74:3264
473. Wittgren B, Wahlund KG (1997) J Chromatogr A 760:205
474. Wittgren B, Wahlund KG (1997) J Chromatogr A 791:135
475. Wittgren B, Borgstrom L, Piculell L, Wahlund KG (1998) Biopolymers 45:85
476. Zahoransky RA, Dummin H, Laile E, Schauer T (1997) Talanta 44:2225
477. Lee H, Kim S, Williams R, Giddings JC (1998) Anal Chem 70:2495
478. Jensen KD, Williams SK, Giddings JC (1996) J Chromatogr 746:137
479. Moon MH, Giddings JC (1996) Ind Eng Chem Res 35:1072

Received: February 1999